Chikungunya virus binds sulfated glycosaminoglycans as attachment factors using specific residues in the E2 glycoprotein

by

Nicole Marie McAllister

BS, Gannon University, 2015

Submitted to the Graduate Faculty of the

School of Medicine in partial fulfillment

of the requirements for the degree of

Doctor of Philosophy

University of Pittsburgh

2021

UNIVERSITY OF PITTSBURGH

SCHOOL OF MEDICINE

This dissertation was presented

by

Nicole Marie McAllister

It was defended on

March 17, 2021

and approved by

Seema Lakdawala, PhD, Assistant Professor, Department of Microbiology & Molecular Genetics

Amy Hartman, PhD, Assistant Professor, Department of Infectious Diseases and Microbiology

Angela Gronenborn, PhD, Professor and Chair, Department of Structural Biology

William Klimstra, PhD, Associate Professor, Department of Immunology

Dissertation Director: Terence Dermody, MD, Professor and Chair, Department of Pediatrics

Chikungunya virus binds sulfated glycosaminoglycans as attachment factors using specific residues in the E2 glycoprotein

Nicole Marie McAllister, PhD

University of Pittsburgh, 2021

Chikungunya virus (CHIKV) is an arthritogenic alphavirus that causes a debilitating musculoskeletal disease. Currently, there are no vaccines or antiviral agents licensed to treat CHIKV disease. Studying the host requirements for CHIKV infection, such as cell attachment factors, may inform the development of therapeutics. Some CHIKV strains depend on cell-surface glycosaminoglycans (GAGs) for efficient infection. However, the specific types of GAGs and other glycans to which CHIKV binds is not fully understood. Using glycan microarray analyses with virus-like particles, we found that CHIKV preferentially binds GAGs relative to nine other glycan groups. Results indicate that sulfate groups on GAGs are essential for CHIKV binding, and CHIKV binds to GAGs as a function of chain length. We determined that strains representing all three CHIKV clades displayed dependence on GAGs for efficient cell-binding, which varied slightly by strain. Enzymatic cleavage of cell-surface GAGs and genetic alterations that diminish GAG expression result in diminished binding and infectivity. Additionally, alanine mutagenesis of the viral attachment protein, E2, enabled the identification of eight E2 residues required for GAG binding, three of which that are required for Mxra8 entry receptor binding. Future work will use these low GAG-binding mutant viruses to test the importance of GAG-binding in a mouse model of CHIKV infection. Collectively, these studies provide evidence for a critical function of GAGs in CHIKV infection, begin to define the GAG-binding region on the virus, and contribute new knowledge about the engagement of host cells by CHIKV.

Table of Contents

List of Tables

List of Figures

Preface

I am grateful for the financial support that made this dissertation possible, including the public health service awards Engagement of Glycosaminoglycans during Chikungunya Virus Infection (F31 AI147440), Immunology of Infectious Diseases training program (T32 AI60525), and Chikungunya Virus Replication and Pathogenesis (R01 AI123348). Additionally, I am thankful for funding provided by the Vira I. Heinz endowment awarded to Dr. Dermody that has supported some of my research.

I am incredibly grateful to have learned from several phenomenal mentors throughout my graduate studies. I am eternally grateful to Terence Dermody, my PhD mentor, for his continuous support and encouragement. His thoughtful mentorship has been integral in my development as a scientist and educator. As I prepared for an academic career focused on teaching, Terry without hesitation always supported the time I spent away from the bench learning and practicing how to teach. For this, I am so grateful. Terry is one of the most kind, humble, and dedicated people I know, and I am incredibly fortunate to have trained with him. Throughout my time in Terry's lab, I have learned the importance of the words we choose to write and speak, how to thoughtfully and selflessly lead through service, and to appreciate the gift of time.

I am also extremely grateful for the mentorship of Laurie Silva. As an expert in CHIKV and the scientist that laid the foundation for my dissertation research, she has been an extraordinary person to learn from. Laurie dedicates herself 110% to her team, and I am so fortunate that I could continue working with her as she transitioned into starting her own lab. Her thoughtful mentorship and friendship have been integral in my development as a scientist, educator, and individual. During my graduate studies, Laurie has taught me the importance of consistent self-reflection and

self-improvement, how to be an exceptional mother, friend, and teacher all at once, and how to enjoy life while kicking ass and pursuing your passions.

I feel very fortunate to have also worked with the caring and brilliant scientists that are currently and were previously led by Terry Dermody and Laurie Silva. It has been an amazing experience to work with such a great team of people. They have been my role models, my cheerleaders, my teachers, and my best friends. I want to especially thank Judy Brown, my rotation mentor. Her patience, leadership, and faith are aspiring. She was the first to teach me how to study viruses, how to NOT dispose of dried ice (and thanks to her guidance several lab sinks are still intact), and how to unapologetically follow your own path in life. I am extremely grateful for her mentorship and friendship over the years. Additionally, I am especially thankful for Anthony Lentscher. Throughout graduate school, he has been my rock, my best friend, and my favorite person to be around. His kindness, patience, and dedication are aspiring. Anthony's constant support and friendship have made my graduate training experience full of laughter, encouragement, and joy. I will forever be grateful for the brilliant experiments we've done together, the endless 11 AM lunches, and all of the celebratory margaritas we've finished sitting across from each other.

I want to thank the past and present members of the CHIKV team in the Dermody and Silva labs for the thoughtful discussions, encouraging words, and friendship over the years. Thanks to Alison Ashbrook, Adam Brynes, Adaeze Izuogu, Anthony Lentscher, and Krishnan Raghunathan for your infectious curiosity and unyielding dedication to your research. Thanks to James Martin and Abby Orzechowski for your continuous support, excitement, and help to push my research forward (even when it meant months of troubleshooting ELISA and qPCR protocols). I am extremely grateful to this team of CHIKV researchers.

I am also thankful for the past and present members of the Reovirus team in the Dermody lab. A special thanks to Danica Sutherland, an extraordinary scientist with unyielding curiosity and excitement for all of our team's research stories. She has set the bar for beautifully structured and delivered talks, manuscripts, and posters. I have had the fortune to not only learn from her but also be supported by her (usually with a glass or two of whiskey). For that, I am eternally grateful. Thanks to Gwen Taylor, Pam Brigleb, and Kelly Urbanek for your friendship and encouragement. Our discussions of science and life have made my time in lab an absolute joy. Thanks to Kira Griswold (my favorite [and only] rotation student – you're a rock star), Xay Somoulay, Kay Fiske, Olivia Welsh, Alexa Roth, Chris Lee, and Pengcheng Shang for being great teammates and always having a kind word to say. Finally, I especially want to thank the graduate students, post-doctoral scholars, and researchers that comprised the Dermody lab when I joined and are the shoulders on which I stand. Alison Ashbrook, Pavi Aravamudhan, Judy Brown, Solomiia Khomandiak, Jon Knowlton, Anthony Lentscher, Kristen Ogden, Andrea Pruijssers, Laurie Silva, Danica Sutherland, and Paula Zamora showed me how to keep rising the bar of excellence, how to be an empathetic teammate, and how to kindly teach new generations of scientists. I could not think of a better team of people to begin my graduate training with.

I am grateful to Seema Lakdawala, Amy Hartman, Angela Gronenborn, and William Klimstra for their mentorship and guidance. These passionate and incredibly intelligent scientists served on my thesis committee and provided ideas and feedback that were integral to my research and training. I am grateful for the mentorship and guidance of my undergraduate research advisors at Gannon University as well, Sarah Ewing and Michael Ganger. These phenomenal teachers and scientists were the first to teach me science and how to conduct research. They introduced me to the idea of graduate school and have been supportive of my decision to pursue a PhD since the

very beginning. I also want to thank the PMI graduate student coordinator, Kristin DiGiacomo, for her tireless work to help the program run smoothly and, most importantly, for her love and dedication to each student that crosses her path. I am so grateful to call her a colleague and friend.

I am also grateful for Ten Feizi, who was kind enough to host me in her lab for a month at the Imperial College of London while I learned how to conduct glycan microarrays. My time in her lab provided incredible training, and I am thankful to have had the opportunity to work with the thoughtful and talented team she has assembled. In particular, I thank Yan Liu, Lisete Silva, and Wengang Chai, who all were unbelievably generous and made me feel so welcome.

Finally, I would like to thank my friends and family that have supported and encouraged me on this journey. To my Gannon friends (Marissa Kutrufis, Jason Brandl, Sarah Miller, David McCartney, and Morgan Thompson) and my Pittsburgh friends (Anthony Lentscher, Brandon Pickel, and Danica Sutherland) – thank you for accompanying me at coffee shops and kitchen tables where I studied endlessly for my comprehensive exam and wrote furiously to submit grants and manuscripts. Thank you for making sure I take breaks from lab, rest my mind, and have fun. I will always cherish the game nights, happy hours, celebratory toasts, and relaxing evenings that made up the best parts of graduate school. A special thanks to Marissa Kutrufis, who continuously shows me how to live life to the fullest with every spontaneous trip, tattoo, and piercing, Jason Brandl, who reminds me to slow down and be present (usually with a beer in one hand and a new movie in another), Danica Sutherland, who always makes sure I stay true to myself (and am well-nourished with red starbursts and whiskey), and Anthony Lentscher, who reminds me to enjoy the small moments in life like a favorite glass of wine, a new recipe, or long night playing games with friends. Thank you all for being at my side every single step of the way in graduate school and making sure I felt supported and confident enough to keep going!

And to my family – thank you for loving me, supporting me, encouraging me, and believing in me. I am forever grateful for my husband (Scott Conrad), mother (Colleen McAllister), grandparents (Denise McAllister, Susan Kuras, and Al Kuras), sister (Ashly McAllister), mother and father in-law (Patti and Bill Conrad), brother in-law (Eric Conrad), cousins (Tinka Schaeffer and Chell Chell Loadman), and aunts (Dee McAllister and Angela Kuras). I am incredibly fortunate to have so many cheerleaders in my life. Your support and excitement have meant the world to me. A special thanks to my husband (Scott Conrad), mother (Colleen McAllister), and grandparents (Denise McAllister, Susan Kuras, and Al Kuras), who have traveled all over the country to support me in my journey to become a scientist. To my sister, my confidant, and friend – thank you for always being just a phone call away, thank you for (sometimes) thinking I'm way cooler than I actually am, and thank you for your unwavering faith in me. Without your love and torment, I would not be the person I am today. To my grandmothers – your unyielding love and tireless work for our family is aspiring. I am so thankful to have learned from you and been loved by you. To my grandfather – your curiosity and interest in my work has continuously made me more excited and thankful to be doing the work I love to do. Thank you for always thinking about me, always being interested in what I have to say, and always wanting to know more. To my mother – your strength, resilience, and independence throughout life is enviable. You have shown the world at a very young age how dedication and love can accomplish anything. I am extremely grateful to have been raised by you, and I hope to emulate that kind of dedication and love in all the things I aim to do. And to my husband – you have supported every big dream, listened to all the details of each troubleshooted experiment, and always reassured me that I could accomplish it all. Your kindness and love have made me such a better version of myself. I am so incredibly grateful for you and our life together.

1.0 Introduction

1.1 Thesis Overview

To initiate infection, viruses interact with a variety of cell-surface molecules, including proteins, carbohydrates, and lipids (1, 2). Binding to abundantly expressed cell-surface molecules, which are sometimes called attachment factors, concentrates viral particles at the plasma membrane, which enhances the probability of engagement with an entry receptor (2). The interaction between a virus and an attachment factor is usually of low-affinity (2). In contrast, interactions with entry receptors are usually of high-affinity and often trigger conformational changes in viral surface proteins that promote viral entry (2). Expression of attachment factors and entry receptors is often a determinant of viral tropism and can influence disease (3), making it important to identify these host factors and characterize their function in viral replication. When multiple attachment factors or entry receptors are used by a virus, defining the function of each during viral infection can be complex. Overall, the molecular mechanisms by which viruses bind to host cells and how such virus-receptor interactions influence tropism and disease are still not completely understood, especially for emerging viruses.

Mosquito-transmitted alphaviruses are a global health threat that periodically reemerge to cause epidemics of disease in many parts of the world (4). Alphavirus introductions into naïve populations have resulted in large epidemics, such as the chikungunya virus (CHIKV) epidemics that began in 2004 and 2013, which collectively resulted in more than 8.5 million cases and the spread of the virus into new geographic regions, including the Western Hemisphere (5–11). CHIKV causes disease in approximately 80% of those infected (12, 13). CHIKV disease is usually

self-limited and rarely fatal, but infection can cause acute and chronic disabilities that impair quality of life (14). Up to 60% of infected individuals experience debilitating arthralgia and arthritis that persist for months to years after infection (15, 16). Additionally, large CHIKV epidemics have severe social and economic consequences (17). Despite the severity of CHIKV disease, there are no licensed antivirals or vaccines for treatment or prevention. Since attachment factors and receptors are determinants of viral tropism and pathogenesis, understanding these virus-host interactions can enhance knowledge of CHIKV infection and facilitate the development of antiviral therapeutics targeting the CHIKV attachment step.

In Chapter 1, I review CHIKV epidemiology, replication, tropism and pathogenesis, and our current knowledge about the attachment factors and entry receptors bound by CHIKV. In Chapter 2, I describe the identification of specific glycosaminoglycans (GAGs) to which multiple CHIKV strains bind as well as the requirement of CHIKV-GAG interactions for binding to and infection of cells. In Chapter 3, I report structural and genetic analyses of the CHIKV E2 glycoprotein to define the residues required for GAG binding. Finally, in Chapter 4, I summarize my thesis studies and discuss ideas for the future continuation of this work. Collectively, research described in this dissertation answers critical questions about the cell-surface interactions that occur when CHIKV encounters a cell. This research identified specific GAG attachment factors to which CHIKV binds and the viral protein residues that are required for CHIKV-GAG interactions.

1.2 Alphaviruses

The alphavirus genus, consisting of 31 species, is one of two genera in the *Togaviridae* family (18). Members of the genus have historically been organized into two groups based on the regions where the viruses were isolated and the type of disease caused, known as Old World and New World. However, geographical nomenclature has become outdated as the global distribution of alphaviruses has expanded. Old World alphaviruses cause arthritogenic disease and include chikungunya (CHIKV), Mayaro (MAYV), O'nyong-nyong, Ross River, and Sindbis viruses. In contrast, New World alphaviruses cause encephalitis and include eastern equine encephalitis virus (EEEV), Venezuelan equine encephalitis virus (VEEV), and western equine encephalitis virus (19). Alphavirus transmission typically occurs between arthropod vectors, such as mosquitoes, ticks, lice, and cliff swallow bugs (20, 21), and vertebrate hosts, including humans. Unlike other alphaviruses, CHIKV titers in the serum of infected humans can be sufficiently high to allow human-mosquito-human transmission, which is not achieved by other alphaviruses (22) (Figure 1). The serious diseases caused by alphaviruses and their continued emergence and geographical spread underlines the importance of studying these viruses.

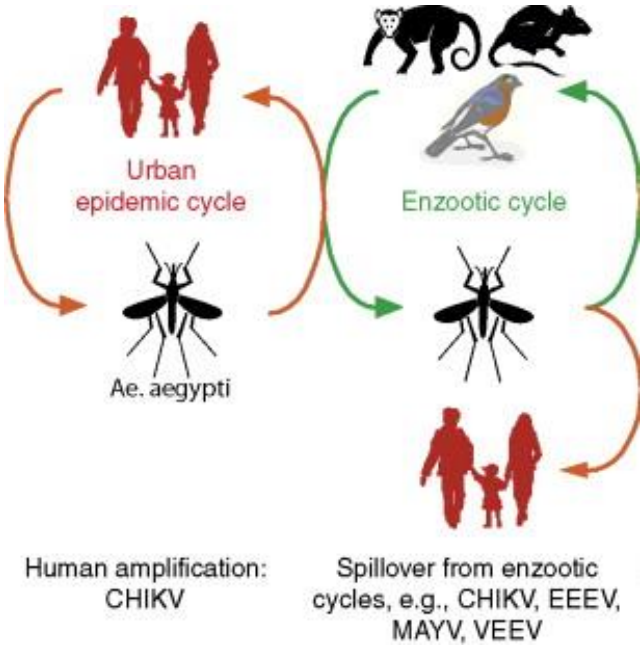

Figure 1. Alphavirus transmission cycles.

Alphaviruses are transmitted by a mosquito vector in either an urban or enzootic cycle. CHIKV, unlike other alphaviruses, can be transmitted in an urban cycle between mosquito and human hosts. CHIKV and other alphaviruses, such as EEEV, MAYV, and VEEV, are transmitted in enzootic cycles between mosquito and animal hosts with occasional spillover into human populations. Figure adapted with permission from (23).

1.3 Chikungunya virology

CHIKV was first isolated in Tanzania in 1953 (24). Although circulating in enzootic cycles throughout Africa, the virus occasionally spilled over into human populations, causing outbreaks that were frequently mistaken for dengue virus infections. Symptoms elicited by CHIKV and dengue virus infections are similar, often leading to misdiagnoses even today (25). The name chikungunya is derived from the Kimakonde language, translating to “that which bends up,” referring to the clinical manifestations observed in the joints that are associated with CHIKV infection (26).

Virions of CHIKV, which are structurally similar to other alphaviruses, are composed of an icosahedral glycoprotein layer embedded in a lipid envelope and an icosahedral core, surrounding the positive-sense, single-stranded RNA genome (27, 28) (Figure 2). The RNA genome is approximately 12 kb and resembles a host messenger RNA with a 5' 7-methylguanosine cap and a 3' poly-A tail (28). The genome contains two open reading frames (ORFs) flanked by 5'- and 3'-terminal non-coding regions. The first ORF encodes non-structural proteins, which function in viral RNA replication, while the second ORF encodes structural proteins (29, 30). Together, both ORFs encode a total of 10 proteins (Table 1).

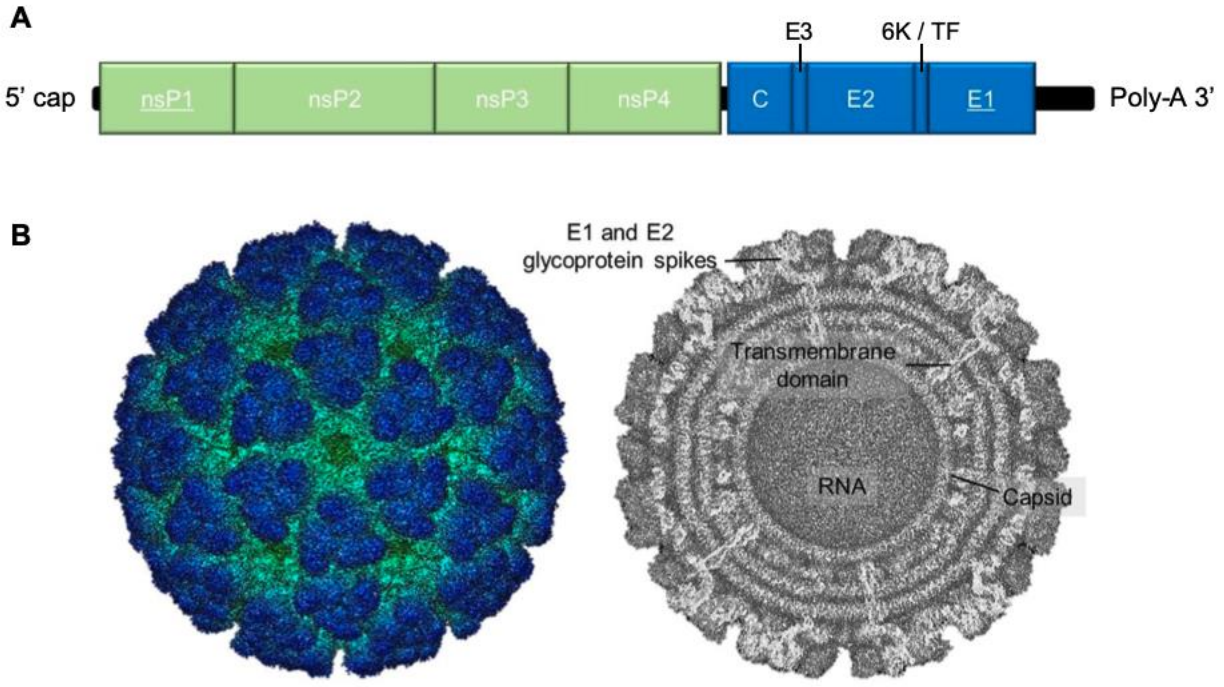

Figure 2. CHIKV genome and virion structure.

(A) Diagram of the CHIKV genome (nonstructural genes, green; structural genes, blue). (B) Structure of the CHIKV virion determined by cryo-electron microscopy (virion surface, left; virion cross section, right). Figure adapted with permission (31).

Table 1. Chikungunya virus proteins.

Protein	Size (aa)	Function
Nonstructural protein cassette		
nsP1	535	Methyltransferase and guanylyltransferase activity that caps viral RNA; sole membrane anchor for replicase complex
nsP2	798	N-terminal NTPase, helicase, and RNA triphosphatase activities; C-terminal cysteine protease activity responsible for processing of nonstructural polyprotein
nsP3	530	Phosphoprotein important for minus-strand synthesis; contains macro domain and SH3-binding regions; unknown functions likely mediated through host protein interactions
nsP4	611	RNA-dependent RNA polymerase (RdRp); putative terminal transferase activity
Structural protein cassette		
Capsid	261	Encapsidates genomic RNA to form nucleocapsid core; carboxyl domain is an autocatalytic serine protease
E3	64	N-terminal domain is uncleaved leader peptide of E2; may help shield fusion peptide in E1 during egress
E2	423	Mediates binding to receptors and attachment factors on the cell membrane; major target of neutralizing antibodies
6K	61	Leader peptide for E1; putative ion channel; may enhance particle release
TF	76	Transframe protein resulting from ribosomal frameshifting; shares N-terminus with 6K; putative ion channel; may enhance particle release; expression prevents synthesis of E1
E1	439	Type II fusion protein; mediates fusion of viral envelope and cellular membrane via fusion peptide

Table adapted with permission from (11).

1.4 CHIKV Disease and Treatment

CHIKV is the causative agent of an acute arthritogenic disease called chikungunya fever (CHIKF), which can develop into a chronic disease in some persons. Symptoms of acute disease in humans develop after an incubation period of about two to six days and include fever, rash, nausea, myalgia, and severe, often debilitating polyarthralgia and polyarthritis (Figure 3). Typically these symptoms resolve after seven to ten days (5, 11, 32). Approximately 87%-98% of infected individuals experience polyarthralgia, the most characteristic symptom of CHIKF. Polyarthralgia reported during acute illness usually occurs in small, peripheral joints. Other symptoms are experienced less often (5). Asymptomatic infections also have been observed with reported case rates between 3.8% to 27.7% (33, 34).

Interestingly, up to 60% of infected individuals develop chronic illness, experiencing debilitating arthralgia and arthritis that persists for months to years after infection (15, 16). Risk factors for developing chronic disease include age, preexisting joint disease, and the severity of symptoms experienced during acute illness (35, 36). During chronic stages of disease most infected individuals develop musculoskeletal disorders. However, about 5% of chronic cases include destructive and deforming inflammatory rheumatism (37).

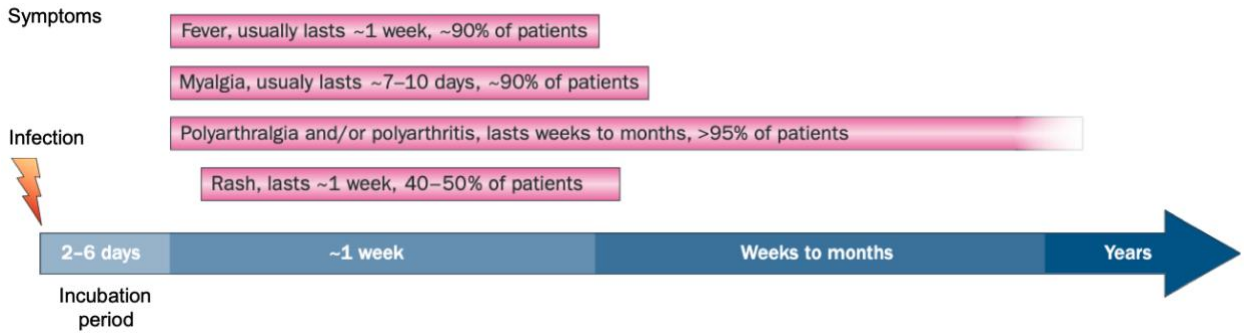

Figure 3. Timeline of CHIKV disease.

After an incubation period of 2-6 days, infected individuals experience fever, myalgia, polyarthralgia, polyarthritis, and rash. The typical duration of each symptom and the average percentage of patients that experience each symptom is shown. Figure adapted with permission (38).

In addition to common acute and chronic disease manifestations, atypical CHIKV disease manifestations have been observed less frequently. Neurological complications, such as seizures, encephalopathy, encephalitis, and Guillain-Barre syndrome, as well as conjunctivitis, myocarditis, pneumonia, nephritis, hepatitis, and pancreatitis have been reported. The development of atypical manifestations is most prevalent in neonates, the elderly, and those with comorbidities (5, 39–42).

Despite the severity of CHIKV disease, there are no licensed antivirals or vaccines to treat or prevent infection. However, supportive therapy can be used to relieve symptoms. Treatment with non-steroidal anti-inflammatory drugs (NSAIDs), disease-modifying anti-rheumatic drugs (DMARDs), anti-tumor necrosis factor-alpha antibodies, muscle relaxant drugs, and acupuncture have been recommended (43, 44). Although there is a lack of FDA-licensed drugs for CHIKV disease, putative CHIKV antivirals that target various stages in the viral lifecycle have been identified using chemical libraries and target-based approaches, but no drugs have advanced to clinical trials (45–51). Some medications have been repurposed in an attempt to treat CHIKV

infection, including favipiravir, ribavirin, and suramin (52–54). However, only ribavirin resulted in positive outcomes in human subjects, although the sample size studied was small (55). Antibody responses are critical for the control and clearance of CHIKV (56–59), suggesting the potential efficacy of antibody therapy. Neutralizing monoclonal antibodies protect immunodeficient mice from CHIKV challenge (59–62) and mediate rapid viral clearance and diminished joint swelling in CHIKV-infected non-human primates (63).

The development of CHIKV vaccines also is underway. The first CHIKV vaccine candidate was a live-attenuated virus, 181/25, which was developed by the United States Army Medical Institute of Infectious Disease (USAMRIID) in 1985. 181/25 was isolated after cell culture passage of a Thailand strain, AF15561, 11 times in green monkey kidney (GMK) cells (64) and 18 times in MRC-5 human fetal lung fibroblast cells (65). Cell-culture adaptation of 181/25 led to mutations in the E2 attachment protein, one of which (G82R) is linked to increased binding efficiency to heparin, a glycosaminoglycan (66, 67), and attenuated virulence in mice and humans (67–69). Protective immune responses were elicited by 181/25 in mice as well as humans in Phase II clinical trials. However, transient arthralgia experienced by a small cohort of vaccinated individuals (~8%) led to the halt of 181/25 development as a CHIKV vaccine in 2000 (65, 69). Currently, live-attenuated virus and virus-like particle (VLP)-based vaccines have shown promising results in clinical studies (70). CHIKV/IRES is a live-attenuated vaccine that contains an internal ribosomal entry site (IRES) in place of the subgenomic promoter, leading to decreased expression of viral structural proteins and overall attenuation in mammalian cells. The CHIKV/IRES vaccine in mice and non-human primates is safe and highly immunogenic (71, 72). VLP vaccines also have been promising thus far. One CHIKV VLP vaccine candidate expresses the structural proteins of a West African CHIKV strain, 37997. This vaccine was found safe and

highly immunogenic in mice, non-human primates, and humans. Phase II clinical trials were recently completed, and Phase III clinical trials are planned to further investigate this vaccine (73–75). Other CHIKV vaccine candidates have been developed and are at various stages of preclinical and clinical evaluation (11, 76).

1.5 Epidemiology and evolution

Phylogenetic analyses suggest that CHIKV originated in Africa over 500 years ago (77). Endemic in sub-Saharan Africa and Southeast Asia, CHIKV has historically been maintained in an enzootic transmission cycle, spreading mostly between *Aedes* species of mosquitoes and nonhuman primates (24, 78, 79). Outbreaks of CHIKV disease in humans occur through the introduction of the virus into more populated areas (78), leading to an urban transmission cycle between mosquitoes and humans (80). In Africa, CHIKV diverged into two main clades, known as West African (WA) and East/Central/South African (ECSA) (22) (Figure 4). CHIKV strains in the West African clade have been responsible for most of the enzootic transmissions and human outbreaks throughout western Africa (6). The ECSA clade eventually emerged in Thailand (81), circulating in an urban transmission cycle and diverging into a new distinct Asian clade (6, 82) (Figure 4).

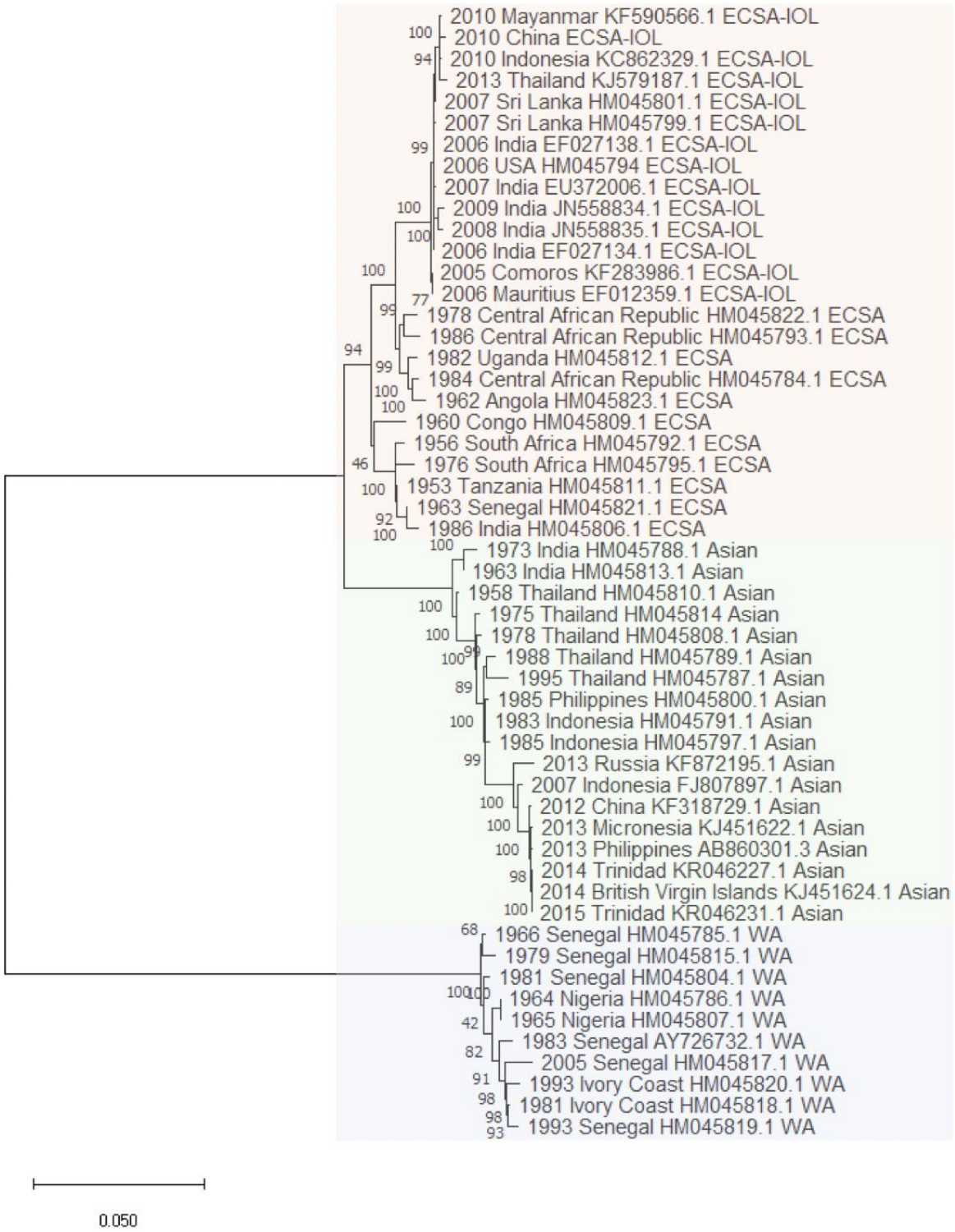

Figure 4. Phylogenetic tree analysis of CHIKV strains.

Viruses from the *Togaviradae* family were analyzed using their complete coding regions available on GenBank. Maximum Likelihood and General Time Reversible model was used to infer evolutionary history, and analyses were

completed in MEGA X. The three main CHIKV clades are color coded (ECSA, red; Asian, green; WA, blue). Indicated next to each branch is the percentage of trees in which the associated taxa are clustered together. The length of each tree branch is measured in the number of substitutions per site. Figure adapted with permission from (83).

Since the identification of CHIKV in 1953, sporadic epidemics of CHIKV occurred mainly in countries in Asia and sub-Saharan Africa (82) (Figure 5). However, recent outbreaks of the virus in the early 2000's led to the geographical expansion of CHIKV into Europe and the Western Hemisphere (Figure 5). In late 2004, an outbreak that began in Kenya led to over six million estimated cases of CHIKV infection and autochthonous spread (local transmission) of the virus to Indian Ocean islands, India, Southeast Asia (5–7, 84), and Europe (9, 85, 86). During this epidemic, a sub-group of the ECSA clade, known as the Indian Ocean lineage (IOL) evolved in the Indian Ocean islands and Southeast Asia (77). Some strains within this sub-group acquired an adaptive mutation in the E1 glycoprotein (A226V), which increased viral fitness in *Aedes albopictus* mosquitoes, one of two mosquito species primarily responsible for CHIKV transmission (87). Importantly, the adaptive A226V mutation requires epistatic interaction in the E1 (98A) and E2 (211T) glycoproteins, which are not observed in the Asian clade, limiting the capacity of these strains to be transmitted by *Aedes albopictus* mosquitoes (88). The enhanced vector competence in *Aedes albopictus* was a notable adaptation because of the broad geographical range of *Aedes albopictus* mosquitoes compared to *Aedes aegypti*, increasing the capacity for CHIKV to spread into naïve populations (87).

The most recent CHIKV outbreak began in December 2013 and led to the first cases of autochthonous spread in the Western Hemisphere (Figure 5). CHIKV was identified in French St. Martin, an island in the Caribbean, and continued to emerge throughout Central, South, and North

America (89, 90). Viral spread in Brazil was attributed to strains of the ECSA clade. However, most cases throughout the 2013 epidemic were attributed to strains of the Asian clade, which limited vector transmission to only *Aedes aegypti* mosquitoes. In the height of the epidemic between December 2013 and December 2017, over 2.5 million cases were identified in almost 50 different countries (90). Additionally, the epidemic led to severe social and economic consequences (17). Overall, these epidemics in the 21st century demonstrated that the emergence of CHIKV into naïve populations can result in large, devastating epidemics, and the possibility of such outbreaks is amplified with increases in human travel, geographical range and presence of vectors due to climate change (91), and adaptations in vector transmission (87).

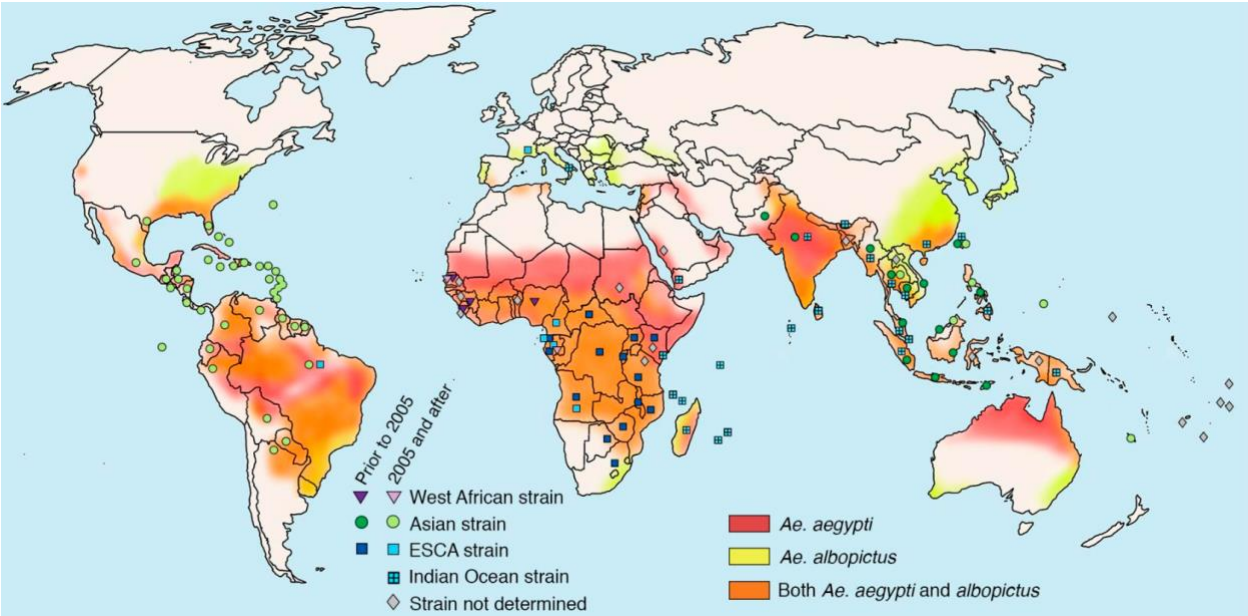

Figure 5. CHIKV and mosquito vector global distribution.

Autochthonous cases (locally transmitted between mosquito and human hosts) of CHIKV are indicated by the symbols, which are color coded by CHIKV clade (WA, purple; Asian, green; ECSA, blue) and date (prior to 2005, darker hue; after 2005, lighter hue). Shaded regions represent the geographical range of each mosquito vector (*Aedes aegypti*, red; *Aedes albopictus*, yellow; both, orange). Figure adapted with permission (11).

1.6 CHIKV replication cycle

The replication cycle of CHIKV in mammalian cells (Figure 6) is comparable to that of other alphaviruses. However, there are key differences that are still being investigated, such as attachment factor and receptor binding, host factor interactions and requirements, and the location of spherule and cytopathic vesicle (CPV) formation. CHIKV cell attachment and entry are mediated by the E1 and E2 glycoproteins, which form a heterodimer. Three E1/E2 heterodimers complex together, creating a trimeric spike. The virion surface is studded with 80 of these spikes that form the icosahedral shape of CHIKV (27). The E2 glycoprotein functions as the attachment

protein, interacting with host molecules to adhere the virion to the cell surface (92, 93). A variety of cell-surface molecules may act as attachment factors for CHIKV, including lectin DC-SIGN, prohibitin 1 (PHB1), and T-cell immunoglobin and mucin 1 (TIM-1) (94–98). Additionally, work from our laboratory, as well as this research, indicate that glycosaminoglycans (GAGs) are attachment factors (66, 67, 99, 100). The engagement of attachment factors provides low-affinity interactions between virions and the cell surface, allowing the virus to concentrate at the plasma membrane before binding to a high-affinity receptor that triggers viral entry into the cell (2, 101). Matrix remodeling associated 8 protein (Mxra8) is an entry receptor for CHIKV and other arthritogenic alphaviruses (102). However, absence of Mxra8 expression in several cell types does not completely abrogate CHIKV infection (102), suggesting that CHIKV can use other entry receptors that are yet to be identified

After attaching to host cells, CHIKV is internalized by clathrin-mediated endocytosis (92, 103, 104). Within endosomes, acidification triggers conformational changes in the E1 glycoprotein, exposing the E1 fusion loop and leading to the insertion of the fusion loop into the endosomal membrane. The nucleocapsid is released into the cytoplasm where it can disassemble and release the viral RNA (93). Since the viral RNA is structurally similar to a cellular messenger RNA (mRNA) with a 5’ cap and 3’ poly-A tail, it can be translated to produce the nonstructural replicase polyprotein, P1234. Alternatively, strains with an opal stop after the nsP3 gene can produce two possible polyproteins (P123 or P1234) (105). The P123 polyprotein and nsP4 function together to transcribe the negative-sense genome (106, 107). Negative-strand synthesis is housed in vesicular structures that form at the plasma membrane, termed spherules. The dsRNA intermediates of genome replication are enclosed inside spherules, protecting them from host sensing and responses, and the nsPs are localized at the neck of the vesicle. Spherules are

eventually internalized and form a large CPV, termed CPV-I (30, 108, 109). The nonstructural polyprotein is post-translationally cleaved into individual proteins (nsP1-4) by the proteolytic action of nsP2 (110). At this point, negative-sense genome synthesis halts, and positive-sense genome synthesis is initiated. This switch is important because positive-sense synthesis is required to produce copies of genomic RNA that will be packaged into progeny virions and for the transcription of the subgenomic RNA that encodes the structural proteins (106, 107). Following translation of the structural polyprotein, it transits the host secretory pathway, during which the polyprotein is cleaved into individual proteins (capsid, E3, E2, 6K, and E1) by various host and viral proteases (111–116). Capsid is the first to be cleaved from the structural polyprotein by autoproteolysis, which allows the capsid protein to interact with newly synthesized genomes, forming intact nucleocapsids (28). 6K is a viral accessory proteins that is not a component of virions but instead may function as an ion channel (117). The envelope glycoproteins (E1, E2, and E3) are extensively processed in the secretory pathway, undergoing conformational changes, palmitoylation, N-linked glycosylation, and furin-mediated release of E3 to form mature E1/E2 heterodimers at the plasma membrane (115, 116). Late in infection, a second CPV is formed, termed CPV-II, which contains helical arrays of E1 and E2 glycoproteins along with nucleocapsids (118–120). CPV-IIs are thought to be intermediate structures that promote assembly of progeny virus particles (120). Ultimately, when intact nucleocapsids enclosing one molecule of the RNA genome are recruited to membrane-associated E1 and E2 glycoproteins, virion particles are assembled and bud from the cell (30).

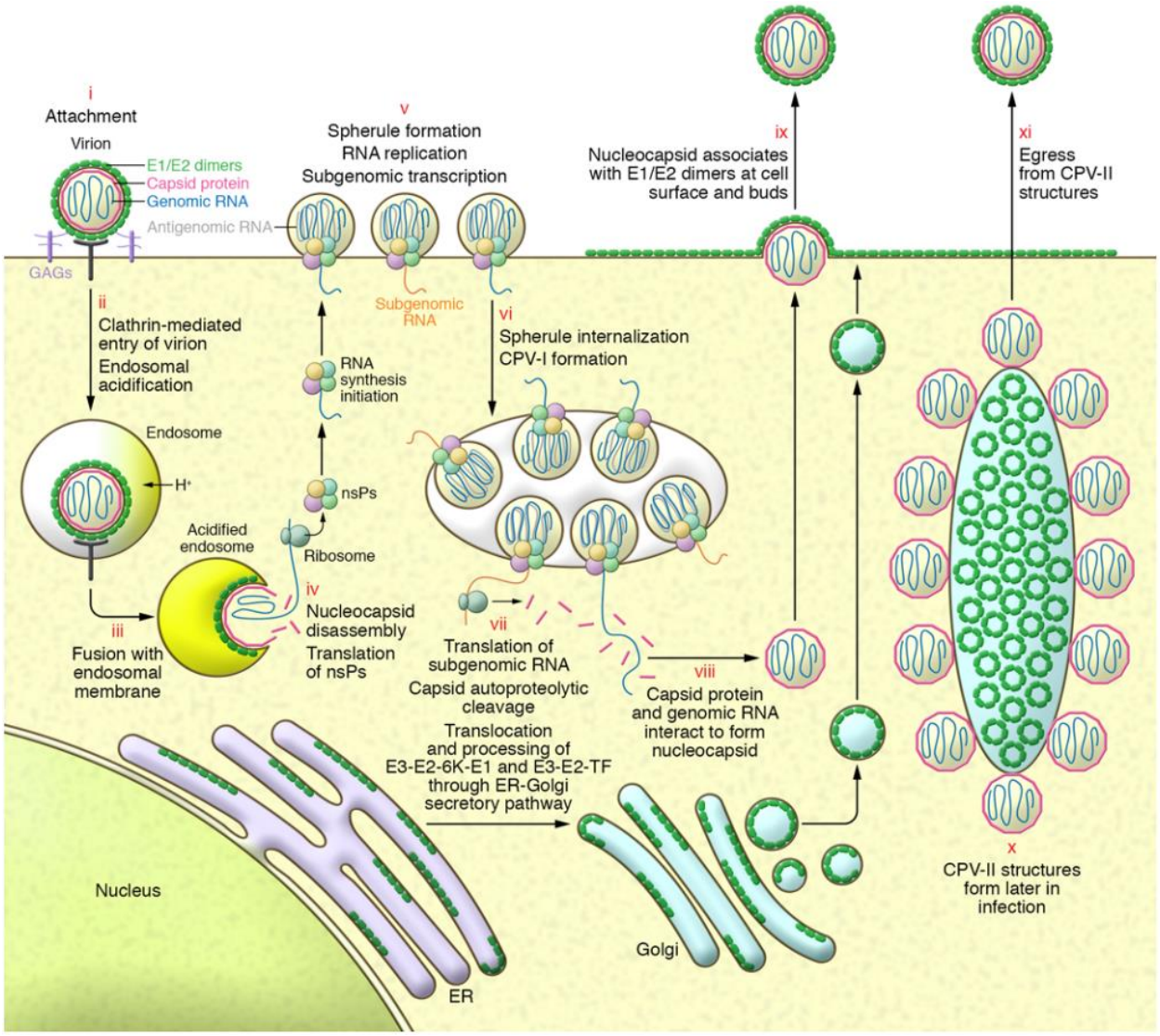

Figure 6. CHIKV replication cycle.

During infection of mammalian cells, (i) CHIKV virions attach to the cell surface by binding to GAG attachment factors and proteinaceous entry receptors like Mxra8. (ii) After entry receptor binding, virions are internalized into the cell using clathrin-mediated endocytosis. Acidification of endosomes causes conformational changes in the E1 glycoprotein. (iii) The viral membrane then fuses with the endosomal membrane and (iv) allows release of the nucleocapsid and viral genome, which is directly translated by the host cell to produce nsPs. (v) Spherules are formed at the plasma membrane with nsPs at the base of these formations. RNA is replicated, and subgenomic transcription occurs. (vi) Spherules are internalized to form CPV-Is. (vii) The mRNA encoding the structural proteins is translated, and the structural polyprotein undergoes post-translational cleavage. Capsid is autoproteolytically cleaved. The

structural polyprotein intermediate is further processed through the ER-Golgi secretory pathway, leading to the translocation of E1/E2 glycoprotein dimers associating with the cell surface. (viii) The capsid protein interacts with genomic viral RNA to form the nucleocapsid, (ix) which is translocated to the plasma membrane to interact with the E1/E2 glycoprotein dimers on the cell surface. Progeny virus is formed and egresses via budding. (x) CPV-II structures form later in infection, (xi) promoting the formation and eventual egress of more progeny virus. Figure adapted with permission (11).

1.7 CHIKV tropism

CHIKV is capable of broad species, tissue, and cell tropism. There is some evidence that CHIKV infects a variety of mammalian and avian species in nature (121–123). However, CHIKV primarily appears to circulate in mosquitoes, nonhuman primates, and humans (78). While CHIKV infection in cell culture is well characterized, less is understood about CHIKV tropism in mosquito and human hosts. Most of the work defining CHIKV tropism has used a variety of animal models, including insect, murine, and nonhuman primate models.

CHIKV infection has been studied in various mosquito cells (66, 67, 124, 125). Additionally, CHIKV infection has been investigated in whole mosquitoes including *Aedes aegypti* and *Aedes albopictus* (126–131) as well as *Drosophila* (132). Virus is ingested by a mosquito through a bloodmeal. CHIKV infects the epithelial cells of the midgut where it replicates and disseminates to sites of secondary infection (133, 134). CHIKV has been detected in the salivary glands, fat bodies, ovaries, legs, and wings (135–137) (Figure 7). Importantly, replication and maintenance of CHIKV in salivary glands is required for transmission of the virus to vertebrate hosts during a bloodmeal (134, 138).

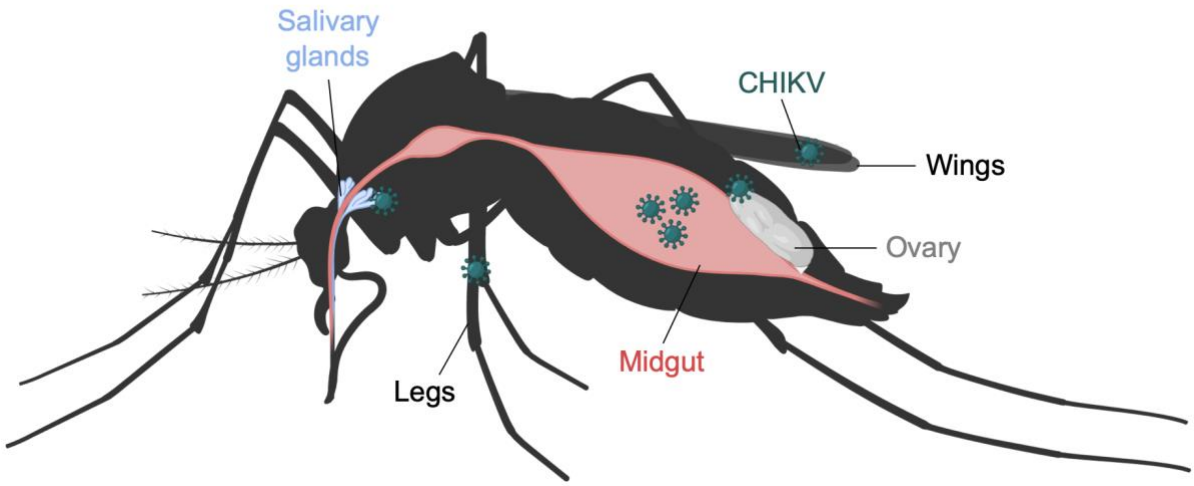

Figure 7. CHIKV tropism in the mosquito vector.

CHIKV is ingested by a mosquito during a bloodmeal. The virus infects the midgut where it replicates and then disseminates to sites of secondary infection, including the ovaries, legs, wings, and salivary glands. The virus must access the salivary glands for transmission from mosquito to vertebrate host. Figure created using BioRender.

Mammalian models of CHIKV disease include immunocompetent and immunodeficient mice (139) as well as nonhuman primates (140). Following the bite of an infected mosquito, virus enters the skin or bloodstream where primary CHIKV replication can occur in fibroblasts, keratinocytes, macrophages, and endothelial cells (Figure 8). Dermal fibroblasts are susceptible to CHIKV in cell culture and in mice (92, 141, 142). There is conflicting evidence about CHIKV infection in human keratinocyte cells *in vitro* (102, 143, 144). However, studies using mice suggest that CHIKV can infect keratinocytes in the absence of interferon regulatory factors 3 and 7 (145). Human macrophages in cell culture are susceptible to CHIKV (146), and viral persistence in macrophages has been observed in nonhuman primates (147). CHIKV can infect primary human endothelial cells, but there is variability in viral susceptibility among endothelial cell lines (92).

CHIKV can spread to sites of secondary infection through the lymphatic system (56, 148, 149). Replication in these peripheral tissues leads to an enormous increase in the viral load observed in the serum, which can exceed 10^9 particles/ml (150). CHIKV disseminates in mice to muscle, joints, and tendons (56, 142, 148, 149). More specifically, CHIKV infection has been observed in synovial fibroblasts and macrophages of the joints (56, 151, 152), chondrocytes and osteoblasts of cartilage and bone (102, 145, 153), and myofibers, satellite cells, and muscle fibroblasts of skeletal muscle (142, 154) (Figure 8).

In addition to the musculoskeletal system, CHIKV disseminates to other peripheral tissues, albeit less frequently and with lower viral loads. CHIKV has been detected in the spleen, liver, and heart of mice and nonhuman primates (56, 129, 140, 148) (Figure 8). Cell types of the central nervous system, such as glial cells, neuroblastoma cells, and microglial cells, are susceptible to CHIKV infection *in vitro* (155–158). In CHIKV-infected neonatal mice, virus is observed in neurons, astrocytes, ependymal cells, and oligodendrocytes (56, 159). CHIKV also has been detected in cells within ocular tissues of infected individuals (Figure 8), including keratocytes, fibroblasts of the sclera, and smooth muscle cells of the ciliary body (160). Overall, the many cells and tissues that support CHIKV infection *in vitro* and *in vivo* showcase the broad tropism of the virus in mosquito and mammalian hosts.

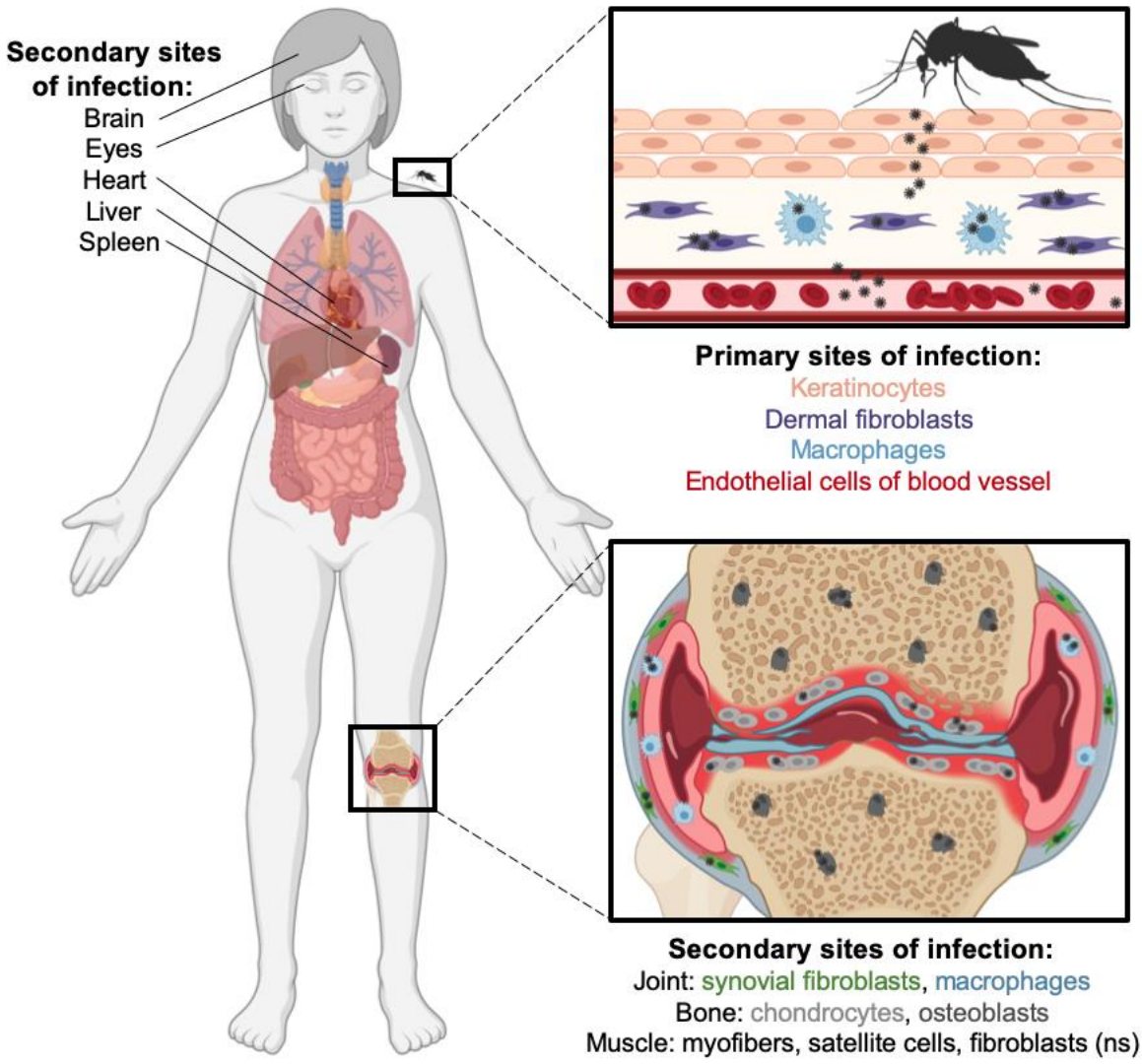

Figure 8. CHIKV tropism in a mammalian host.

When CHIKV enters the body through the bite of an infected mosquito, virus infects and replicates in keratinocytes (peach), dermal fibroblasts (purple), macrophages (light blue), and endothelial cells (red) lining the blood vessels. CHIKV can disseminate to sites of secondary infection, including the brain, eyes, heart, liver, spleen, and musculoskeletal tissues. CHIKV infects synovial fibroblasts (green) and macrophages (light blue) of the joints, chondrocytes (light grey) and osteoblasts (dark grey) of cartilage and bone, and myofibers, satellite cells, and fibroblasts of the skeletal muscle (ns – not shown). Figure created using BioRender.

1.8 CHIKV pathogenesis

The pathogenesis of CHIKV disease and the immune responses elicited by CHIKV are challenging to study in humans. Therefore, much of our knowledge about CHIKV pathobiology is based on animal models of disease, including immunocompetent and immunodeficient mice (139). Immunodeficient mice that lack type I interferon receptors (IFNAR-/-) rapidly succumb to CHIKV infection, limiting their utility in viral pathogenesis studies (56, 139). In contrast, immunocompetent 3-to-4-week-old C57BL/6 mice develop signs that mimic the human disease and are used to investigate CHIKV pathogenesis. Following subcutaneous inoculation of CHIKV into the footpad, these mice develop acute metatarsal swelling in the infected footpad and histological evidence of arthritis, myositis, and tenosynovitis (148, 149).

The tissue injury and disease observed during CHIKV infection in humans and mice is attributed to inflammatory responses elicited by the virus. Following infection, interferon alpha and gamma levels are increased (151, 161), as are levels of cytokines and chemokines (161–163), and immune cells infiltrate into infected tissues (151, 164), causing inflammation and immune-mediated damage. Specifically, severe CHIKV disease is associated with increased production of interleukin-1 beta (IL-1 beta), IL-6, C-X-C motif chemokine ligand 10 (CXCL10), CXCL9, C-C motif chemokine ligand 2 (CCL2), and ***r***egulated upon ***a***ctivation, ***n***ormal ***T*** cell ***e***xpressed and ***s***ecreted chemokine (RANTES) (161–163). Following CHIKV infection in mice, enhanced serum levels of these chemokines correlate with the severity of joint swelling (148, 165). Furthermore, inhibition of CCL2 in mice using bindarit reduces arthritis, myositis, and bone erosion (166, 167). These studies emphasize the critical role of cytokines and chemokines in CHIKV pathogenesis.

CHIKV-induced cytokines and chemokines recruit innate immune cells, including dendritic cells, macrophages, neutrophils, and natural killer (NK) cells, to infected tissues (149,

168–170). Afterwards, cells of the adaptive immune system, including B cells, $CD4^+$ T cells, and $CD8^+$ T cells, infiltrate CHIKV-infected joints (148, 149). Neither $CD4^+$ or $CD8^+$ T cells are required for the clearance of CHIKV. Based on studies using CD4-null mice, $CD4^+$ T cells appear to contribute to joint swelling and tissue damage (171–173). Importantly, macrophages and antibody responses are required for the clearance of CHIKV (57, 148).

1.9 Alphavirus attachment factors and receptors

To initiate infection, viruses interact with a variety of cell-surface molecules, including proteins, carbohydrates, and lipids (1, 2). Virion binding to host molecules abundantly expressed on the cell surface, which are often called attachment factors, concentrates viral particles on the cell membrane and enhances the probability of engagement with an entry receptor that may be expressed at lower levels (2). The interaction between a virus and an attachment factor is usually of low affinity (2). In contrast, interactions with entry receptors are usually of high affinity and often trigger conformational changes in viral surface proteins that promote viral entry (2). Expression of attachment factors and entry receptors can determine viral tropism and influence disease (3), making it important to identify these host factors and characterize their function in viral replication. When multiple attachment factors or entry receptors are used by a virus, defining the function of each during viral infection can be complex. Overall, the molecular mechanisms by which viruses bind to host cells and how such virus-receptor interactions influence tropism and disease are still not completely understood for most viruses.

Alphavirus engagement of attachment factors and receptors is complex, and the field still has an incomplete understanding of this process. The broad cell and tissue tropism observed for

many alphaviruses suggests that these viruses either bind a single receptor expressed by all susceptible cells or can engage multiple receptors specific to each cell type. The variety of attachment factors and possible entry receptors that have been identified over the years for alphaviruses (Figure 9) indicates that the latter possibility is likely true.

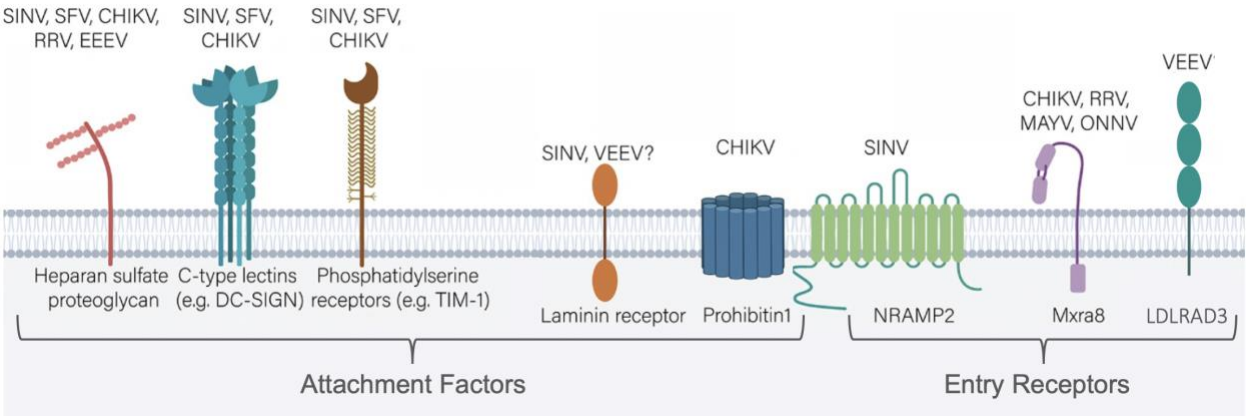

Figure 9. Alphavirus attachment factors and entry receptors.

Several cell-surface molecules have been identified as alphavirus attachment factors and entry receptors. The viruses that engage these attachment factors and entry receptors are shown (CHIKV, chikungunya virus; MAYV, Mayaro virus; ONNV, O'nyong'nyong virus; SINV, Sindbis virus; SFV, Semliki forest virus; RRV, Ross River virus; VEEV, Venezuelan equine encephalitis virus). Figure adapted with permission from (174).

1.9.1 Alphavirus entry receptors

The identification of bona fide alphavirus entry receptors has been challenging. Most studies lack evidence of a direct interaction between viral attachment proteins and putative receptors (174, 175). Additionally, many studies report residual virus binding to and infection of

cells lacking the proposed receptor, suggesting that receptor engagement is either highly cell-type specific or results from a complex interaction with multiple receptors. Alternatively, these studies also could indicate that the putative receptor functions as an attachment factor (174). However, research initiatives have identified three cell-surface molecules as putative alphavirus entry receptors, which include natural resistance-associated macrophage protein (NRAMP) (176), low-density lipoprotein receptor class A domain-containing 3 (LDLRAD3) (177), and matrix remodeling associated protein 8 (Mxra8) (102, 132, 178, 179). These molecules have been deemed alphavirus entry receptors because the following evidence has been collected: (1) direct binding interaction between virus and receptor, (2) cellular susceptibility to virus correlates with receptor expression, (3) virus infection is blocked by receptor-specific antibodies or drugs that inhibit the receptor, and (4) receptor mediates the internalization of the virus. While not always possible, animal studies assessing receptor requirements for viral tropism and pathogenesis further support the role of entry receptors. Putative entry receptors that do not meet the criteria listed above are more likely to function as attachment factors.

Natural resistance-associated macrophage protein (NRAMP) is an entry receptor for the alphavirus Sindbis virus (SINV). NRAMP is a divalent metal ion transporter expressed on cellular targets of SINV infection, including neuronal cells and macrophages. Direct interaction between NRAMP and SINV was confirmed by co-immunoprecipitation assays (176). In insect and mammalian cells, NRAMP gene silencing or treatment with exogenous iron to downregulate NRAMP blocked SINV infection (176, 180). Furthermore, viral RNA transfection experiments that allow viral replication while bypassing a requirement for receptor interactions suggest that NRAMP is specifically involved in the binding and entry of SINV. Ross river virus (RRV) does not require NRAMP, but whether CHIKV or other alphaviruses use this receptor is unclear.

Although NRAMP is required for SINV infection in adult flies (176), the role of NRAMP in mammalian hosts is unknown.

Low-density lipoprotein receptor class A domain-containing 3 (LDLRAD3) is an entry receptor for the alphavirus Venezuelan equine encephalitis virus (VEEV) (177). LDLRAD3 is a scavenger receptor expressed on neurons and epithelial cells (181) and modulates amyloid precursor protein functions in neurons (182). In neurons, LDLRAD3 gene silencing reduces viral infection. Virus attachment to and internalization into neurons is enhanced by LDLRAD3 expression and blocked following the treatment of cells with anti-LDLRAD3 antibodies. Direct interaction between LDLRAD3 and VEEV was observed using ELISAs and surface plasmon resonance (SPR) assays. Furthermore, VEEV infection in mice is diminished with LDLRAD3-Fc blocking treatments and genetic ablation of LDLRAD3. The i*n vitro* and *in vivo* requirements of LDLRAD3 were not observed with other encephalitic or arthritogenic alphaviruses, including CHIKV (177).

Matrix remodeling associated 8 (Mxra8) is an entry receptor for several alphaviruses, including CHIKV. Mxra8 is a cell-adhesion molecule expressed on many cellular targets of alphavirus infection, including epithelial, mesenchymal, and myeloid cells. Mxra8 receptor use appears specific to a subset of Old World arthritogenic alphaviruses. While infection of CHIKV, ONNV, MAYV, and RRV is diminished in mouse embryonic fibroblast (MEF) cells genetically deleted of Mxra8, infection of SINV, SFV, and New World encephalitic alphaviruses (e.g., VEEV, WEEV, and EEEV) is not significantly reduced in Mxra8-lacking MEFs. Furthermore, viral RNA transfection experiments suggest that Mxra8 is specifically required for viral binding and cell entry.

Direct binding of CHIKV and Mxra8 was confirmed by ELISA (102), biolayer interferometry (BLI), SPR, and cryo-electron microscopy (cryo-EM) (178, 179). Structural analyses of Mxra8 in complex with CHIKV or the E1/E2 glycoprotein heterodimer have defined CHIKV E1 and E2 residues that are required for Mxra8-virus binding. The Mxra8 ectodomain is composed of two Ig-like domains oriented head-to-head. The ectodomain binds three E1/E2 heterodimers at a time, contacting two heterodimers on one CHIKV spike and a third heterodimer of an adjacent spike (Figure 10). Mxra8-binding residues are located in domains A and B of the E2 glycoprotein as well as in the fusion loop and domain II of the E1 glycoprotein (178, 179).

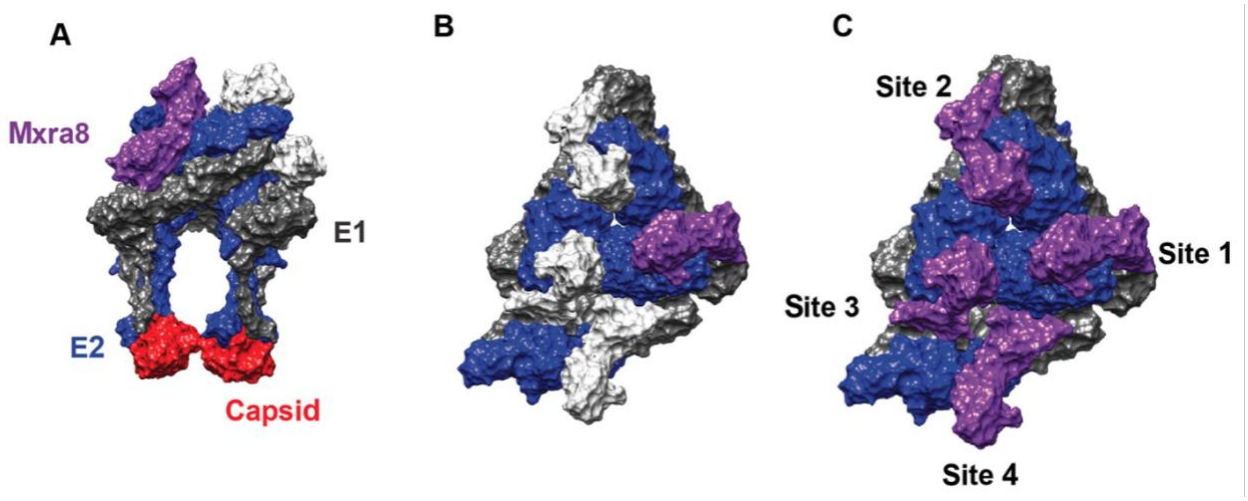

Figure 10. Mxra8 binding interactions with CHIKV.

Structures of Mxra8 and CHIKV in complex together as determined by cryo-EM (PDB: 6NK6). (A) Side view and (B and C) top view of the CHIKV E1/E2 trimer spike binding to Mxra8 (E1, grey; E2, blue; capsid, red; Mxra8, purple). (A and B) A single Mxra8 binding site is shown. (C) Four of the possible Mxra8-binding sites are shown on two adjacent E1/E2 trimers. Figure adapted with permission from (174).

In addition to *in vitro* studies, the requirement of the Mxra8 entry receptor has been reported using mice and *Drosophila* (102, 132). Transgenic flies expressing Mxra8 have increased susceptibility to CHIKV (132). CHIKV infection in mice is diminished with blocking Mxra8-Fc treatments, anti-Mxra8 antibody treatments, and genetic ablation of Mxra8. Viral titers and footpad swelling are reduced when Mxra8 is blocked or genetically disrupted (102, 132). Similarly, MAYV, RRV, and ONNV produce lower titers and less footpad swelling following infection of Mxra8-deficient mice (132). However, viral infection is not completely abrogated by Mxra8 disruption for any virus tested, as indicated by an appreciable viral titer observed in organs of infected mice with blocked or genetically altered Mxra8 expression (102, 132). These data indicate that although Mxra8 is most likely a bona fide entry receptor for CHIKV and some other arthritogenic alphaviruses, other entry receptors yet to be identified also are used.

1.9.2 Alphavirus attachment factors

Alphavirus attachment factors are continually being identified. In fact, several cell-surface molecules originally described as putative receptors have been subsequently defined as attachment factors because of new evidence suggesting attachment factor function. Possible alphavirus attachment factors include: C-type lectins (97, 183, 184), phosphatidylserine receptors (95, 185, 186), laminin receptor (187, 188), prohibitin 1 (94, 189), ATP synthetase beta subunit 1 (96), and glycosaminoglycans (GAGs) (93, 174, 190).

C-type lectins have been suggested to act as attachment factors for some alphaviruses. Specifically, dendritic cell-specific intercellular adhesion molecule-3-grabbing non-integrin (DC-SIGN) and liver-specific SIGN (L-SIGN) aid in virus-cell attachment for SINV, SFV, and CHIKV (97, 183, 184). These c-type lectins function in cell migration and serve as pattern recognition

receptors (PRRs) (191, 192). Cells transfected with DC-SIGN or L-SIGN show increases in CHIKV, SFV, and SINV infection (97, 183). Interestingly, mannose processing of viral N-linked glycans influences virus interaction and dependence on DC-SIGN and L-SIGN. SINV and SFV only bind to these lectins when virus contains high- and pauci-mannose N-linked glycans, which occurs when virus is propagated in mosquito cells (184, 193). Moreover, CHIKV infection is not altered in mice deficient in DC-SIGN and L-SIGN (194). These data suggest a role for DC-SIGN and L-SIGN during *in vitro* alphavirus infection. However, the physiological importance of these c-type lectins *in vivo* is still in question.

Phosphatidylserine (PS) receptors, including the T cell immunoglobulin mucin 1 (TIM-1), milk fat globule-epidermal growth factor-factor 8 (MFG-E8), growth arrest-specific gene 6 (Gas6), and CD300a, are proposed alphavirus attachment factors (95, 185, 186). These molecules bind phosphatidylserine, a component of cell membranes that often is included in the host-derived lipid bilayer of enveloped viruses (195). PS receptors often function during apoptosis (196). CHIKV, SINV, RRV, and EEEV infection of cultured cells increases when TIM-1 is expressed (95, 186). However, viral infection appears to require TIM-1 binding of PS and not the direct engagement of TIM-1 by virus (95). Additional studies using pseudotyped viruses expressing SINV envelope proteins show that expression of MFG-E8, Gas6, and CD300a increases viral infection *in vitro*, suggesting possible attachment factor roles for these molecules (185). The contribution of virus-PS receptor interactions *in vitro* for viral entry and *in vivo* for tropism and disease requires further investigation.

The laminin receptor was identified as a possible SINV entry receptor. However, evidence suggesting a role as an entry receptor rather than an attachment factor is lacking. The laminin receptor is expressed at the cell surface and binds basement membrane laminin and functions in

cell development and tumor metastasis (197). Transfection of the laminin receptor into Chinese hamster ovary (CHO) cells and baby hamster kidney (BHK) cells increases susceptibility to SINV. Antibodies against the laminin receptor can inhibit SINV infection (187). However, whether the laminin receptor is required for internalization of virus into host cells is undetermined, suggesting that this molecule is a SINV attachment factor. Evidence of direct interaction between the laminin receptor and SINV also is lacking. One study observed binding interactions between the c-terminal domain of the laminin receptor and VEEV E2 glycoprotein, but the function of the laminin receptor for VEEV and other alphaviruses, including CHIKV, is unknown.

Similar to the laminin receptor, identification of prohibitin 1 (PHB1) as a putative CHIKV entry receptor is still in question and remains categorized as an attachment factor. PHB1 is expressed on cell and mitochondrial membranes, functioning in cell proliferation and mitochondrial integrity (198). In microglial cells, gene silencing of PHB1 and treatment with anti-PHB1 antibodies reduces CHIKV infection. Immunofluorescence microscopy and co-immunoprecipitation indicate direct binding between CHIKV and PHB1 (94). However, whether PHB1 is actually required for the internalization of the virus is unknown, so it is currently classified as a CHIKV attachment factor. Although PHB1 is suggested to function as an attachment or entry ligand for dengue virus (DENV) (189), the requirement of PHB1 for other alphaviruses and in other cell types is undetermined.

While many studies have investigated alphavirus attachment factor binding in mammalian cells, ATP synthase beta subunit 1 (ATPS-beta 1) was identified as a possible attachment factor in insect cells. ATPS-beta 1 is expressed at the plasma and mitochondrial membranes. The binding interaction between ATPS-beta 1 and CHIKV was discovered in a virus overlay protein binding assay, followed by mass spectroscopy. In insect cells, gene silencing and treatment with anti-

ATPS-beta 1 antibodies reduce CHIKV infection (96). However, more work is required to determine how this molecule mediates CHIKV infection, whether the ATPS-beta 1 ortholog is required in mammalian cells, and whether other alphaviruses depend on ATPS-beta 1 for binding and infection of insect cells.

1.9.3 GAG attachment factors

The most studied alphavirus attachment factors are glycosaminoglycans (GAGs), which are negatively charged, linear polysaccharide glycans found at the cell surface (174, 199–202). Many pathogenic viruses bind GAGs as attachment factors (66, 67, 99, 101, 200, 202–214). Multiple studies conducted with alphaviruses have indicated the importance of heparan sulfate (HS), a specific type of GAG, for virus-cell attachment (67, 100, 199, 203–205, 213, 215–222). Increased HS binding has been identified as a cell-culture adaptation resulting from passaging alphaviruses in cells, which has been a method used to select attenuated vaccine candidates like CHIKV 181/25 (65, 124, 165, 223). However, field-isolated alphavirus strains also use GAGs as attachment factors for efficient *in vitro* infection. These studies used gene silencing of GAGs, enzymatic cleavage of GAGs, blocking treatments of viral particles with exogenous soluble GAGs, and viral mutagenesis to yield enhanced GAG-binding viruses, which defined the requirement of GAGs for CHIKV (66, 67, 99, 100, 224), EEEV (203, 204, 221), RRV (222), SINV (205, 225), SFV (225, 226), and VEEV (213). Furthermore, recent studies have begun to determine the specific GAG moieties required for virus binding. Gene silencing of various GAG biosynthetic enzymes in cells demonstrated that N-sulfation of HS chains is required for efficient CHIKV infection *in vitro* (100). Future studies are required to further define the specific GAG moieties that mediate CHIKV-GAG interactions.

Direct binding interactions between GAGs and alphaviruses have been observed. Binding of SINV and RRV to heparin, HS, and CS was determined with assays using radiolabeled immobilized GAGs (205, 223). RRV binding to heparin was observed by cryo-electron microscopy, which identified the distal tip of the E2 glycoprotein as a heparin-binding region (206). EEEV and heparin (approximately 6 kD monomers) binding also was revealed by cryo-electron microscopy, which identified HS-binding sites in the E2 glycoprotein in axial (spike center) and peripheral (spike periphery) locations (221).

Direct engagement of CHIKV and GAGs also has been observed. CHIKV directly binds heparin as assessed by heparin-agarose bead assays (66, 67). The specific residues of the CHIKV glycoproteins that mediate GAG-binding are yet to be identified. However, by studying viral mutants with increased GAG-binding, regions of the CHIKV E2 glycoprotein have been identified that influence GAG interactions, including residues near G82 and E79. When these residues are altered to an arginine or lysine, respectively, GAG-binding capacity is enhanced (66, 67, 165). Furthermore, molecular docking techniques have identified CHIKV HS-binding residues R104, R107, and R144 in the E2 glycoprotein domain A and arch (218). While direct interactions between GAGs and CHIKV have been reported and preliminarily mapped, the GAG-binding sites on CHIKV are still largely undetermined. Cryo-electron microscopy paired with viral mutagenesis studies to further analyze virus-GAG contact sites are required.

Virus-GAG interactions assessed *in vivo* have been reported to influence tropism and virulence in mouse models of infection with CHIKV (58, 67, 165, 227), EEEV (204), SFV (228), and SINV (219, 223, 229, 230). The contribution of HS binding to alphavirus pathogenesis is complex and differs depending on inoculation method. Intracranial inoculation of HS-binding WT EEEV strains increases neurovirulence and boosts viral titers in the brain relative to low HS-

binding strains. In contrast, subcutaneous infection of HS-binding WT EEEV strains results in decreased neurovirulence as determined by illness and death as well as decreased viral titers when compared to low HS-binding strains (204). Similarly, SINV strains with increased HS binding results in increased neurovirulence when inoculated intracranially and decreased virulence when inoculated subcutaneously (219, 229). During SFV intracranial infection, increased viral HS binding alters viral tropism, allowing virus to more efficiently cross the blood-brain barrier and replicate to higher titers in the brain (228). Overall, following intracranial inoculation, neurotropic alphaviruses with increased HS binding are more neurovirulent. In contrast, following subcutaneous inoculation, alphaviruses with increased HS binding are attenuated in mice, causing reduced disease, rapid viral clearance, and reduced dissemination *in vivo*.

For CHIKV, subcutaneous infection of strains with enhanced HS binding capacity results in attenuated disease characterized by reduced footpad swelling, diminished inflammation and pathology in musculoskeletal tissues, reduced viral titers, and rapid viral clearance (58, 67, 165, 227). This is similar to the *in vivo* phenotypes observed for subcutaneous inoculation of EEEV and SINV. While infection with high GAG-binding CHIKV strains have been assessed, CHIKV strains that are abrogated for GAG binding have yet to be identified and analyzed for tropism and virulence.

1.10 GAG structure and biology

GAGs are glycans expressed ubiquitously on the cell surface and in the extracellular matrix of human and mosquito cells (226, 231, 232). These negatively charged linear polysaccharides are composed of repeating disaccharide units of an N-acetylated or N-sulfated hexosamine and either

a uronic acid (glucuronic acid [GlcA] or iduronic acid [IdoA]) or galactose. There are four main types of GAGs characterized based on the differences in their repeating disaccharide units, including heparin/heparan sulfate (HS), chondroitin sulfate (CS)/dermatan sulfate (DS), keratan sulfate (KS), and hyaluronan. With the exception of hyaluronan, the other types of GAGs are highly sulfated (231). Variations in GAG disaccharide units and the degree and pattern of sulfation are determined by the expression and relative abundance of specific GAG biosynthetic enzymes. Five types of sulfatases (N-sulfatase, 2-O-sulfatase, 3-O-sulfatase, 4-O-sulfatase, 6-O-sulfatase), two types of epimerases (Glce and Dse), and various transferases catalyze GAG modification reactions that lead to the diversity observed among GAG chains (231, 233).

1.10.1 Proteoglycans

Some GAG chains can be attached to core proteins to create complex proteoglycan (PG) structures (Figure 11). Hyaluronan and heparin are the only two GAGs that do not form PGs. In contrast, HS, CS, DS, and KS are covalently attached to a core protein to form a PG. There are many different types of PGs, which are categorized by the core protein, types of GAGs, and distribution in the cell (secreted or membrane-bound). PGs can consist of one or multiple GAG types with variability in the number of GAG chains present (231).

HS, CS, and DS link to serine residues in core proteins through a xylose. A xylotransferase catalyzes the addition of a xylose to a serine residue in the core protein. This reaction is followed by the transfer of two galactose residues, which is catalyzed by galactosyltransferases, and one GlcA catalyzed by a glucuronosyltransferase. The xylose, two galactoses, and GlcA form the tetrasaccharide linkage that is required for HS, CS, and DS PG formation (231). Interestingly, sulfation of this tetrasaccharide linkage likely dictates which type of GAG chain is added to the

PG protein core. However, the exact mechanism remains unknown (234). Once the tetrasaccharide linkage is established, N-acetylglucosamine (GlcNAc) is added by the enzymatic activity of EXTL3 to initiate heparin and HS assembly, or N-acetylgalactosamine (GalNAc) is added by the enzymatic activity of CSGALNACT1/2 to initiate CS and DS assembly (231, 233).

There are four major PG families that are named according to the core protein: glypicans, lecticans, small leucine-rich family of proteoglycans (SLRPs), and syndecans (235). Glypicans are anchored into the plasma membrane by a glycosylphosphatidylinositol (GPI) linkage and consist of only HS GAG chains and a core protein of 56 to 59 kDa in size (231, 235–238). Lecticans are found in the extracellular matrix usually aggregated with hyaluronan chains and consist of CS or KS GAG chains and a large core protein of 96 to 373 kDa in size (231, 235, 238). SLRPs are often found in the extracellular matrix and consist of CS, DS, or KS GAG chains and a small core protein of 25 to 42 kDa in size (231, 235, 238). Finally, syndecans are transmembrane molecules that consist of HS, CS, or DS GAG chains and a small core protein of 22 to 43 kDa in size (231, 235–239). These proteoglycans mediate a variety of functions, including cell adhesion, cell migration, cell signaling, collagen matrix assembly, regulation of inflammation, extracellular matrix assembly, and pathogen binding (231, 239–241).

1.10.2 Heparin and heparan sulfate

Heparin and HS are composed of repeating units of GlcNAc and either GlcA or IdoA (Figure 11). The polymerization of heparin and HS chains is catalyzed by EXT1 and EXT2. GlcA monosaccharides on heparin and HS chains can be epimerized to IdoA through the enzymatic activity of an epimerase called Glce. Heparin is composed of approximately 80% more iduronic acid than HS and is also more sulfated than HS. While both heparin and HS can contain 6-O- and

N-sulfated GlcNAc, over 70% of GlcNAc molecules in heparin chains are N-sulfated. Additionally, IdoA, which largely comprises heparin chains, contains a 2-O-sulfate more often than GlcA (231, 242). These structural differences between heparin and HS explain the more sulfated, negatively charged nature of heparin. In the laboratory, heparin is often used instead of HS due to better accessibility and lower cost (231, 243). However, because of the structural differences between heparin and HS, conclusions based on experiments using only heparin should be conservative. Heparin chains are not attached to core proteins to form PGs and instead are found in the extracellular matrix of endothelial cells, cells of the connective tissue, and glial progenitor cells. Heparin functions as an anti-coagulant and a regulator of cell proliferation and migration. In contrast, HS chains compose glypicans and syndecan proteoglycans as well as perlecan, agrin, collagen type XVIII, and betaglycans (231, 235). In mosquitoes, HS is expressed in the ovaries, midgut, and salivary glands (226, 244, 245). In mammals, HS is expressed ubiquitously throughout the body and in abundance on epithelial cells, fibroblasts, endothelial cells, skin, and muscle (231, 236, 246, 247). Generally, HS functions in cell migration, extracellular matrix assembly, cell adhesion, and inflammation (231, 248, 249).

1.10.3 Chondroitin sulfate and dermatan sulfate

CS is composed of repeating units of GalNAc and GlcA (Figure 11). CS chain polymerization is catalyzed by CHSY1, CHSY3, and CHPF, which constitute the CS-polymerase. Chains of DS are formed when GlcA monosaccharides are epimerized to IdoA by the enzymatic activity of an epimerase called Dse. CS and DS chains are further modified by sulfation, which is used to categorize the different CS chains. CS-A chains contain 4-O-sulfated GalNAc, CS-B chains (also known as DS) contain 4-O-sulfated GalNAc and 2-O-sulfated IdoA, CS-C chains

contain 6-O-sulfated GalNAc, CS-D chains contain 6-O-sulfated GalNAc and 2-O-sulfated GlcA, and CS-E chains contain 3-O- and 6-O-sulfated GalNAc. Although CS is categorized by these different sulfation patterns, many CS chains are hybrid structures containing more than one type of CS. CS/DS chains are found in syndecan, lectican, and SLRP proteoglycans as well as collagen type IX, CSPG4, and neuroglycan-C (231, 235). In mosquitoes, CS/DS are expressed in the ovaries, midgut, and salivary glands (226, 244, 245). However, these forms of CS/DS are unsulfated in invertebrates (231). In mammals, CS/DS are mainly found in cartilage, connective tissue, fibroblasts, macrophages, and endothelial cells (231, 250). Generally, CS/DS chains form collagen matrices, cushion compressive forces, regulate cell adhesion and signaling, and stabilize cartilage collagen fibrils (231, 249, 251).

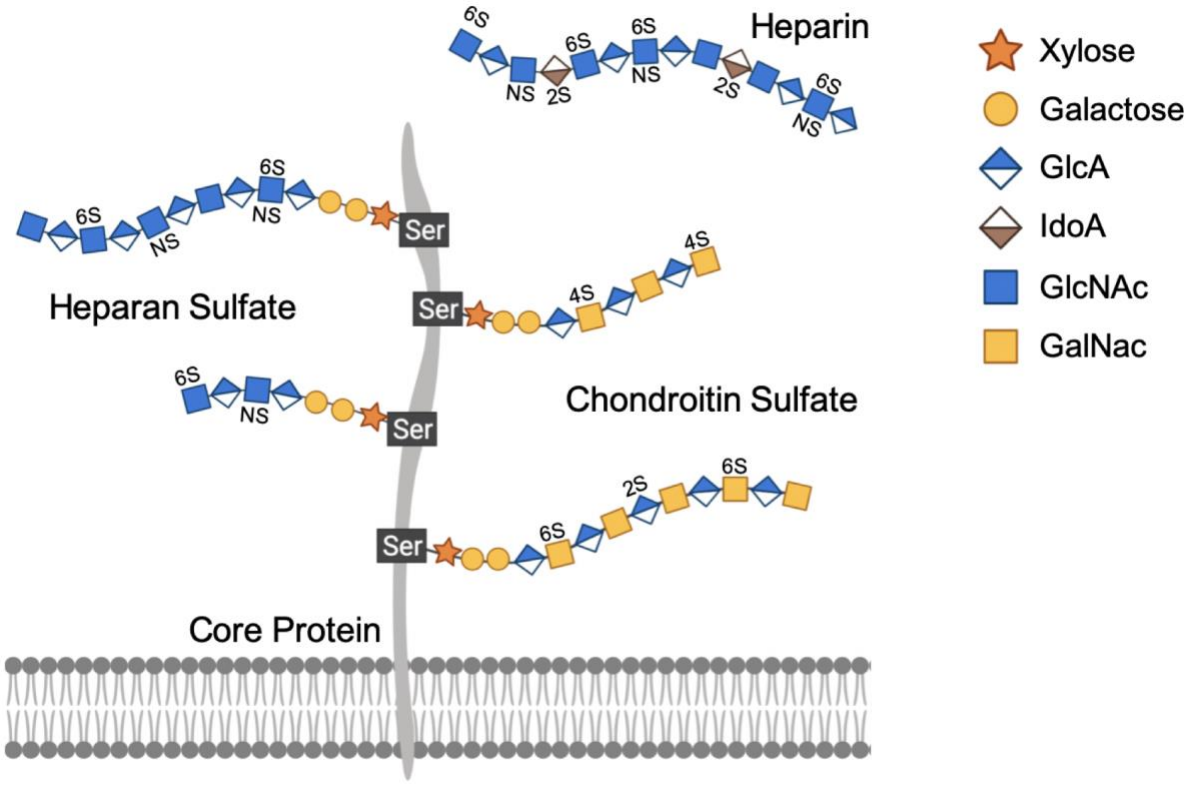

Figure 11. GAG and PG structure.

Chain structures of heparan sulfate, chondroitin sulfate, and heparin. Variations in chain length and sulfation are indicated for heparan sulfate and chondroitin sulfate (NS, N-sulfation; 2S, 2-O-sulfation; 4S, 4-O-sulfation; 6S, 6-O-sulfation). Heparan sulfate and chondroitin sulfate are shown attached to a core protein anchored into the plasma membrane to form a PG. The GAG chains are linked to a serine residue of the core protein by a tetrasaccharide linkage, consisting of xylose, two galactoses, and GlcA. Figure created using BioRender.

1.10.4 Keratan sulfate

Similar to HS and CS/DS, KS also can attach to a core protein to form a PG structure. However, the linkage between KS and a core protein is unique. In general, KS is composed of repeating units of galactose and GlcNAc, which can be 6-O-sulfated. There are two types of KS that differ in linkage to a core protein. KS I is linked to a core protein by an N-glycan attached to

an asparagine protein residue. KS II is linked to a core protein by an O-glycan attached to a serine or threonine protein residue. Chains of KS I are usually longer than those of KS II, found in cornea tissues as part of SLRP PGs like keratocan and lumican, and function in corneal transparency. Chains of KS II are found in the brain and cartilage on lectican PGs like aggrecan. KS II forms a hydrated extracellular matrix to counter compressive forces (231, 235).

1.10.5 Hyaluronan

In contrast to other GAG types, hyaluronan (also known as hyaluronic acid) is the only unsulfated GAG chain. Similar to heparin, it is found in the extracellular matrix and not in complex with a core protein. Hyaluronan is composed of repeating subunits of GlcNAc and GlcA (231). The polymerization of hyaluronan is catalyzed by hyaluronan synthases. Chains of hyaluronan have a high molecular weight and are the largest polysaccharides in vertebrates (231, 252). Furthermore, within the extracellular matrix, multiple hyaluronan chains can interact to form matrices with themselves and lectican PGs like aggrecan (231, 235, 252). Hyaluronan is not found in invertebrates, but it is ubiquitously expressed in most vertebrate cells, functioning in cell differentiation, cell proliferation, and cell signaling (231, 252).

1.10.6 Summary of GAGs and CHIKV

GAGs are structurally and functionally diverse glycans found on most cells and tissues. The broad expression of GAGs makes these molecules ideal cell-surface targets for virus attachment (101, 200, 202, 253). Many pathogenic viruses bind specific types of GAGs as attachment factors to anchor and accumulate at the cell surface (66, 67, 99, 101, 200, 202–214).

Importantly, the types and abundance of GAGs expressed varies among different cells and tissues, which can influence the tropism and virulence of viruses that bind GAGs as attachment factors (101, 200–202).

Our current understanding of the engagement of GAGs by CHIKV is incomplete. Biochemical assays show direct binding of CHIKV to heparin, and a few residues in the CHIKV E2 glycoprotein influence GAG binding (66, 67). However, other specific GAGs to which CHIKV binds and the full GAG-binding pocket on CHIKV have not been identified. *In vitro* evidence indicates a requirement for GAGs for efficient CHIKV infection (66, 67, 224). N-sulfation of HS chains is specifically required for CHIKV infection of culture cells (100). However, the *in vitro* requirement of other specific GAGs and other sulfation modifications on GAG chains for CHIKV binding and infection is unclear, especially on cells with varying levels of GAG and Mxra8 entry receptor expression. Furthermore, whether GAG dependence differs among CHIKV strains from the three genetically distinct clades is undetermined. Finally, the *in vivo* contribution of CHIKV-GAG interactions has been assessed using high GAG-binding CHIKV strains, which are attenuated and rapidly cleared (58, 67, 165, 227). However, *in vivo* infection by CHIKV strains that fail to bind GAGs has not been reported. Such experiments will enhance an understanding of the effects of CHIKV-GAG binding on viral tropism and virulence. The research described in this dissertation addresses these gaps in knowledge.

1.11 Significance of research

Arbovirus infections are a global health threat, contributing to outbreaks of disease in many parts of the world. Recent epidemics in 2004 and 2013 caused by CHIKV, an arthritogenic

alphavirus, resulted in more than 8.5 million cases as the virus spread into new geographic regions, including the Western Hemisphere. CHIKV causes disease in the majority of people infected, leading to severe and debilitating arthritis. Despite the severity of CHIKV disease, there are no licensed therapeutics. Since attachment factors and receptors found on the surface of susceptible host cells are determinants of viral tropism and disease, understanding these virus-host interactions will enhance knowledge of CHIKV infection and may illuminate new antiviral drug targets.

The overall goal of this research is to identify the specific GAG attachment factors bound by CHIKV and define the residues in the E2 glycoprotein required for CHIKV-glycan binding. I analyzed over 670 glycans and identified GAGs as the main glycan bound by CHIKV. I defined specific GAG components required for CHIKV binding and assessed strain-specific differences in GAG-binding capacity and dependence. Finally, I identified eight basic, surface-exposed residues in domain A, domain B, and arch of the CHIKV E2 glycoprotein required for GAG binding. Future studies will define specific GAG structures bound by CHIKV, identify other GAG-binding residues in the CHIKV E1 and E2 glycoproteins, and investigate the role of CHIKV-GAG interactions during *in vivo* CHIKV infection in mice. Overall, these studies provide insight about cell-surface molecules that CHIKV binds, which will help facilitate the development of antiviral therapeutics targeting the CHIKV attachment step.

2.0 CHIKV specifically binds longer, sulfated gags as attachment factors

2.1 Introduction

Several cell-surface molecules have been identified to facilitate CHIKV attachment and entry. CHIKV binds Mxra8 as an entry receptor (102, 132), but absent or decreased expression of Mxra8 in cells and mice does not completely abrogate CHIKV infection, suggesting that CHIKV can use other entry receptors (102, 132). Additionally, a variety of cell-surface molecules may act as attachment factors for CHIKV (94–98), including GAGs (66, 67, 99, 100). Since attachment factors and receptors are determinants of viral tropism and pathogenesis, understanding these virus-host interactions can enhance our knowledge of CHIKV infection. It is not clear whether CHIKV preferentially binds to different GAG types, nor whether CHIKV strains from the three genetically distinct clades differ in GAG binding. Moreover, the requirement of specific GAGs for CHIKV binding and infection of cells with varying levels of GAG and Mxra8 expression has not been defined.

To identify the types of GAGs and other glycans to which CHIKV binds, I used glycan microarray technology in collaboration with the laboratory of Dr. Ten Feizi. Due to the diverse and heterogenous nature of glycans and the inability to readily clone glycans, as they are the product of numerous biosynthetic enzymes, high-throughput screening of protein-glycan interactions is challenging. Microarray technology is one of few methods available to analyze glycan binding in a high-throughput approach. Microarrays have been used to analyze the binding interactions of a variety of molecules, including DNA (254), proteins (255), tissues (256), and

chemical compounds (257). In the early 2000s, this technology was adapted to investigate carbohydrates (258–260).

Microarrays are an ideal method to study carbohydrate interactions. Not only is this a high-throughput approach, but it also requires small amounts of material, which is beneficial since large quantities of homogenous glycans are challenging and expensive to prepare (258). Additionally, glycans are presented in a multivalent display on a microarray chip. This strategy allows for more avid substrate binding, which aids in the detection of the often weak interactions that occur between carbohydrates and their binding partners (258). Glycan microarray approaches have been developed to analyze what binds to monosaccharides (259), oligosaccharides (261), and polysaccharides (260). To conduct microarray analyses, glycans are immobilized to a glass slide, substrate is added, and glycan-substrate binding is quantified, usually by fluorescence intensity (258–263). One of the main differences among glycan microarray approaches is the method by which glycans are immobilized, which is an important factor in ensuring that glycans are retained on the slide and that glycan epitopes are preserved. Either covalent or non-covalent strategies can be used. The first reported glycan microarray by Wang et al. in 2002 used non-covalent immobilization by spotting carbohydrates onto glass slides coated with a nitrocellulose polymer (259). Houseman and Mrksich in 2002 used covalent, Diels-Alder-mediated immobilization of carbohydrates onto gold-coated glass slides (260). While covalent glycan immobilization can provide better glycan retainment on the slide and prevent nonspecific binding, non-covalent glycan immobilization is a less complex approach, which when optimized, can provide the same benefits.

In our studies, we used a glycan microarray approach of non-covalent glycan immobilization through a lipid linker (Figure 12). This method requires the conjugation of an oligosaccharide by reductive amination to an aminolipid called 1,2-dihexadecyl-sn-glycero-3-

phosphoethanolamine (DHPE) (261–263). These glycan-lipid conjugates are called neoglycolipids (NGLs) (261–263). The advantage of the lipid tag approach is that it promotes more efficient glycan mobilization, while also allowing glycans to assume a more natural conformation than provided by the covalent approach, which prevents glycan mobility (261–263). Liu et al., the first group to report the development and use of NGL microarrays, emphasize that the "noncovalent presentation mimics to some extent the arrangement of clustered oligosaccharide structures at the cell surface (263)," making this approach the best high-throughput method currently developed to analyze carbohydrate binding. Thus, we used this technology to identify the types of GAGs and other glycans to which CHIKV binds.

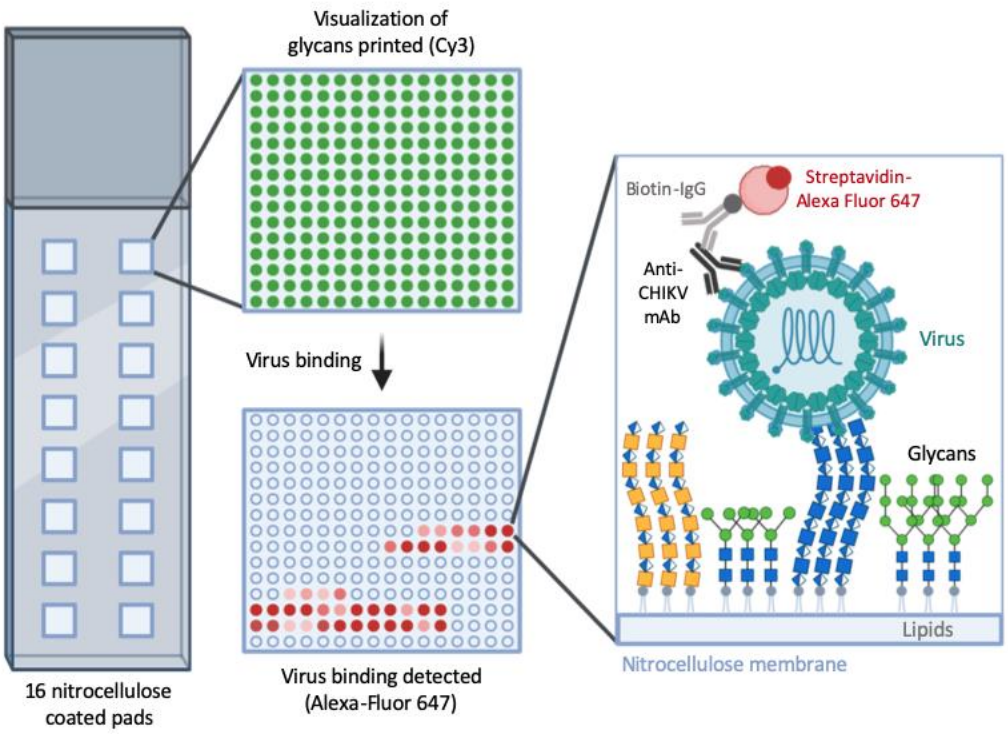

Figure 12. NGL-based glycan microarray.

Illustration of glycan microarray technology. Glass slides are coated with 16 nitrocellulose pads. Each pad is printed with 64 lipid-linked glycans (NGLs) in two concentrations (2 and 5 fmol) for a total of 256 NGLs. NGL preps are diluted in Cy3 dye as a marker. After NGLs are printed onto each pad, imaging is conducted to visualize the glycans to verify spot location and quality. After virus is bound, glycan-virus interactions are detected using an anti-CHIKV monoclonal antibody, biotin-conjugated IgG, and streptavidin-conjugated Alexa Flour 647. Pads are reimaged, and glycan-virus binding is reported as fluorescence intensity.

The glycan microarray work described in this chapter was a collaborative effort between our lab and Dr. Ten Feizi's team, which included Drs. Yan Liu, Lisete Silva, Wengang Chai, Barbara Mulloy, Tomas Frenkiel, and Nian Wu. The chikungunya virus-like particles that were tested on glycan microarrays were obtained from Emergent BioSolutions Inc. with help from Drs. Lo Vang, Jeff Alexander, and Kelly Warfield. Studies to validate the microarray results using

GAG ELISAs were analyzed and interpreted with help from Krishnan Raghunathan (Figure 15 and Table 3). Dr. Laurie Silva's lab team, including James Martin and Abby Orzechowski, aided in the characterization of cell lines (Figure 18D). Cell-binding and infection studies conducted to determine the requirement of CHIKV-GAG binding during infection were completed in collaboration with Dr. Anthony Lentscher and Ms. Kira Griswold (Figures 20 and 21). Technical assistance with flow cytometry was provided by Kelly Urbanek, Pam Brigleb, Joshua Michel, and Alexis Styche. Adam Brynes and Adaeze Izuogu provided technical assistance with RT-qPCR and transient gene complementation. Reagents critical to the work in this chapter, including Hap1 cell lines, Mxra8 antibodies, and CHIKV infectious clones were provided by Drs. Yusuke Maeda, Atsushi Tanaka, Michael Diamond, Mark Heise, and Stephen Higgs.

2.2 Results

2.2.1 CHIKV binds specifically to GAGs

Some strains of CHIKV bind directly to heparin *in vitro* (66, 67). To identify other glycans to which CHIKV binds, we conducted glycan microarray analyses using virus-like particles (VLPs). Chikungunya VLPs are structurally indistinguishable from native chikungunya virions (74) and can be used in experiments at a lower biosafety level than pathogenic CHIKV. The VLPs used in our experiments are composed of the structural proteins of West African clade CHIKV strain 37997 (264) and are currently in advanced development as a vaccine candidate by Emergent BioSolutions (73, 75, 265). The microarray contained 672 sequence-defined lipid-linked

oligosaccharides, representing the major types of mammalian glycans found on glycoproteins, glycolipids, and proteoglycans, as well as those derived from glucan polysaccharides of bacteria, fungi, and plants (Figure 13). Ten heparin-derived oligosaccharides (2-mer to 20-mer chains) were included in this array as representatives of GAG-related sequences. Chikungunya VLPs were overlaid onto the microarray, and VLP binding was detected by indirect immunofluorescence.

Among the 672 glycans tested in the microarray, CHIKV VLPs bound to approximately 30 glycans with signal above background (Figure 13). The ten highest VLP-binding signals were produced by heparin GAGs of varying lengths (Figure 13), suggesting that GAGs are the preferred glycan type bound by CHIKV. Binding was observed with a heparin dimer, and binding signals increased with increasing length of heparin chains. Among the non-GAGs bound, most are negatively charged, including three of the strongest bound non-GAG glycans: 'ring-opened' NeuAc monosaccharide (position 637), SU-3GlcAβ-3Galβ-4Glc (position 36), and Carra-Hexa-4S (position 669; Figure 13; Table S1 in (224)). Collectively, these data demonstrate that GAGs are preferentially bound by chikungunya VLPs *in vitro* and highlight a potential role for GAG chain length in the efficiency of virus binding.

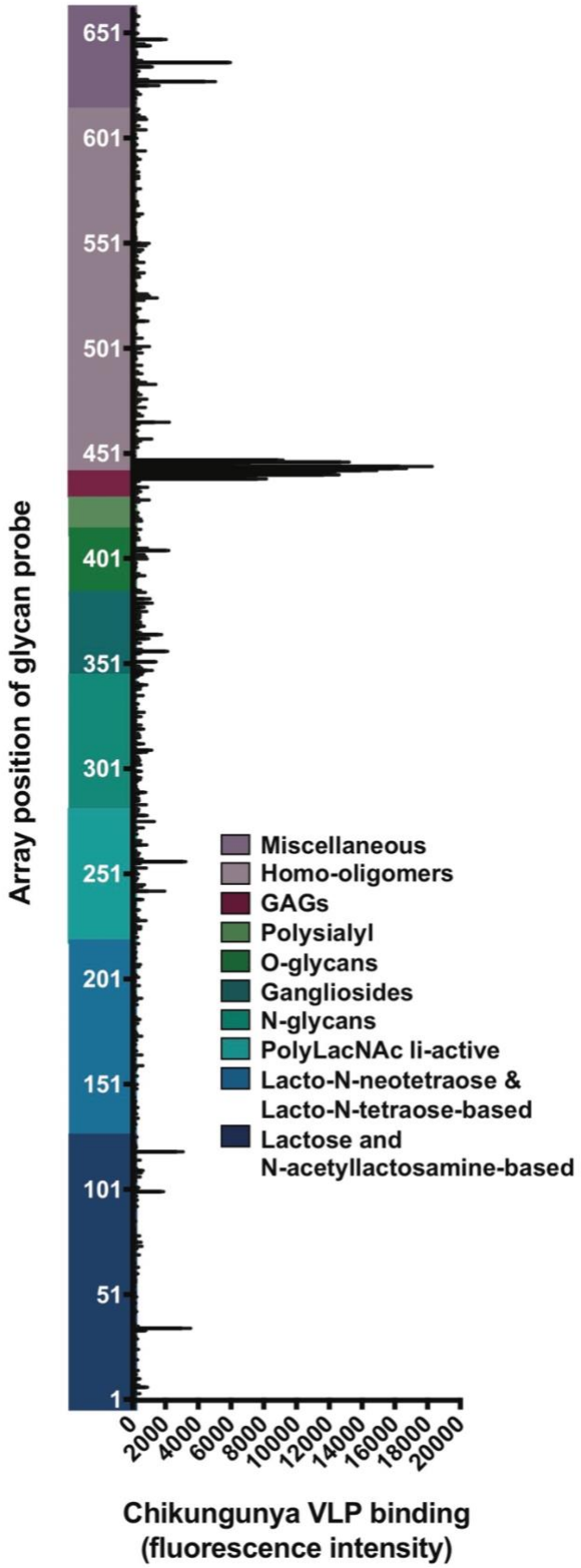
Array position of glycan probe
651
601
551
501
451
401
351
301
251
201
151
101
51
1
0
2000
4000
6000
8000
10000
12000
14000
16000
18000
20000
Chikungunya VLP binding
(fluorescence intensity)
Miscellaneous
Homo-oligomers
GAGs
Polysialyl
O-glycans
Gangliosides
N-glycans
PolyLacNAc li-active
Lacto-N-neotetraose &
Lacto-N-tetraose-based
Lactose and
N-acetyllactosamine-based

Figure 13. Chikungunya VLPs bind specifically to GAGs.

A glycan microarray composed of 672 lipid-linked glycan probes was incubated with purified chikungunya virus-like particles (VLPs, 50 μg/mL). Bound VLPs were fixed with 4% PFA and detected using anti-CHIKV E2-specific monoclonal antibody (CHK-152), followed by biotin-conjugated IgG and streptavidin-conjugated Alexa Fluor 647. VLP-glycan binding is reported as the mean fluorescence intensity of duplicate spots of each lipid-linked glycan probe printed at 5 fmol. The glycan groups tested are arranged according to their backbone sequences as annotated. The glycans tested, probe sequences, and binding intensities are listed in Table S1. Binding data shown are representative of two independent experiments. Error bars represent half of the difference between the two values.

2.2.2 CHIKV binds to longer, sulfated, iduronic acid-containing GAGs

To identify the GAG binding specificities of CHIKV, we used GAG-focused microarrays. These microarrays included 15 size-defined oligosaccharides derived from different types of GAGs: heparin, HS, CS-A, CS-B (DS), CS-C, KS, and hyaluronan, which was the only non-sulfated GAG in this analysis (Figure 14). Short (6- or 10-mer) and long (up to 14-mer) chains were included for each GAG type except for the hyaluronan 12-mer, HS 6-mer, and HS 8-mer (Figure 14). Larger size-defined fractions of HS oligosaccharides were not available for the study due to the sequence heterogeneity of HS relative to other GAG types. Two non-GAG polysaccharides, dextran sulfate and dextran (266), also were included as controls for highly sulfated and neutral saccharides, respectively. Chikungunya VLPs were overlaid onto the GAG-focused array, and VLP binding was detected by indirect immunofluorescence.

Whereas VLPs bound to dextran sulfate, binding to unsulfated dextran was not detected, and very little binding was observed to hyaluronan, an unsulfated GAG (Figure 14A). These data suggest an important function for sulfation in CHIKV-glycan interactions. VLPs bound all sulfated

GAGs above background with varying intensities (Figure 14A). The strongest binding signals were observed with heparin, followed by HS, CS-B, CS-C, CS-A, and weakest for KS (Figure 14A). In general, stronger binding signals were observed with longer GAG oligosaccharides, especially with heparin 14-mer, HS 8-mer, and CS-B 14-mer, which all reached statistical significance. Interestingly, the GAGs bound strongest by CHIKV, including heparin, HS, and CS-B (DS), all contain iduronic acid monomers, while the other GAG types do not (231) (Figure 14B), suggesting that iduronic acid may contribute to CHIKV binding. Overall, CHIKV binds with greatest avidity *in vitro* to longer, sulfated chains of GAGs, with a preference for HS and heparin.

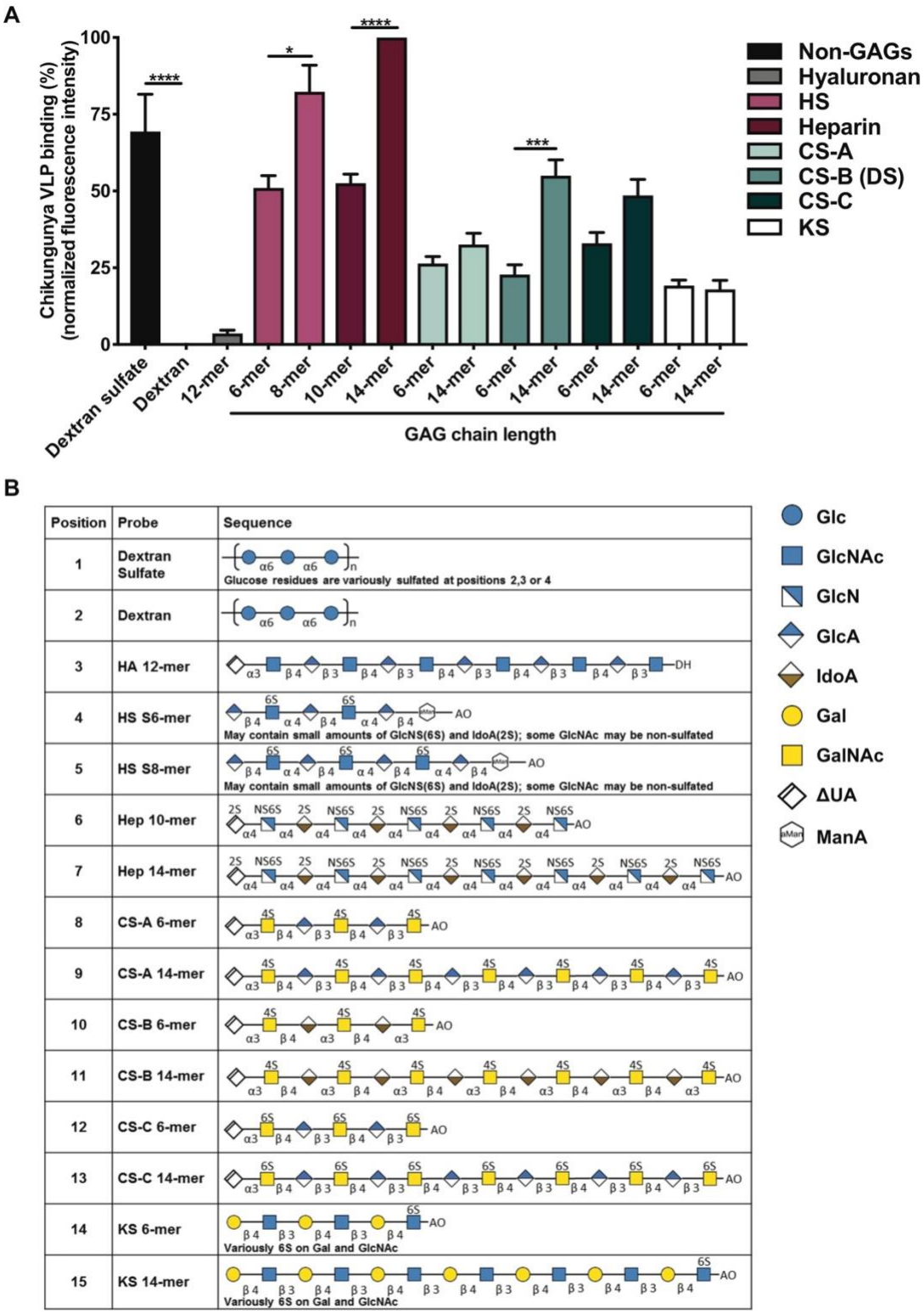

Figure 14. Chikungunya VLPs bind to longer, sulfated, iduronic acid-containing GAGs with a preference for heparin and HS.

(A and B) A GAG-focused microarray composed of GAGs differing in length (indicated by #-mer) and sulfation was incubated with chikungunya VLPs. Dextran and dextran sulfate, non-GAG glycans, also were included in the array to assess sulfation requirements for binding. (A) Chikungunya VLPs were incubated on the microarray. Bound VLPs were fixed with 4% PFA and detected using either anti-CHIKV E2-specific monoclonal antibody (CHK-152) or anti-CHIKV ascites fluid, followed by biotin-conjugated IgG and streptavidin-conjugated Alexa Fluor 647. Fluorescence intensity was determined from duplicate spots of each glycan probe printed at 5 fmol for GAG NGL probes and 0.1 ng for dextran and dextran sulfate. VLP-glycan binding is normalized to heparin 14-mer fluorescence intensity signals. Binding data shown are an average of five independent experiments, except for results with HS, which are from three independent experiments. Error bars indicate standard error of the mean (SEM). *P* values were determined by one-way analysis of variance (ANOVA) followed by Tukey's multiple comparison test (*, $P < 0.05$; ***, $P < 0.001$; ****, $P < 0.0001$). Statistics presented within the graph only indicate statistical significance between samples of each glycan type. (B) The backbone sequences for each glycan probe used on the microarray are listed. (Glc, glucose; GlcNAc, N-acetyl glucosamine; $GlcNH_2$, glucosamine; GlcA, glucuronic acid; IdoA, iduronic acid; GalNAc, N-acetyl galactosamine; dUA, 4,5-unsaturated hexuronic acid; ManA, 2,5-anhydro-mannose; DH and AO, lipid moieties of NGLs prepared by reductive amination and oxime ligation, respectively)

2.2.3 Multiple CHIKV strains directly bind heparin and chondroitin sulfate

To determine whether GAG-binding efficiency differs between CHIKV strains and to validate the microarray results, we assessed viral binding to heparin and CS by ELISA. Three CHIKV strains, SL15649 (149), H20235 (267), and 37997 (264), were selected to represent the three CHIKV genetic clades (ECSA, Asian, and West African, respectively) (Table 2). Importantly, the strains chosen for analysis were isolated from infected humans or mosquitoes and minimally passaged in cell culture prior to sequencing and construction of infectious cDNA clones (Table 2). We used CHIKV strain 181/25 as a positive control for heparin binding. Strain 181/25

was derived from plaque-to-plaque passaging of parental strain AF15561 of the Asian CHIKV clade (64, 65). Cell-culture adaptation of 181/25 led to mutations in the E2 attachment protein, one of which (G82R) is responsible for increased heparin binding efficiency (66, 67) and attenuated virulence in mice and humans (67–69).

Table 2. CHIKV strains used in this study.

Clade	Strain	Isolation	Passage history
Asian	Attenuated 181/25	Tissue culture passage of AF15561 strain	11 passages in GMK cells 18 passages in MRC-5 cells
ECSA	Sri Lanka SL15649	Human patient in Sri Lanka (2006)	3 passages in Vero cells
Asian	Caribbean H20235	Human patient in St. Martin (2013)	3 passages in Vero cells
W. African	Senegal 37997	Mosquito in Senegal (1983)	1 passage in AP-61 cells 2 passages in Vero cells

Serial dilutions of viable virus were adsorbed to ELISA plates coated with either heparin or CS, and bound virus was quantified. We calculated a relative binding strength (RBS) for the binding of each strain to heparin and CS, where the RBS values refer to the relative concentration of virus at which 50% of GAG-binding sites are occupied. As expected, the attenuated 181/25 strain displayed the highest-avidity binding to heparin (Figure 15A) and had the lowest RBS value of 7.9×10^6 genomes/sample (Table 3). The other strains tested also bound to heparin in a dose-dependent manner (Figure 15A). The second-highest heparin-binding signals were detected for the ECSA strain with an RBS value of 1.8×10^7 genomes/sample, followed by moderate binding for

the Asian and West African strains (Figure 15A). The RBS values for heparin binding for the Asian strain was 2 x 10^7 genomes/sample and 3.6 x 10^7 genomes/sample for the West African strain (Table 3). In addition, all strains except the attenuated 181/25 strain bound to CS in a dose-dependent manner (Figure 15B). For this reason, an RBS value for 181/25 binding to CS could not be calculated (ND, not determined; Table 3). A similar preference for HS binding relative to CS binding by 181/25 is observed during *in vitro* binding and infection of mutant Chinese hamster ovary cells (66). Similar to heparin binding, the highest binding signals to CS were detected for the ECSA strain, followed by moderate binding for the Asian and West African strains (Figure 15B). The RBS values for CS binding were 1.4 x 10^7 genomes/sample for the ECSA strain, 2 x 10^6 genomes/sample for the Asian strain, and 10^7 genomes/sample for the West African strain (Table 3). Notably, binding signals were generally lower in the CS binding assays relative to the heparin binding signals (Figure 15). Collectively, these data indicate that CHIKV strains from each clade directly bind *in vitro* to heparin and, to a lesser degree, CS, validating the microarray results that used CHIKV strain 37997 VLPs. These data also demonstrate strain-specific differences in GAG binding with the ECSA strain binding to heparin and CS with the highest avidity and the Asian strain binding to heparin and CS with the lowest avidity.

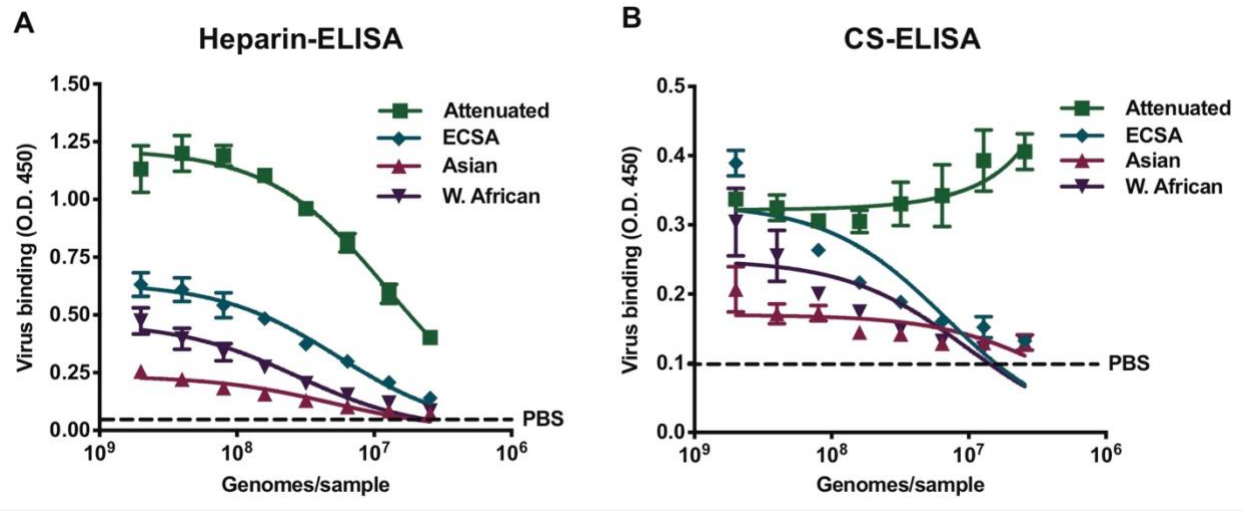

Figure 15. CHIKV strains bind directly to heparin and chondroitin sulfate.

(A and B) Serial dilutions of each CHIKV strain, quantified by genome number, were adsorbed to wells of avidin-coated ELISA plates bound with (A) biotinylated heparin or (B) biotinylated CS. (A and B) PBS was adsorbed to wells coated with heparin and CS as a negative control. Following washes to remove unbound virus, virus binding was detected using mouse monoclonal anti-CHIKV E2 antibody (CHK-187), secondary goat anti-mouse HRP-conjugated antibody, and TMB substrate. Absorbance was measured at 450 nm for duplicate wells from three independent experiments. The dotted line indicates background levels of binding, as determined using PBS control wells. Error bars indicate SEM. Data were fit using a non-linear regression curve.

Table 3. CHIKV binding to heparin and CS.

Virus	Heparin RBS	Heparin - 95% CI	CS RBS	CS - 95% CI
Attenuated	7.9×10^6	$6.13 \times 10^6 – 1.0 \times 10^7$	ND	ND
ECSA	1.8×10^7	$1.3 \times 10^7 – 2.5 \times 10^7$	1.4×10^7	$8.8 \times 10^6 – 2.4 \times 10^7$
Asian	2.0×10^7	$1.4 \times 10^7 – 2.9 \times 10^7$	2.0×10^6	$5.9 \times 10^5 – 4.4 \times 10^6$
W. African	3.6×10^7	$2.2 \times 10^7 – 5.9 \times 10^7$	1.0×10^7	$4.3 \times 10^6 – 2.5 \times 10^7$

2.2.4 Characterization of cell lines

While microarray and ELISA results demonstrate that multiple CHIKV strains directly bind GAGs, it was not clear whether this virus-glycan interaction contributes to virus binding and infection of cells. We characterized several cell lines to identify the most appropriate cells to test the requirement of GAGs for virus binding and infection in assays using enzymatic cleavage of GAGs or genetic disruption of GAG biosynthetic enzymes. Cell lines were assessed for GAG expression, Mxra8 (CHIKV entry receptor (102)) expression, CHIKV susceptibility, and karyotype. These were important parameters to test, as cell-surface receptor expression (102, 226, 231, 236, 244–247, 250) and viral susceptibility (56, 92, 135, 136, 142, 143, 146, 148, 149, 154) vary by cell type. Quantification of the expression of GAG attachment factors and the Mxra8 entry receptor in our experimental system was essential to enable accurate conclusions to be drawn from our studies. We further considered the karyotype of cell lines to determine those most amenable to genetic disruption. We searched for a cell line with high HS and CS expression to conduct studies using enzymatic cleavage of cell-surface GAGs and a cell line with high HS or CS expression with a haploid or diploid karyotype as an ideal model to engineer GAG-expression genetic knock-out cells. Additionally, the identification of cell lines that express or lack Mxra8 were of interest to investigate the requirement of GAGs for CHIKV binding and infection in the presence and absence of Mxra8.

Baby hamster kidney fibroblasts (BHK-21) and African green monkey kidney epithelial cells (Vero-81), which are cell lines typically used to prepare and titer CHIKV stocks, respectively, express relatively high levels of cell-surface HS (Figure 16A and B). Vero cells also express high levels of CS; while BHK cells express little CS (Figure 16A and B). Murine cell lines, including 3T3 fibroblasts and BV-2 microglial cells, also were assessed for GAG expression. 3T3 cells

express high levels of HS and low levels of CS (Figure 16C and D). BV-2 cells express relatively low levels of both HS and CS (Figure 16E and F). Finally, GAG expression was analyzed for four human cell lines: osteosarcoma (U-2 OS) cells, telomerized foreskin fibroblasts (HFF-1), immortalized synovial fibroblasts, and Hap1 cells. Relatively high levels of HS and CS are detected on U-2 OS cells (Figure 16A-L), synovial fibroblasts (Figure 16I and J), and HFF-1 cells (Figure 16G and H). Only HS is detected on Hap1 cells (Figure 16K and L). U-2 OS cells, which are commonly used for studies of CHIKV replication, were compared to each cell type analyzed for GAG expression (Figure 16). Interestingly, the level of GAG expression detected on U-2 OS cells changes slightly with each U-2 OS cell preparation, which may correlate with passage number. Higher HS expression was observed in cells passaged longer in cell culture (Figure 16 and data not shown). Overall, the only cell types expressing both HS and CS are Vero, U-2 OS, HFF-1, and synovial fibroblast cells. Several cell types express HS with little to no expression of CS, including BHK, 3T3, and Hap1 cells. In contrast, little to no HS or CS are expressed on BV-2 cells.

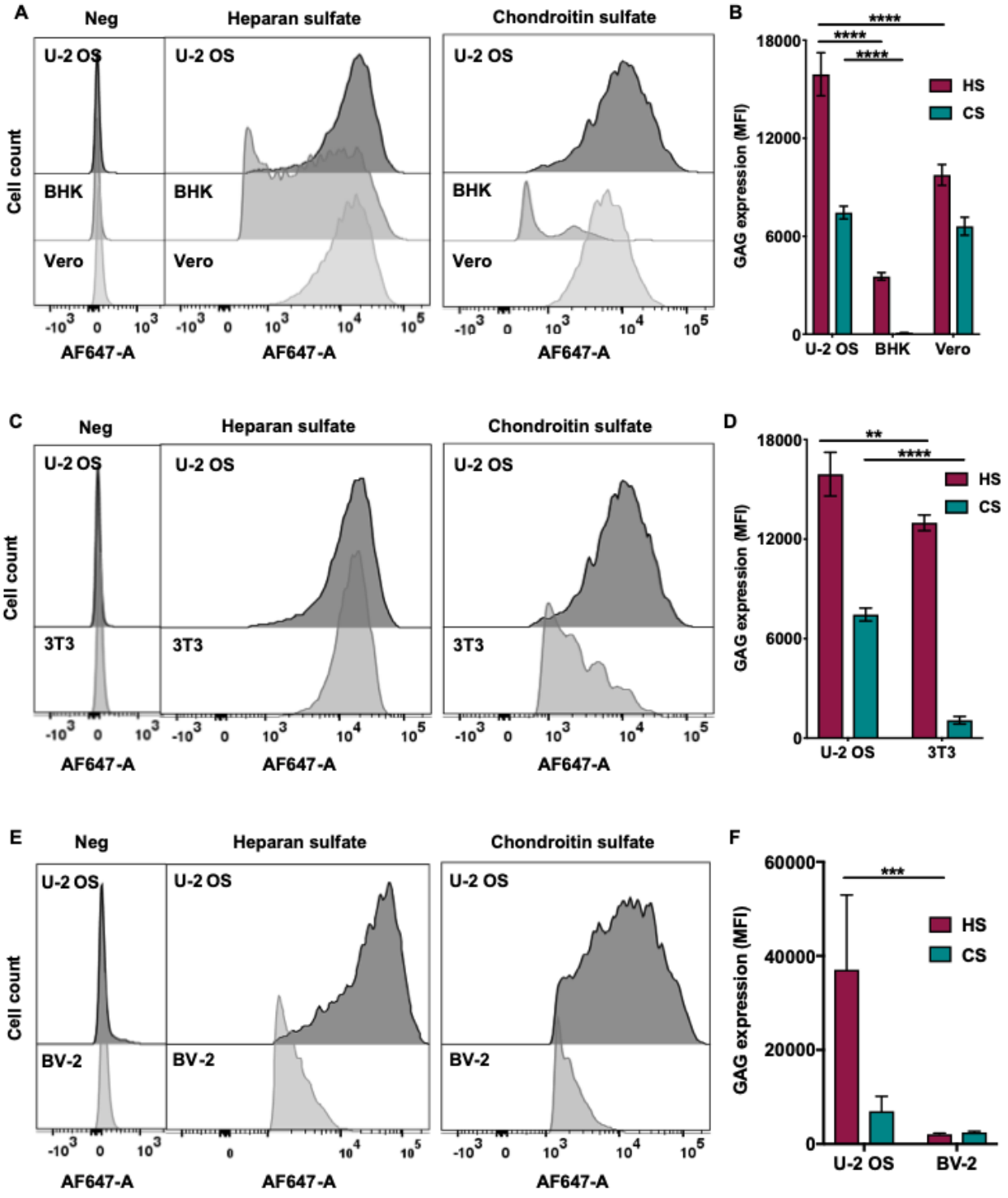
A
Neg
Heparan sulfate
Chondroitin sulfate
U-2 OS
BHK
Vero
Cell count
AF647-A
B
GAG expression (MFI)
HS
CS
U-2 OS
BHK
Vero
C
3T3
D
E
BV-2
F

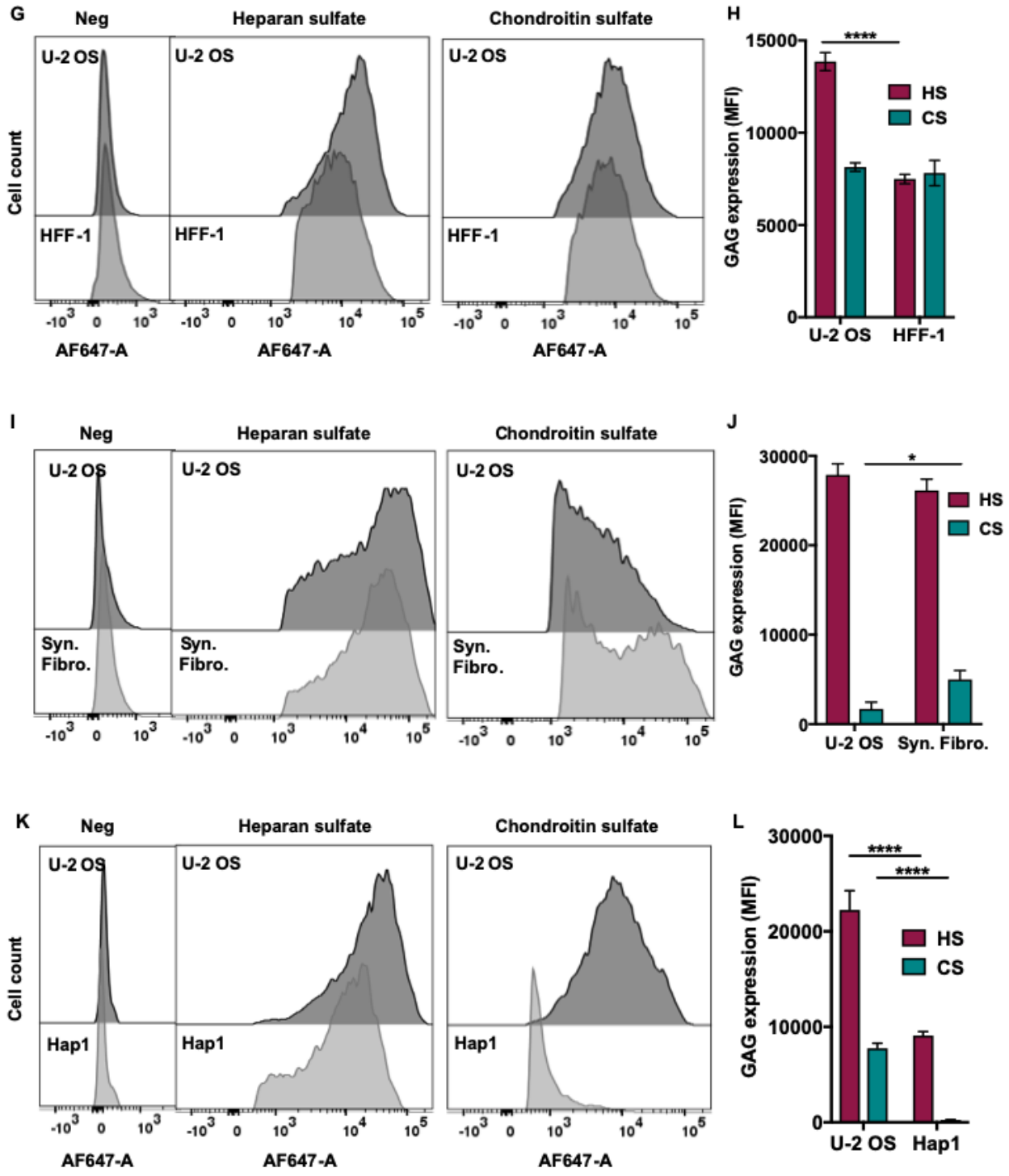

Figure 16. U-2 OS cells express relatively high levels of GAGs.

(A-L) U-2 OS, (A and B) BHK, Vero, (C and D) 3T3, (E and F) BV-2, (G and H) HFF-1, (I and J) synovial fibroblast, and (K and L) Hap1 cells were stained with antibodies specific for HS or CS, followed by Alexa-647 antibody. Cells were fixed with 4% PFA, and median fluorescence intensity (MFI) was quantified using flow cytometry. (A, C, E, G, I, K) Representative flow cytometric plots and (B, D, F, H, J, L) quantification of GAG profiles for triplicate wells from two-to-three independent experiments are shown. Data were normalized to secondary-antibody-only negative controls. Error bars indicate SEM. *P* values were determined by two-way ANOVA followed by Tukey's multiple comparison test (*, $P < 0.05$; **, $P < 0.01$; ***, $P < 0.001$; ****, $P < 0.0001$).

Mxra8 expression on mouse and human cell lines was analyzed using an approach analogous to that used to characterize GAG expression. U-2 OS cells express relatively high levels of Mxra8 (Figure 17). In contrast, 3T3 and Hap1 cells express little to no Mxra8 (Figure 17). Of the cell lines tested, we identified a cell line with high HS, CS, and Mxra8 expression (U-2 OS cells) as well as two cell lines that express high HS levels and little to no CS or Mxra8 (3T3 and Hap1 cells). These cell lines were used to define the requirement of GAGs and Mxra8, when expressed independently or together, for CHIKV binding and infection.

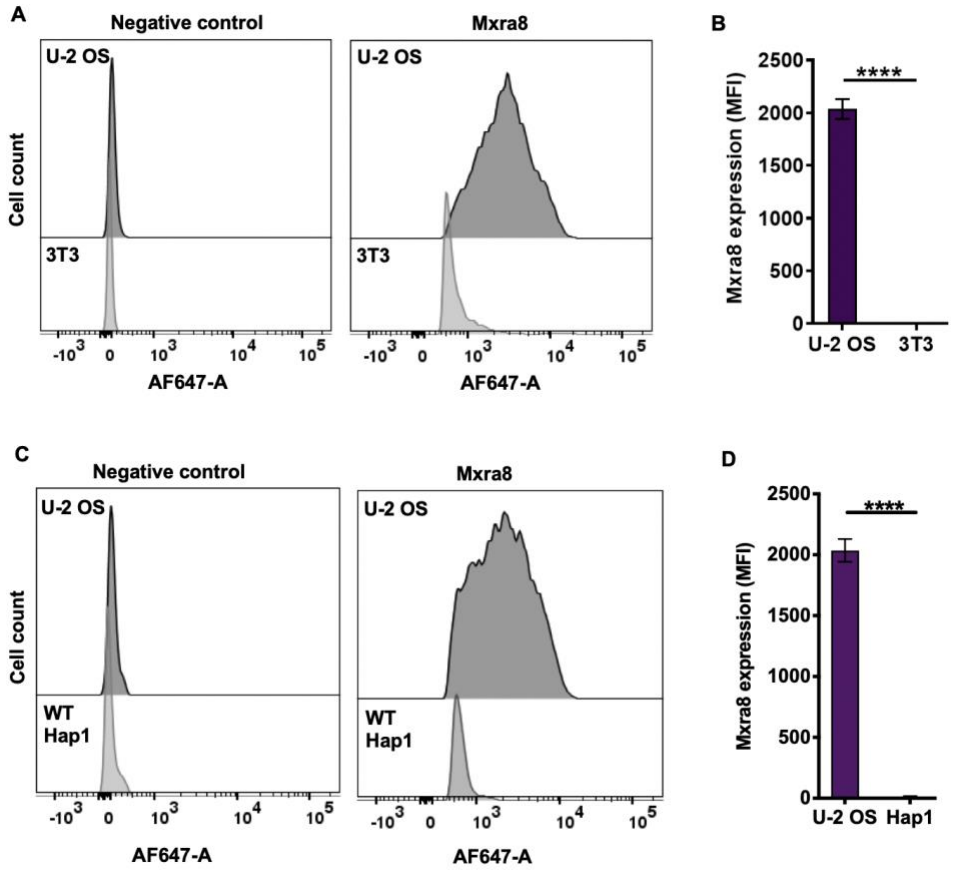

Figure 17. U-2 OS cells express relatively high levels of Mxra8.

(A-D) U-2 OS, (A and B) 3T3, and (C and D) Hap1 cells were stained with antibodies specific for Mxra8, followed by Alexa-647 antibody. Cells were fixed with 4% PFA, and median fluorescence intensity (MFI) was quantified using flow cytometry. (A and C) Representative flow cytometric plots and (B and D) quantification of Mxra8 profiles for triplicate wells from three independent experiments are shown. Data were normalized to secondary-antibody-only negative controls. Error bars indicate SEM. *P* values were determined by two-way ANOVA followed by Tukey's multiple comparison test (**, $P < 0.01$; ****, $P < 0.0001$).

To assess CHIKV infection of the various cell lines characterized for receptor expression, we conducted FFU assays following infection of cells with the CHIKV attenuated strain 181/25 and ECSA strain SL15649 at various MOIs. CHIKV infected all cells tested (Figure 18). As

expected, infection with 181/25, which has increased *in vitro* infection capacity (67), resulted in the highest level of infection in all cell lines tested relative to SL15649 (Figure 18). U-2 OS and 3T3 cells were the most susceptible, with about 88% of 181/25 infected cells (MOI of 100 PFU/cell) and 84% of SL15649 infected cells (MOI of 25 PFU/cell) (Figure 18A and B). Similarly, 84% of HFF-1 cells were infected with 181/25 at a MOI of 25 PFU/cell (Figure 18E). Hap1 cells were infected less efficiently by both strains (Figure 18D). BV2 cells and synovial fibroblasts were least susceptible to 181/25 (Figure 18C and F). Overall, infection levels of 181/25 and SL15649 were the greatest in U-2 OS and 3T3 cells, followed by HFF-1 and Hap1 cells.

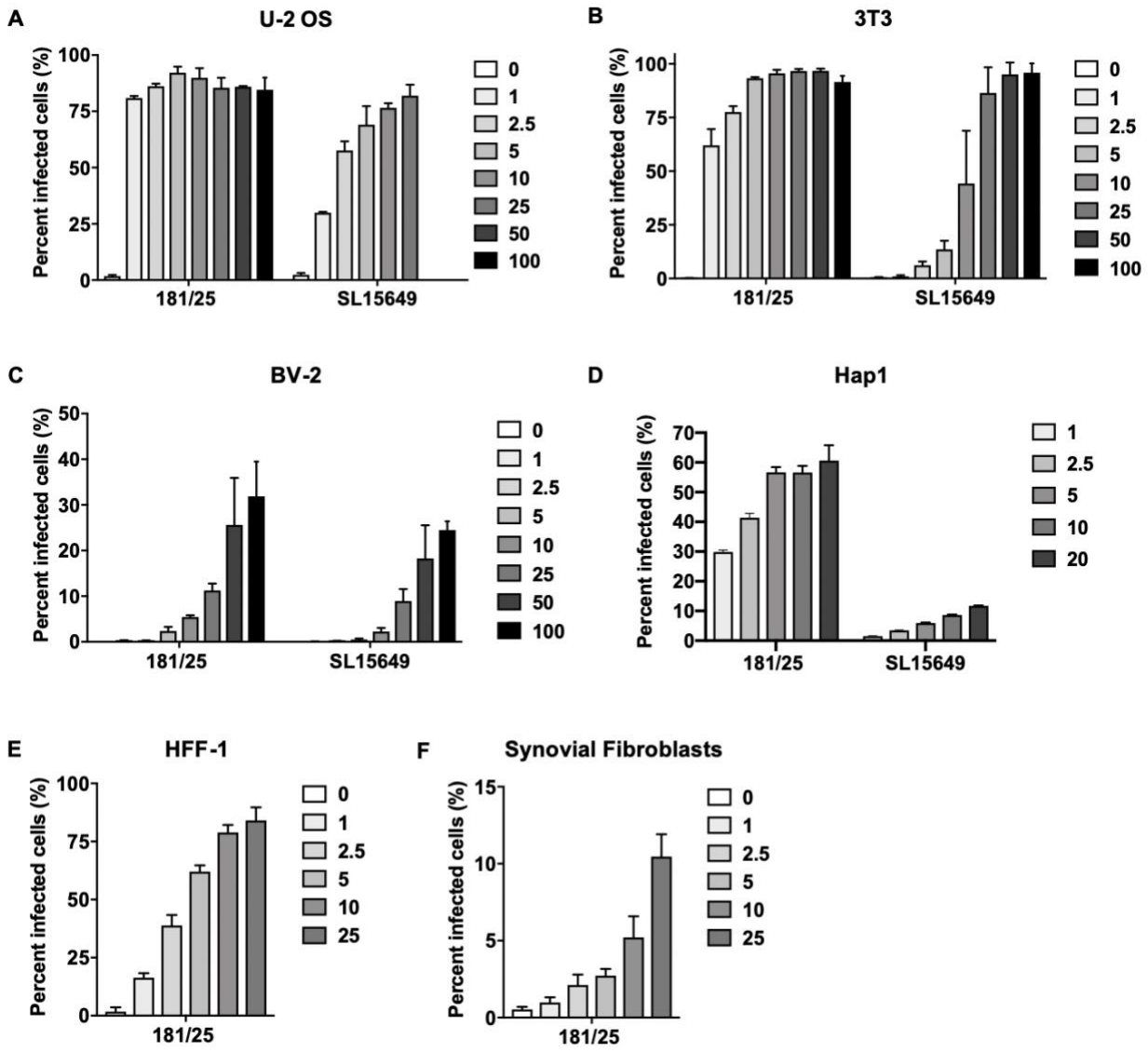

Figure 18. U-2 OS and 3T3 cells are most permissive to CHIKV.

(A) U-2 OS, (B) 3T3, (C) BV-2, (D) Hap1, (E) HFF-1, and (F) synovial fibroblast cells were adsorbed with CHIKV attenuated strain 181/25 or ECSA strain SL15649 at various MOIs. Cells were fixed with methanol at (A-C, E and F) 6 h post-adsorption or (D) 18 h post-adsorption. (A-F) The percentage of infected cells was determined using an immunofluorescence FFU assay. Results are expressed as the mean percentage of infected cells for four fields of view per well in triplicate wells from two independent experiments. Error bars indicate SEM.

Finally, to identify a cell type amenable to genetic disruption using CRISPR-Cas9 technology, I conducted a karyotyping analysis using ten G-banded metaphase spreads. Eight HFF-1 cell spreads had an apparently normal human male karyotype, while two spreads were tetraploid (Figure 19A and D). Each of the ten synovial fibroblast spreads had an abnormal and different karyotype with multiple rearrangements (Figure 19B and D). Dicentrics and marker chromosomes, which are structurally abnormal and ambiguous chromosomes, were present in eight of the synovial fibroblast spreads (Figure 19B and D). Two of the synovial fibroblast spreads contained decondensed, shredded chromosomes that were not amenable to counting (Figure 19B and D). The karyotype of U-2 OS cells also was abnormal. Each of the ten U-2 OS spreads had multiple rearrangements and marker chromosomes (Figure 19C and D). Nine U-2 OS spreads contained a single X chromosome, and one spread was devoid of any sex chromosomes (Figure 19C and D). Overall, HFF-1 cells are the only cell type tested with a normal diploid karyotype.

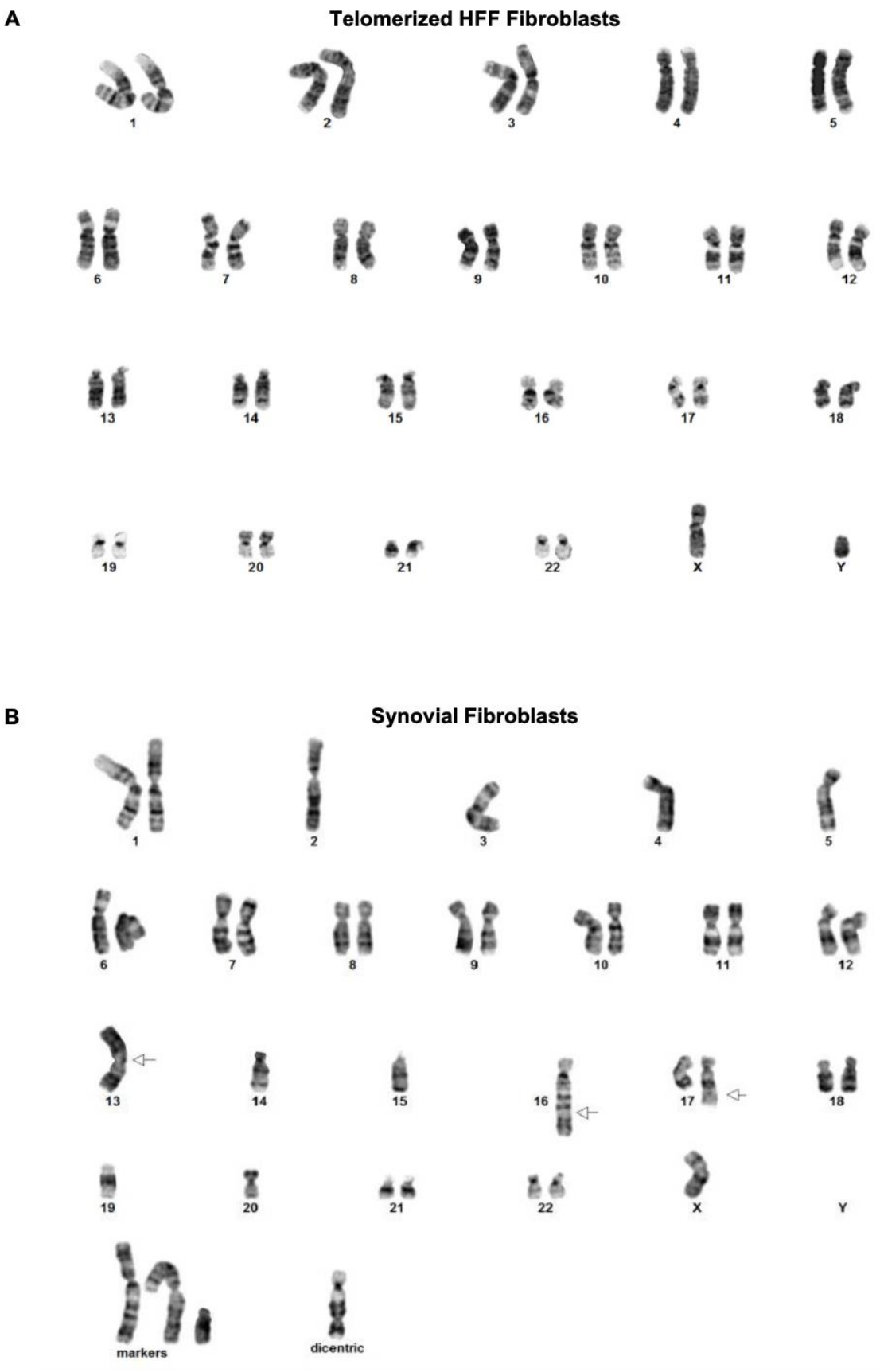
A
Telomerized HFF Fibroblasts
1
2
3
4
5
6
7
8
9
10
11
12
13
14
15
16
17
18
19
20
21
22
X
Y
B
Synovial Fibroblasts
1
2
3
4
5
6
7
8
9
10
11
12
13
14
15
16
17
18
19
20
21
22
X
Y
markers
dicentric

C

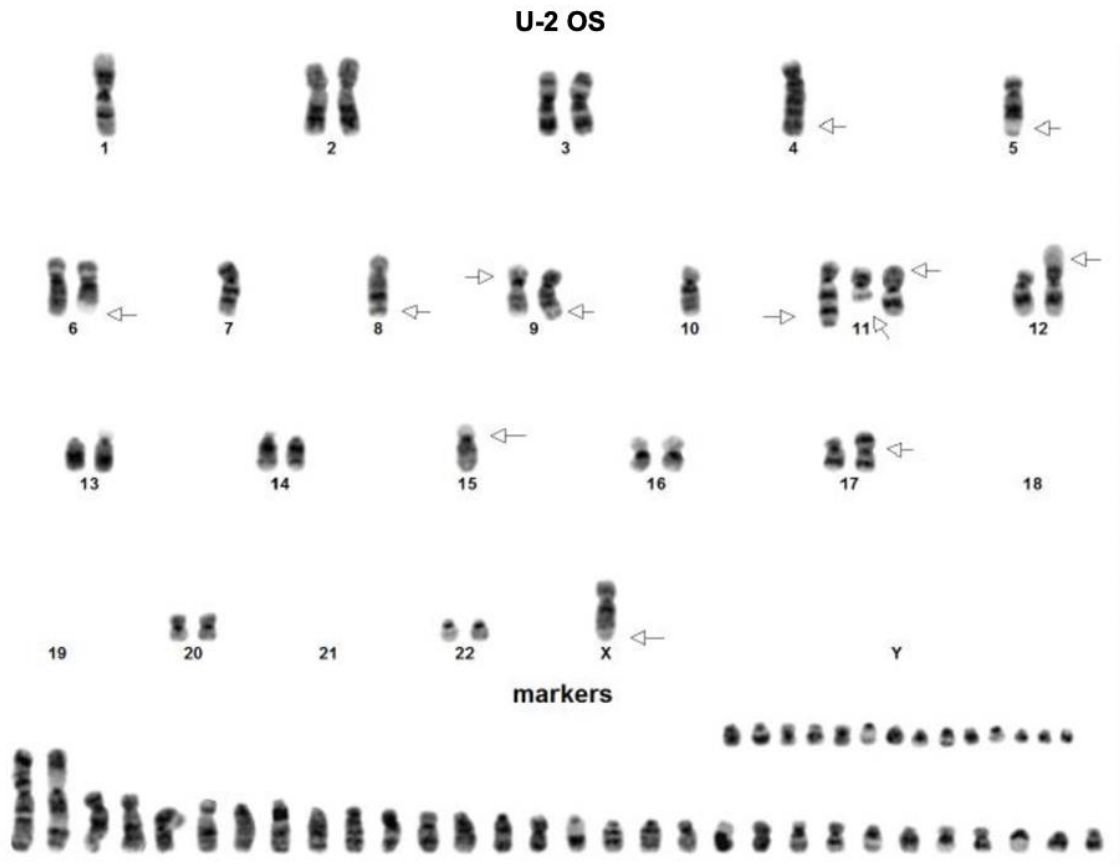

D

Cell Type	Summary of Karyotyping Results
HFF-1	8 spreads – apparently normal human male karyotype 2 spreads – tetraploid
Synovial fibroblasts	All spreads – abnormal, different karyotypes with multiple rearrangements 8 spreads – dicentrics and marker chromosomes 2 spreads – decondensed (shredded) chromosomes
U-2 OS	All spreads – multiple rearrangements and marker chromosomes 9 spreads – single X chromosome 1 spread – no sex chromosomes

Figure 19. Synovial fibroblasts and U-2 OS cells have abnormal karyotypes.

(A) HFF-1, (B) synovial fibroblast, and (C) U-2 OS cell preps were sent to KaryoLogic for cytogenetic analysis. Ten G-banded metaphase spreads were analyzed for ploidy. A representative karyotype of a full metaphase spread is shown

for each cell type. Arrows point to aberrant chromosomes with partial deletions or additions. Dicentrics indicate chromosomes that do not pass through mitosis, leading to genetic instability over time. Marker chromosomes are structurally abnormal chromosomes that cannot be unambiguously identified by conventional banding cytogenetics.

The characterization of mouse and human cell lines for GAG and Mxra8 expression, susceptibility to CHIKV, and karyotype were conclusive in identifying appropriate cells to test the requirement of GAGs for virus binding and infection. U-2 OS cells expressed the highest HS, CS, and Mxra8 levels (Figure 16 and 17) and were most susceptible to CHIKV infection relative to the other cells tested (Figure 18A), making them appropriate to assess the requirement of GAGs by CHIKV when the Mxra8 entry receptor is present. Hap1 cells expressed high levels of HS with no detectable CS or Mxra8 (Figure 16K and L; Figure 17C and D), making them appropriate to assess the requirement of HS by CHIKV in the absence of other known attachment factors and receptors. Additionally, the unique haploid nature of Hap1 cells (268) makes them more amenable to genetic alteration by CRISPR-Cas9, which is advantageous since the other cell types tested displayed multiploid and abnormal karyotypes (Figure 19). The following studies use U-2 OS and Hap1 cells to determine the requirement of GAGs for CHIKV binding and infection.

2.2.5 CHIKV binding and infection depends on GAG expression

Results obtained thus far demonstrate that multiple CHIKV strains bind GAGs *in vitro*. To determine whether CHIKV-GAG interactions contribute to binding and infection of cells, we treated U-2 OS cells with a combination of heparinases (HSase) or chondroitinases (CSase) and assessed the cells for GAG expression, virus binding, and virus infectivity. Treatment with HSase

I/II/III or CSase ABC specifically and efficiently reduced levels of cell-surface HS and CS, respectively (Figure 20A and B). Following GAG cleavage, Mxra8 expression did not change (data not shown). HS was required for efficient cell binding, as cleavage of HS reduced binding for all CHIKV strains studied (Figure 20C). As expected, binding of the attenuated 181/25 strain, which has enhanced HS binding capacity (66, 68), was reduced by 95% following HS cleavage (Figure 20C). Binding of the mosquito and clinical CHIKV strains was reduced by 23 to 44% following HS cleavage (Figure 20C). Cleavage of CS decreased binding of some CHIKV strains, with the ECSA strain reduced by 29%, a reduction greater than that observed for the other strains (Figure 20C). Additionally, cleavage of HS diminished infectivity of all CHIKV strains by 34 to 55% (Figure 20D). Cleavage of CS did not greatly affect infectivity (Figure 20D), suggesting an importance of HS, but not CS, for CHIKV infection of U-2 OS cells. These data indicate that all strains tested depend on HS to bind to cells, while some strains also depend on CS for efficient cell attachment. Efficient infection of U-2 OS cells requires HS binding.

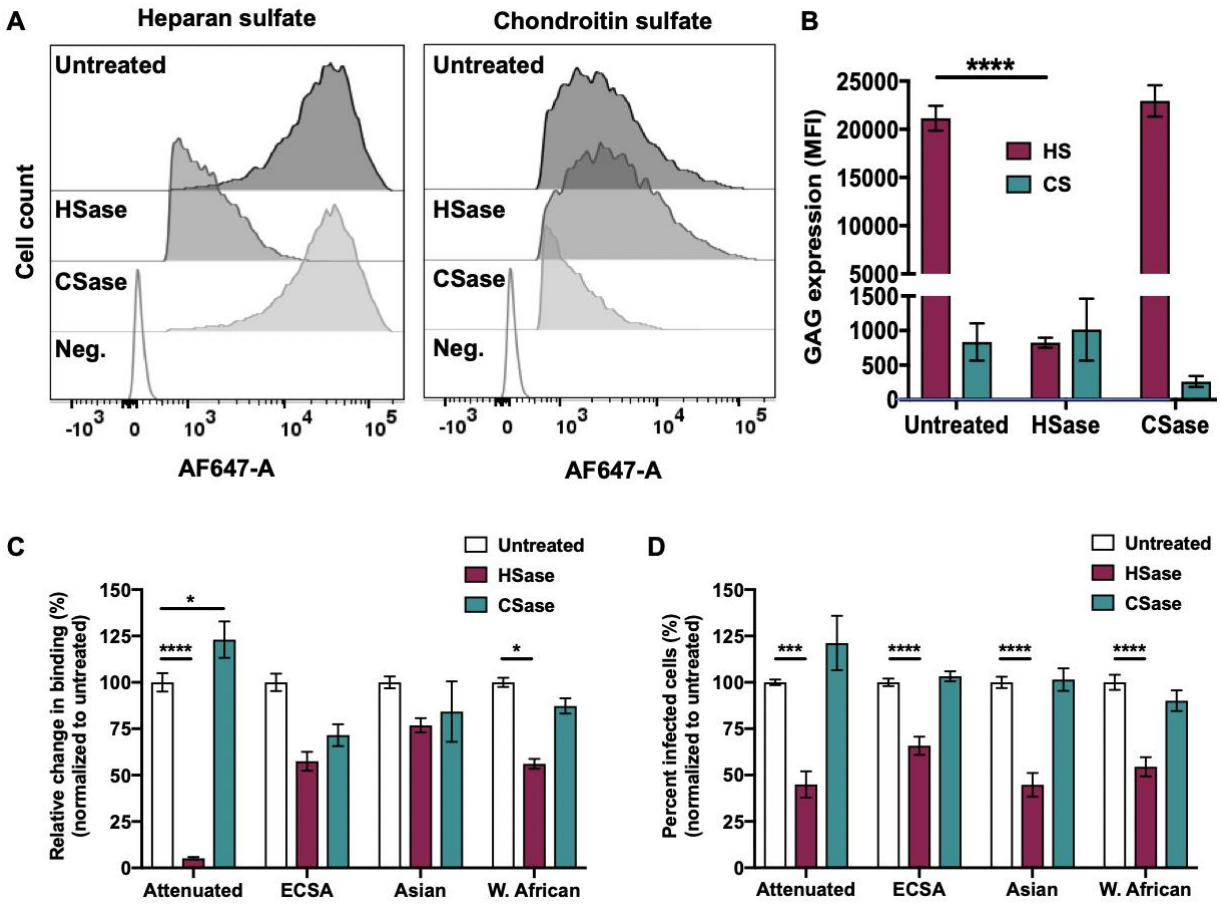

Figure 20. Enzymatic cleavage of HS reduces binding and infection of CHIKV.

(A-D) U-2 OS cells were treated with a combination of heparinases (HSase I/II/III) or chondroitin sulfatases (CSase ABC) at a final concentration of 2 mIU/mL. (A and B) Cells were stained with antibodies specific for HS or CS, followed by Alexa-647 antibody. Cells were fixed with 4% PFA, and MFI was quantified using flow cytometry. (A) Representative flow cytometric plots and (B) quantification of GAG profiles for duplicate wells from three independent experiments. Data were normalized to secondary-antibody-only negative controls. (C) U-2 OS cells were adsorbed with 10^8 genomes/sample of the CHIKV strains shown at 4°C for 2 h and washed three times to remove unbound virus. Total RNA was purified using TRIzol, and CHIKV RNA was quantified using RT-qPCR. (D) U-2 OS cells were adsorbed with the attenuated CHIKV strain (181/25) at an MOI of 1 PFU/cell and the ECSA (SL15649), Asian (H20235), and W. African (37997) strains at an MOI of 5 PFU/cell. Cells were fixed with methanol at 18 h post-adsorption, and the percentage of infected cells was determined using an immunofluorescence FFU assay. (C and D) Data were normalized to untreated controls. Results are expressed as (C) mean percentage of binding in triplicate wells from three independent experiments and (D) mean percentage of infected cells for four fields of view per well

in triplicate wells from three independent experiments. (B-D) Error bars indicate SEM. *P* values were determined by (B) two-way ANOVA followed by Tukey's multiple comparison test or (C and D) one-way ANOVA followed by Tukey's multiple comparison test (*, $P < 0.05$; ***, $P < 0.001$; ****, $P < 0.0001$).

To investigate the requirement of HS for efficient CHIKV cell binding and infection when Mxra8 and CS are absent, we used human haploid Hap1 cells. Wild-type (WT) Hap1 cells abundantly express HS and have low to no expression of CS and Mxra8 (Figures 16 and 17). These features make Hap1 cells suitable for studies to determine whether HS is required for CHIKV binding and infection in the absence of other known attachment factors and receptors. Due to their haploid nature, Hap1 cells also are more amenable to genetic alteration. We used *B3GAT3*$^{-/-}$ Hap1 cells, engineered using CRISPR-Cas9 technology (100), that have a targeted disruption of the *B3GAT3* gene, which encodes beta-1,3-glucuronyltransferase 3 (B3GAT3). B3GAT3 catalyzes the transfer of glucuronic acid to galactose, which is a required step in the biosynthesis of heparin, HS, and CS/DS (231). Compared with WT Hap1 cells, *B3GAT3*$^{-/-}$ cells exhibit diminished GAG expression (Figure 21A and B). However, neither WT Hap1 cells nor B3GAT3-/- cells express detectable levels of Mxra8 (data not shown). *B3GAT3*$^{-/-}$ cells complemented with a B3GAT3-expressing plasmid display GAG expression comparable to WT levels (Figure 21A and B). WT, *B3GAT3*$^{-/-}$, and complemented *B3GAT3*$^{-/-}$ cells were tested for CHIKV binding and infection. Binding of all CHIKV strains tested to *B3GAT3*$^{-/-}$ cells was reduced by 74 to 97% compared with binding to WT cells, and complementation of the *B3GAT3*$^{-/-}$ cells restored binding by 43 to 82% (Figure 21C). Infection of *B3GAT3*$^{-/-}$ cells by all CHIKV strains tested was diminished by 92 to 100% relative to WT cells (Figure 21D). Complementation of *B3GAT3*$^{-/-}$ cells with *B3GAT3* partially restored infection (Figure 21D). The lack of full restoration of binding and infection to

WT levels after complementation of *B3GAT3*$^{-/-}$ cells may be due to differences in HS expression by WT and complemented *B3GAT3*$^{-/-}$ cells (Figure 21A). Overall, these data indicate that CHIKV requires HS for binding to and infection of Hap1 cells and emphasize the importance of HS as a CHIKV attachment factor when other ligands like CS or Mxra8 are absent.

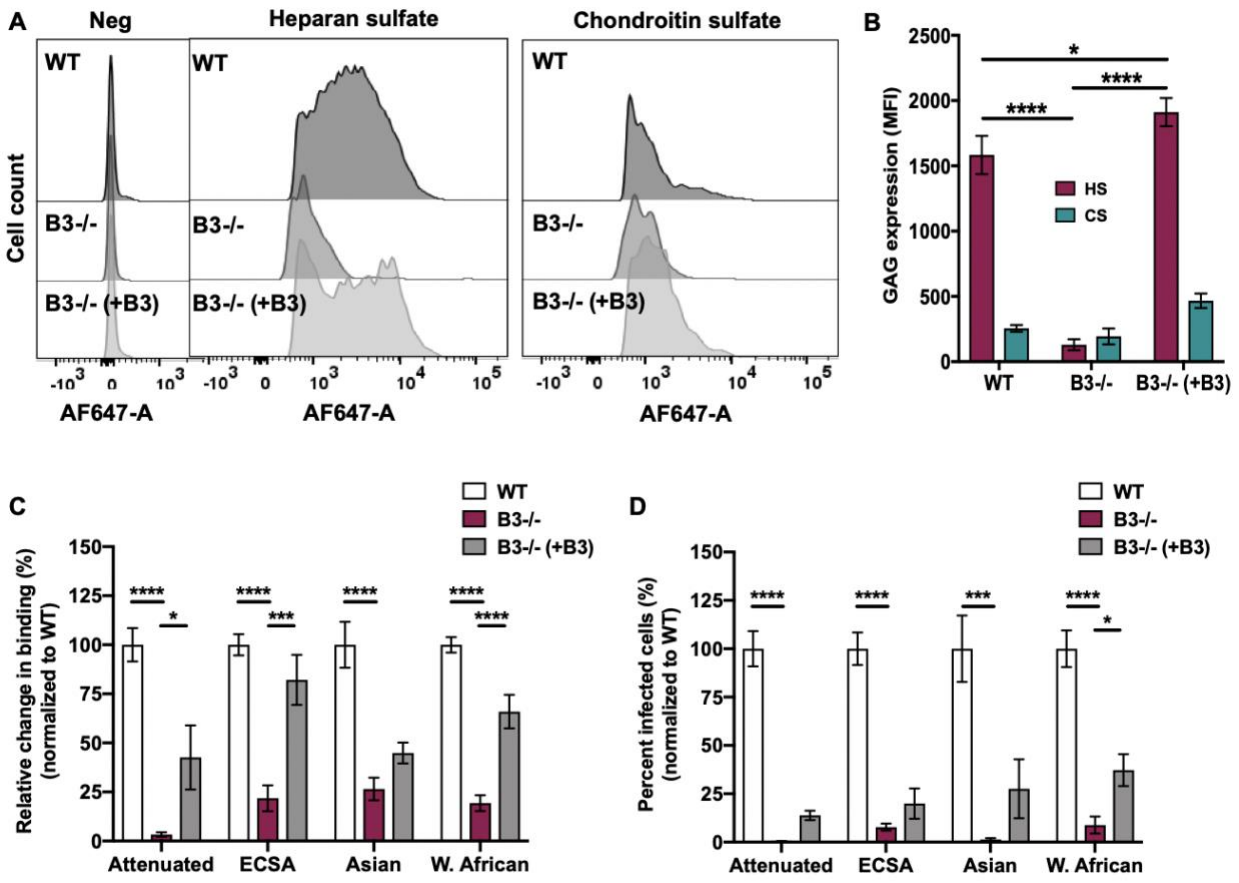

Figure 21. Genetic disruption of GAG biosynthesis reduces CHIKV binding and infection.

(A and B) WT, *B3GAT3*$^{-/-}$, and complemented *B3GAT3*$^{-/-}$ Hap1 cells were stained with antibodies specific for HS or CS, followed by Alexa-647 antibody. Cells were fixed with 4% PFA, and MFI was quantified using flow cytometry. (A) Representative flow cytometric plots and (B) quantification of GAG profiles for triplicate wells from three independent experiments. Data were normalized to secondary-antibody-only negative controls. (C) WT, *B3GAT3*$^{-/-}$, and complemented *B3GAT3*$^{-/-}$ Hap1 cells were adsorbed with 10^8 genomes/sample of the virus strains shown at 4°C for 2 h and washed three times to remove unbound virus. Total RNA was purified using TRIzol, and CHIKV RNA was quantified using RT-qPCR. (D) WT, *B3GAT3*$^{-/-}$, and complemented *B3GAT3*$^{-/-}$ Hap1 cells were adsorbed with the attenuated CHIKV strain (181/25) at an MOI of 2.5 PFU/cell and the ECSA (SL15649), Asian (H20235), and W. African (37997) strains at an MOI of 10 PFU/cell. Cells were fixed with methanol at 18 hpi, and the percentage of infected cells was determined using an immunofluorescence FFU assay. (C and D) Data were normalized to WT cells. Results are expressed as (C) mean percentage of binding in triplicate wells from three independent experiments and (D) mean percentage of infected cells for four fields of view per well in triplicate wells from two independent

experiments. (B-D) Error bars indicate SEM. *P* values were determined by (B) two-way ANOVA followed by Tukey's multiple comparison test or (C and D) one-way ANOVA followed by Tukey's multiple comparison test (*, $P < 0.05$; ***, $P < 0.001$; ****, $P < 0.0001$).

2.3 Discussion

The specific glycans used by different strains of CHIKV as attachment factors have not been well understood. In this chapter, I report that sulfated GAGs are the glycans preferentially bound by CHIKV. The strongest binding occurred with HS and heparin, followed by CS. All human- and mosquito-isolated CHIKV strains tested directly bound to heparin and CS. HS was required for efficient binding and infection of U-2 OS and Hap1 cells, while CS was required only by some strains to efficiently attach to U-2 OS cells. Moreover, the requirement of GAGs for CHIKV binding and infection inversely correlated with levels of Mxra8 receptor expression. Collectively, these data suggest that HS, and to a lesser extent CS, function as attachment factors for several CHIKV strains.

CHIKV displays broad cell, tissue, and species tropism (8, 133), which may correlate with the attachment factors or entry receptors used by the virus. Previous studies, as well as this work, identified sulfated GAGs as CHIKV attachment factors (66, 99, 100) (Figure 20 and 21). These glycans are ubiquitously expressed in humans and mosquitoes (226, 231, 232), including the specific cells and tissues that CHIKV infects. Many pathogenic viruses, including viruses in the alphavirus family (203–206, 213, 221) as well as other virus families (207–212, 214, 269–272), bind GAG attachment factors to attach to cells. For example, enterovirus 71 (EV-71), which displays broad tissue tropism (273) like CHIKV, specifically binds HS as an attachment factor

(214). An alphavirus, eastern equine encephalitis virus, also binds HS attachment factors (204). Strains of both EV-71 and eastern equine encephalitis virus with enhanced HS binding capacity csn display broadened tissue tropism and enhanced virulence (203, 204, 274). Thus, GAG attachment factor binding can influence viral tropism and virulence.

Although GAGs are CHIKV attachment factors, the specific GAG structures required for CHIKV binding had not been defined. GAG types and structures vary in different cells, tissues, and organisms, and the interactions between GAGs and proteins are often mediated by the structural characteristics of GAG chains. GAG types differ in their composition of repeating disaccharide units, which can facilitate specific interactions with chemokines, growth factors, enzymes, and viral proteins (199, 240, 275). The glycan microarray analyses we conducted identified sulfated GAGs as the primary glycan type bound by chikungunya VLPs (Figure 13) with HS and heparin most strongly bound (Figure 14). Similarly, binding signals were generally lower in the CS ELISAs relative to the heparin ELISAs, suggesting a preference of CHIKV for binding to heparin (Figure 15). On the glycan microarrays, some weak binding also was detected to non-GAG glycans, which may prompt further investigation into these CHIKV-glycan interactions. Interestingly, the iduronic acid-containing GAGs, HS, heparin, and CS-B (DS), which are abundantly expressed in cells and tissues infected by CHIKV (226, 231, 232, 236, 244–247), had the highest binding signals with VLPs relative to other GAGs tested (Figure 14). This is reminiscent of the GAG binding properties of respiratory syncytial virus (RSV), which require iduronic acid-containing GAGs for *in vitro* infection (212).

GAG oligosaccharide chain length is another important structural characteristic that influences binding to many ligands, including chemokines, growth factors, tau aggregates, and viral proteins (276, 277). We found that longer, sulfated GAGs are generally bound more

efficiently by CHIKV (Figure 13 and 14). VLPs bound more efficiently to longer rather than shorter chains of almost every GAG type (Figure 15). The requirement of longer GAG chains for virus binding has been observed for many viruses (271, 272, 278–280). For example, RSV requires heparin with a minimum 10-mer chain for efficient binding (271), and Zika virus preferentially binds 8- to 18-mer heparin chains (272). Further investigation is required to determine the optimum chain length required for each GAG type to promote binding of different CHIKV strains.

Sulfation modifications along the GAG chain also regulate ligand binding (281). Our studies indicate that the degree of sulfation is an important factor in CHIKV-GAG binding, which is consistent with previous findings, demonstrating that N-sulfation of HS chains is required for CHIKV infection *in vitro* (100). VLPs bound to all sulfated GAGs and dextran sulfate but not to hyaluronan or dextran, which are unsulfated glycans (Figure 14). GAG sulfation also influences the binding of several other viruses (269–271, 282–284). In fact, specific sulfation modifications on HS chains are important for virus-GAG interactions, such as 3-O sulfation for herpes simplex virus 1 (283, 284) and N-sulfation for RSV (271). Although we found that sulfation of GAG chains is required for CHIKV binding, the specific sulfation patterns necessary for CHIKV engagement remain unknown. Given that expression of many sulfation-modifying enzymes is tissue-specific (233, 285, 286), identifying the specific modifications necessary for CHIKV binding could enhance our understanding of its tropism and help define more specific cell-attachment inhibitors. Collectively, our glycan microarray analyses suggest that CHIKV most efficiently binds longer, sulfated GAGs with a preference for HS and heparin. As GAG mimetics are a possible therapeutic for alphavirus and flavivirus disease (287–290), understanding the unique GAG sequences required for efficient CHIKV binding may foster development of new classes of GAG-based antiviral agents.

In addition to identifying specific GAGs bound by CHIKV, we evaluated strain-specific differences in GAG attachment during infection of cells. Strain differences have been observed in CHIKV tropism and virulence (58, 67, 291). Therefore, it is important to know whether CHIKV strains also differ in attachment factor binding, which often is a determinant of tropism and virulence. Several cell-culture-adapted alphaviruses (223, 225, 292), including CHIKV strain 181/25 (66, 67, 165), bind strongly to GAGs. GAG binding was previously thought to be attributable to a cell-culture adaptation that was dispensable for infection by naturally circulating alphavirus strains. However, evidence has accumulated supporting a role for GAG binding by clinically relevant, non-culture-adapted alphaviruses (66, 67, 204–206, 213). Using viruses that were minimally passaged in culture, we discovered that the ECSA strain bound most efficiently to heparin and CS (Figure 15) and was the only strain that required both HS and CS expression to efficiently bind to U-2 OS cells (Figure 20C). In contrast, the Asian strain bound less efficiently to GAGs (Figure 15), and virus binding was least affected by HS cleavage on U-2 OS cells (Figure 20C) and the absence of HS on Hap1 *B3GAT3*$^{-/-}$ cells (Figure 21C). These results parallel the requirement for Mxra8 utilization for infection of fibroblasts *in vitro*, with Asian and ECSA strains showing full and partial Mxra8-dependence for infection, respectively (102). Similarities between the strains also were observed. All CHIKV strains tested required HS to efficiently bind and infect U-2 OS and Hap1 cells (Figure 20 and 21). Interestingly, following HS cleavage of U-2 OS cells, residual CHIKV binding (56-77%) and infection (44-66%) was observed (Figure 20C and D). However, residual CHIKV binding to (19-26%) and infection of (1-9%) Hap1 *B3GAT3*$^{-/-}$ cells was significantly less (Figure 21C and D). The low expression of Mxra8 and CS on Hap1 cells compared to U-2 OS cells may influence the observed differences in residual binding and infection. These data suggest that although HS is required for efficient CHIKV binding and infection, the

magnitude of the requirement is inversely correlated to the abundance of entry receptor expression. Additionally, the residual binding to and infection of Hap1 *B3GAT3*$^{-/-}$ cells, which express little to no GAGs or Mxra8, suggests the presence of an unidentified cell-surface molecule engaged by CHIKV or a route of viral entry other than receptor-mediated endocytosis.

Findings reported in this chapter contribute to an understanding of the interactions between CHIKV and the cell-surface molecules that promote virus attachment. We have identified specific GAG types to which CHIKV binds as well as differences in the binding efficiency of CHIKV to specific GAGs. Using clinically relevant CHIKV strains, we discovered strain-specific differences in GAG binding and the requirement of GAGs for attachment and infection of cultured cells. Our data demonstrate that multiple strains of CHIKV bind HS and CS as attachment factors, likely promoting initial cell attachment and allowing the virus to concentrate at the cell surface before engaging entry receptors. CHIKV interactions with widely expressed GAGs may contribute to the broad cell, tissue, and species tropism observed for CHIKV. Overall, findings reported here define critical interactions between CHIKV and GAG attachment factors and improve understanding of the multistep process of cell attachment for CHIKV.

3.0 Residues in the CHIKV E2 glycoprotein domain A, domain B, and arch are required for GAG binding

3.1 Introduction

The structural requirements of GAG-protein interactions are complex. GAG chain structure, including sulfation, disaccharide composition, and length are important characteristics that influence ligand binding (242, 276, 293, 294). The pattern of sulfation modifications on GAG chains is referred to as the sulfation code, which is key to ligand recognition. The organization and pattern of sulfated and unsulfated domains of GAG chains contributes to the specificity of protein binding (242). For example, endostatin-HS engagement requires HS chains with two N-sulfated regions separated by at least one unsulfated GlcNAc monosaccharide (295). Specific sulfation modifications also regulate virus-GAG binding. N-sulfation of HS is required for CHIKV and respiratory syncytial virus binding (271), and 3-O sulfation of HS is required for herpes simplex virus 1 binding (283, 284).

Disaccharide composition and sulfation both contribute to the internal mobility of GAG chains. The combination of unsulfated domains and the presence of IdoA residues promotes chain flexibility. The variable flexibility of different regions of a GAG chain can influence protein binding and allow for multiple ligand interactions to occur on the same GAG chain (293, 294, 296). IdoA is required for efficient GAG binding to several proteins, such as fibroblast growth factors (297), respiratory syncytial virus (212), and CHIKV (224) (Figure 14).

GAG chain length also plays a role in the binding of proteins, such as chemokines, growth factors, tau aggregates, and viral proteins (276, 277). Data presented in Chapter 2 indicate that

longer, sulfated GAGs are generally bound more efficiently by CHIKV (224) (Figure 14). Additionally, respiratory syncytial virus requires heparin with a minimum 10-mer chain for efficient binding (271), and Zika virus preferentially binds 8- to 18-mer heparin chains (272).

Structural features of protein binding partners of GAGs also influence the affinity of protein-GAG interactions. Consensus sequences have been identified as common, evolutionarily conserved protein motifs that mediate GAG binding (293). The CW motif, named for the scientists who discovered this sequence (Cardin and Weintraub), is found in heparin and HS-binding proteins. The CW consensus sequences are X-B-B-X-B-X and X-B-B-B-X-X-B-X, where B is an arginine or lysine residue and X is a hydrophobic amino acid. Specific arrangements of these residues in protein secondary structures are important for GAG-protein interactions. Beta-strand and alpha-helical structures containing CW sequences are structured with basic amino acids aligned on one face of the strand or helix and hydrophobic amino acids on the other, pointing into the protein core (298). The three-dimensional arrangement of basic amino acids also influences binding. An analysis of 437 heparin-binding proteins revealed the presence of short, widely-spaced GAG-binding consensus sequences throughout heparin-binding proteins instead of longer conserved sequences. This analysis suggests that the three-dimensional arrangement of consensus sequences is the evolutionarily conserved element rather than the primary sequences of basic amino acids, emphasizing the importance of placement of consensus GAG-binding sequences in the tertiary structure of a protein (299).

In addition to the positively charged arginine, lysine, and histidine residues of GAG-binding consensus sequences, other uncharged, polar residues like asparagine and glutamine also can influence GAG binding (293, 300). Whereas the ionic interactions between positively charged amino acids and negatively charged GAGs are clearly important, non-ionic binding between GAGs

and their ligands can contribute to protein-GAG engagement (242, 301, 302). Hydrogen bonding by uncharged residues like asparagine and glutamine can mediate GAG-protein interactions (293, 300). Computational, biochemical, and structural data have confirmed the requirement of asparagine and glutamine in several GAG-binding proteins (300). Furthermore, a conserved structural motif composed of one polar residue, such as asparagine and glutamine, and two basic residues, such as arginine and lysine, was identified in heparin-binding proteins. The spatial arrangement of the three residues dictates specific distances between basic (cationic) and polar residues. This cation-polar-cation (CPC) motif is the minimum structural requirement for the heparin-binding proteins (303).

Overall, the interactions between GAGs and proteins are complicated and driven by structural features of both molecules. Depending on the protein, GAG binding can be non-specifically mediated by charge, which is observed with HS-thrombin interactions (242, 304). Alternatively, GAG-protein interactions can be specific, requiring particular sulfation modifications or residues. This specific interaction with GAGs is observed for fibroblast growth factor, anti-thrombin, interleukin-8, and interferon-gamma (242, 305–308).

The research described in this chapter was a collaborative project. The structural analysis identifying basic, surface-exposed residues on the CHIKV trimer was conducted by Dr. Laurie Silva. The infectious clone of SINV-CHIKV chimera, consisting of the CHIKV LR2006-OPY structural cassette, was provided by William Klimstra, and Adam Brynes assisted in the cloning of the SINV-CHIKV chimera to incorporate the CHIKV SL15649 structural cassette. Dr. Anthony Lentscher, Adam Brynes, and Abby Orzechowski assisted in the design and generation of single alanine mutant viruses, as well as the quantification (Table 4) and characterization of mutant

viruses (Figures 25, 26, and 28). James Martin and Elana Lancia also assisted in virus quantification (Table 4).

3.2 Results

3.2.1 Structural analysis of the CHIKV trimer

The specific CHIKV residues that mediate virus-GAG interactions are not known. As a first step to define regions of the virion that contact GAG chains, I analyzed the structure of the CHIKV trimer and compared these observations to findings made in mutagenesis studies with CHIKV and other alphaviruses. The CHIKV E2 glycoprotein mediates binding to receptors and attachment factors on the cell membrane (66, 67, 99, 218, 309, 310) and is the most solvent-exposed protein on the virion surface (27). We hypothesized that residues in E2 are most likely to interact with GAG chains. Furthermore, since negatively charged GAGs interact with positively charged amino acids, we sought to identify basic, surface-exposed residues of the CHIKV E2 glycoprotein that potentially bind GAG chains. Following this sequence and structural analyses, 38 basic, surface-exposed residues were identified in E2 (Figure 22A and B).

Regions of the CHIKV E2 glycoprotein that potentially mediate GAG interactions were previously identified in mutagenesis studies, including residues near E79 and G82 (66, 67, 165). When these residues are exchanged with a lysine or arginine, respectively, GAG-binding capacity is enhanced (66, 67, 165). Two surface-exposed, basic amino acids are located near residues 79 and 82 in the tertiary structure of CHIKV E2, R80 and R86, which have yet to be investigated for GAG binding. Molecular docking techniques suggest that residues R104, K107, and R144 in the

E2 glycoprotein domain A and arch interact with GAGs (218). Additionally, studies with other alphaviruses have provided clues about surface-exposed, positively-charged E2 residues that may be important for CHIKV-GAG binding. Mutation of SINV E2 N62 to aspartate decreases HS binding (229). This residue aligns with CHIKV E2 residue T65, which is located near several surface-exposed, basic residues in the E2 tertiary structure, including K57, H62, K66, and R68. A SINV E2 E70K mutation leads to increased HS binding (229). This residue aligns with CHIKV E2 residue N72, which is located adjacent to H73 in the E2 tertiary structure. A SINV E2 S114R mutation as well as VEEV E2 E117K and T120K mutations lead to increased HS binding (217, 220, 223). These residues align with CHIKV E2 residues G114, S118, and S122, respectively. There are several surface-exposed, basic residues in this region of E2, including R119, K120, H123, and H127. SINV E2 R157H and K159E mutations lead to decreased HS binding (229). These residues align with CHIKV E2 Q158 and T160, which are located near K140, R144, and K149. Finally, a SINV E2 K230M mutation causes decreased HS binding (229), and this residue aligns with CHIKV E2 V229, which is located near K200 and R267 in the tertiary structure of CHIKV E2 and near a CW heparin-binding consensus sequence located in E2 domain B from residues 250 to 255 (DRKGKI), which has been implicated in GAG binding (66). Overall, these analyses implicate 18 residues in the CHIKV E2 glycoprotein in GAG-binding (Figure 22C and D).

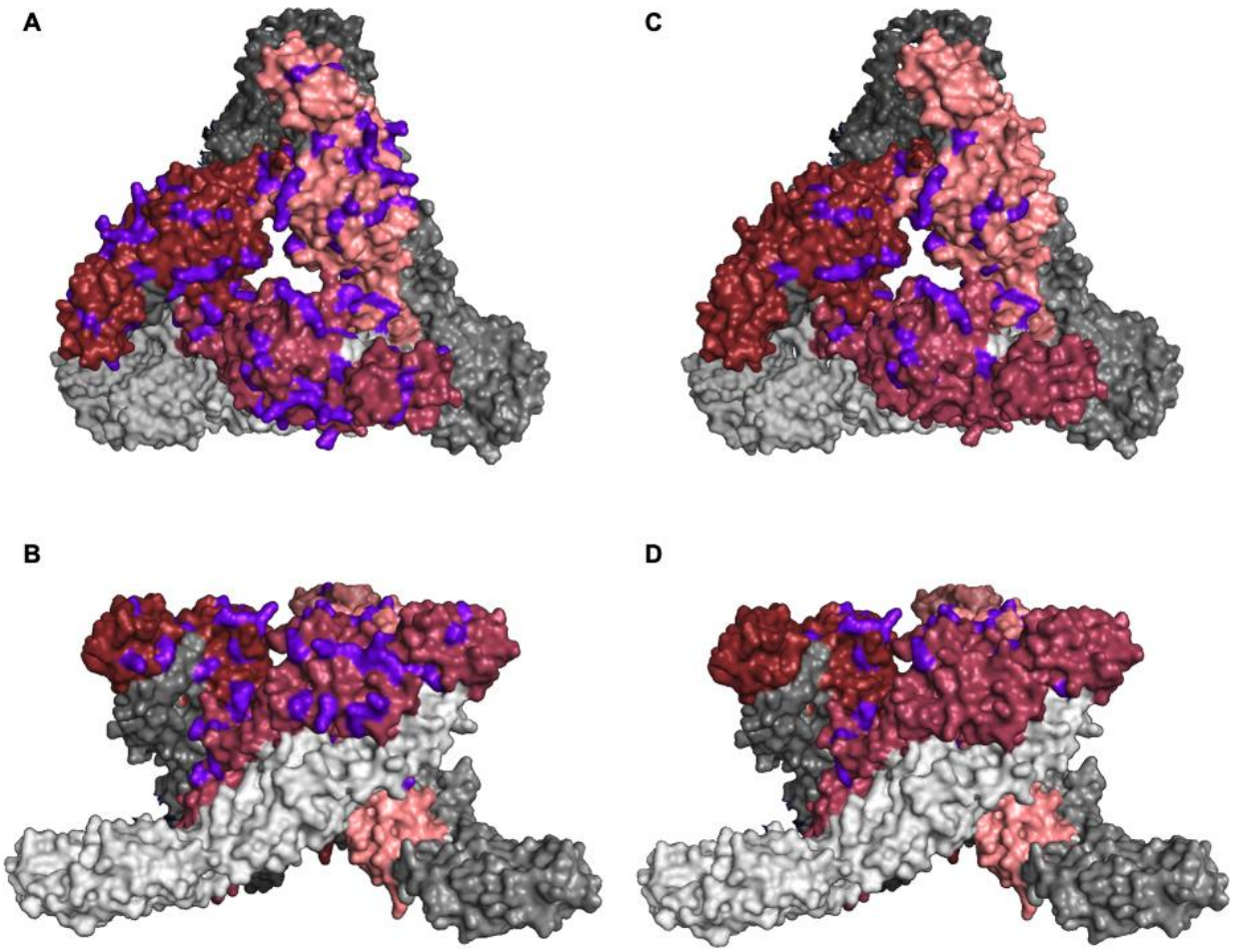

Figure 22. Structural analysis of CHIKV E1/E2 glycoprotein trimer.

(A and C) Top and (B and D) side view of the CHIKV E1/E2 trimer (E1, grey; E2, red). (A and B) All 38 basic, surface-exposed residues in E2 (SL15649 strain) are colored in purple. (C and D) The 18 putative basic, surface-exposed residues that will be tested for their function in GAG binding based on support from published mutagenesis studies using CHIKV and other alphaviruses are likewise colored in purple.

3.2.2 Alanine mutagenesis to recover single alanine mutant viruses

To determine whether the selected 18 putative E2 GAG-binding residues function in GAG interactions, I conducted alanine mutagenesis. Mutant viruses were engineered by individually exchanging the surface-exposed, basic E2 residues of interest with alanine (Figure 23). The 18 residues chosen for mutagenesis were basic, surface-exposed E2 residues that were supported by previously published studies with CHIKV and other alphaviruses. Alanine was used for substitution because of its small, nonpolar, aliphatic nature (311). Mutations were introduced into SINV-CHIKV chimeric viruses, consisting of the SINV non-structural proteins and the CHIKV (SL15649) structural proteins (102, 223) to enable studies using BSL-2 conditions.

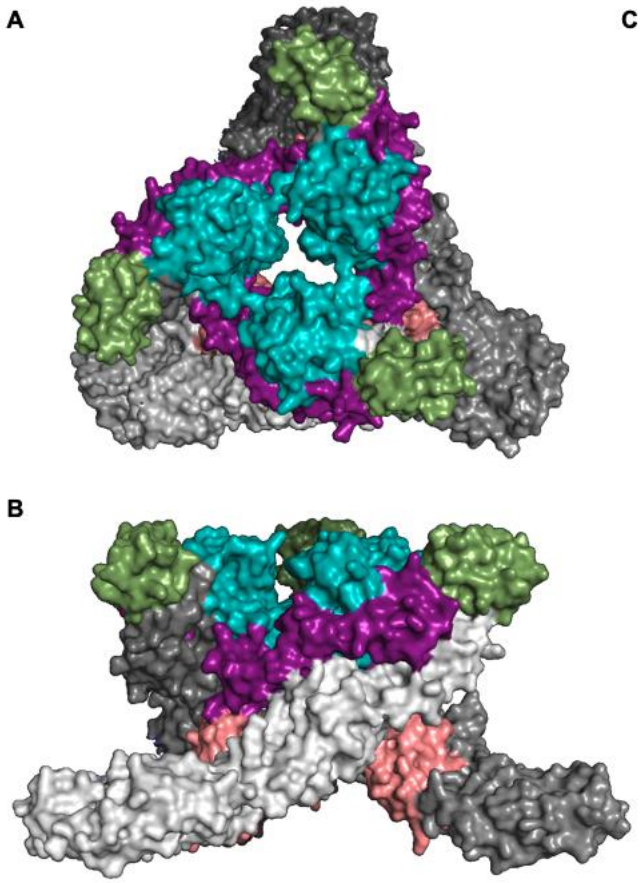

C

Mutation	E2 Region
K57A	Domain A
H62A	Domain A
K66A	Domain A
R68A	Domain A
H73A	Domain A
R80A	Domain A
R86A	Domain A
R104A	Domain A
K107A	Domain A
R119A	Domain A
K120A	Domain A
H123A	Domain A
H127A	Domain A
K140A	Arch
R144A	Arch
K149A	Arch
K200A	Domain B
R267A	Arch

Figure 23. Alanine mutant viruses engineered for this study.

(A) Top and (B) side view of the E1/E2 trimer structure (E1, grey; E2 domain A, blue; E2 domain B, green; E2 arch, purple; E2 domain C, pink). (C) Table of alanine mutant viruses.

Following alanine mutagenesis, stocks of each mutant virus were quantified for infectious virus particles (PFU/mL of culture supernatant) and number of genomes (genomes/mL of culture supernatant) (Table 4). Genome-to-PFU ratios were determined to quantify viral fitness. Higher ratios indicate that progeny virions are not as infectious. Unconcentrated WT virus had a genome/PFU ratio of 84.6 (Table 4). Similarly, K57A, H62A, K66A, R68A, and K107A had genome/PFU ratios ranging from 50.99 to 77.88 (Table 4). Lower genome/PFU ratios were

observed for R80A, R104A, R119A, K120A, and H123A, ranging from 2 to 11 times lower than the WT genome/PFU ratio (Table 4). In contrast, H73A, K144A, and R267A had slightly higher genome/PFU ratios, ranging from 1.2 to 1.7 times higher than WT genome/PFU ratio (Table 4). K140A had a genome/PFU ratio 2.8 times higher than WT genome/PFU ratio (Table 4). K149A and K200A had genome/PFU ratios approximately 3.5 times higher than WT genome/PFU ratio (Table 4). Mutant viruses R86A and H127A had the highest genome/PFU ratios, which were 11 and 46 times higher than the WT genome/PFU ratio, respectively (Table 4). Overall, most alanine mutants had similar or lower genome/PFU ratios relative to WT (K57A, H62A, K66A, R80A, R68A, R104A, K107A, R119A, K120A, and H123A). However, eight viruses (H73A, R86A, H127A, K140A, K144A, K149A, K200A, and R267A) had higher genome/PFU ratios relative to WT, with H127A having the highest ratio, indicating a reduction in viral fitness.

Table 4. Chimeric SINV-CHIKV alanine mutant viruses.

Virus	Genomes/mL	PFU/mL	Genome/PFU ratio
WT*	5.92E9	7.0E7	84.6
K57A	8.8E10	1.13E9	77.88
H62A	1.81E11	3.55E9	50.99
K66A	1.72E11	2.48E9	69.35
R68A	1.17E9	2.2E7	53.18
H73A	1.53E11	1.12E9	136.61
R80A	9.58E10	2.13E9	44.98
R86A	2.02E10	2.2E7	918.18
R104A	2.6E9	3.4E8	7.65
K107A	2.5E10	4.89E8	51.12
R119A	3.85E10	1.2E9	32.08
K120A	2.12E10	1.15E9	18.43
H123A	1.96E9	2.53E8	7.75
H127A	1.25E8	3.23E4	3869.97
K140A	1.69E11	7.08E8	238.70
R144A	6.87E10	6.8E8	101.03
K149A	3.28E11	1.08E9	303.70
K200A	1.95E11	6.68E8	291.92
R267A	9.36E10	6.59E8	142.03

*WT virus was the only virus that was unconcentrated. All other mutant viruses were concentrated according to Chapter 5.0 Material and Methods.

Mutant viruses were assessed for intact glycoprotein folding using ELISAs. Serial dilutions of virus were adsorbed to ELISA plates coated with a conformationally-specific monoclonal antibody (CHK-152), which binds across E2 domain A and B (312) (Figure 24), and bound virus

was quantified. Relative to WT virus as a control, all mutant viruses except R68A and H127A bound to CHK-152 antibody, suggesting that E2 glycoprotein conformation was intact despite the alanine substitution (Figure 25). While all but two mutants bound to CHK-152, variability in binding signal was observed. Some of the residues exchanged with alanine are located near CHK-152-binding sites in the E2 sequence, including K57, H73, R80, and K200 (Figure 24), which could affect recognition of these viruses by CHK-152. H73A, R80A, and K200A were among the many mutants that bound to CHK-152 less efficiently compared with WT virus (Figure 25). Overall, these data suggest that the alanine mutant viruses are structurally intact with the exception of R68A and H127A, which were not included in further analyses.

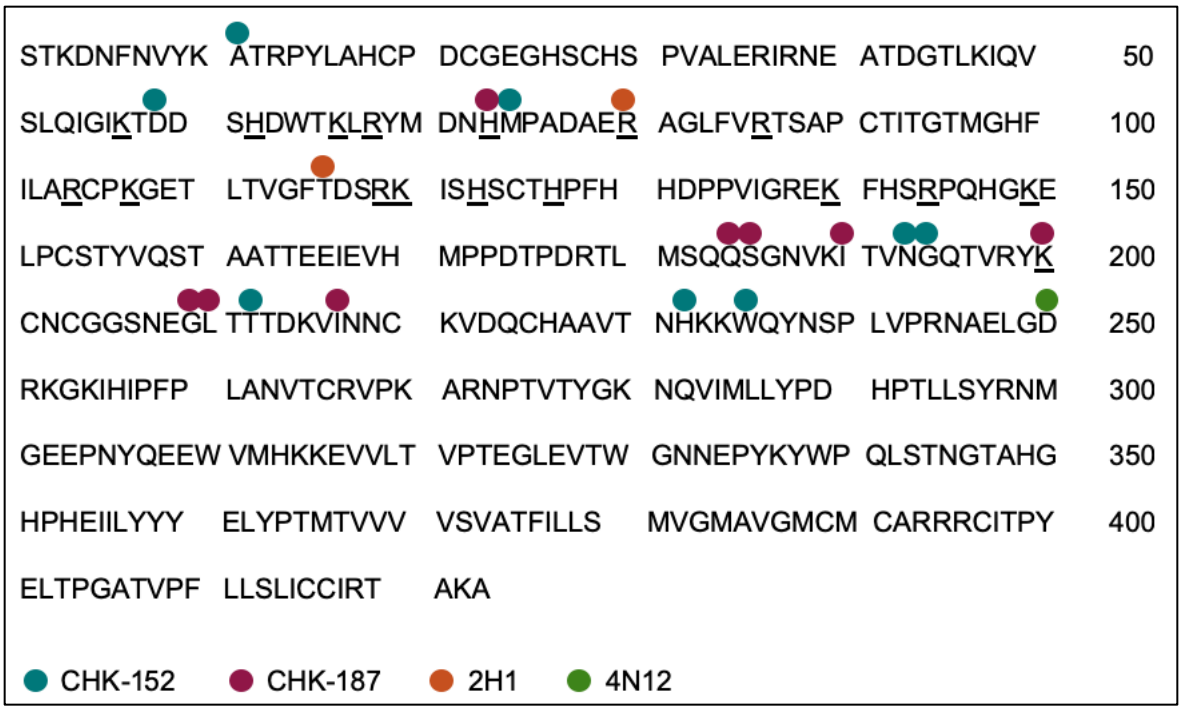

Figure 24. Antibody mapping in the E2 glycoprotein.

The mapped epitopes in the primary CHIKV (SL15649 strain) E2 glycoprotein sequence of mouse monoclonal antibody CHK-152 used in conformational ELISAs, mouse monoclonal antibody CHK-187 used in GAG ELISAs, and human monoclonal antibodies 2H1 and 4N12 used in conformational and Mxra8 ELISAs (312, 313). The 18 putative E2 residues selected for alanine mutagenesis are underlined.

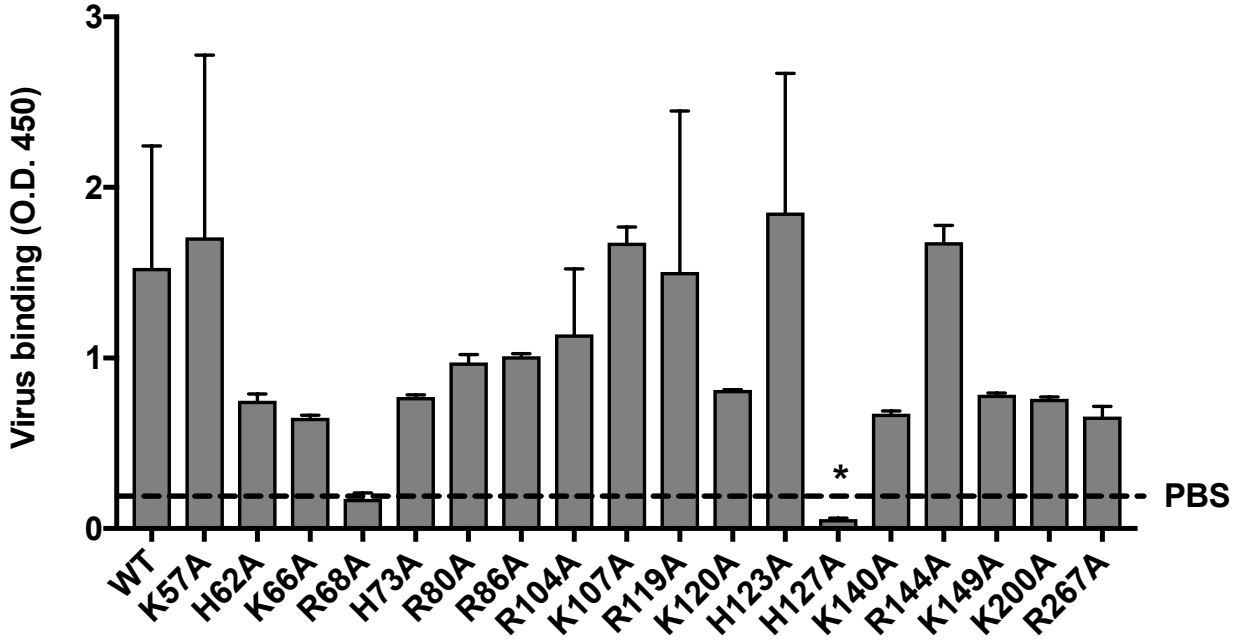

Figure 25. E2 alanine mutant viruses are recognized by a conformationally-specific antibody.

Equivalent genomes/mL of each virus (1.25E8) were adsorbed to ELISA plates bound with conformationally-specific anti-E2 antibody CHK-152. PBS was adsorbed to wells as a control. Following washes to remove unbound virus, virus binding was detected using a mixture of human anti-E2 antibodies 4N12 and 2H1, secondary goat anti-human HRP-conjugated antibody, and TMB substrate. Absorbance was quantified at 450 nm for duplicate wells from one-to-three independent experiments. The dotted line indicates background levels of binding in PBS control wells. Error bars indicate SEM. *P* values were determined by one-way analysis of variance (ANOVA) followed by Tukey's multiple comparison test (*, $P < 0.05$). Statistics presented within the graph indicate statistical significance only of mutant viruses relative to WT virus.

3.2.3 Characterization of attachment factor and receptor binding

To determine the importance of each E2 residue for GAG binding, 16 alanine mutant viruses were tested for heparin binding by ELISA. Serial dilutions of virus were adsorbed to ELISA plates coated with heparin, and bound virus was quantified. Eight mutant viruses displayed

similar or higher binding signals to heparin relative to WT virus (Figure 26A). K66A and R80A bound to heparin with similar binding signals compared with WT virus (Figure 26A). H62A, H73A, K107A, K140A, R144A, and R267A viruses bound to heparin with higher binding signals compared with WT (Figure 26A), with the E2 K107A and K140A viruses displaying the highest binding signals. At 6.25E7 genomes/mL, the K107A and K140A heparin-binding signals were 1.7 and 1.3 times higher than the WT heparin-binding signal, respectively.

In contrast, the other eight mutant viruses, K57A, R86A, R104A, R119A, K120A, H123A, K149A, and K200A, displayed lower binding signals to heparin relative to WT virus (Figure 26B). The greatest effects on heparin binding were observed with the K57A, R104A, R119A, K120A, H123A, and K149A viruses. H123A displayed the largest reduction in heparin binding. At 6.25E7 genomes/mL, the H123A heparin-binding signal was just above background levels and 7 times lower than the WT heparin-binding signal. Overall, these data suggest that E2 residues K57, R86, R104, R119, K120, H12A, K149, and K200 in domain A, domain B, and arch (Figure 27) function in GAG binding.

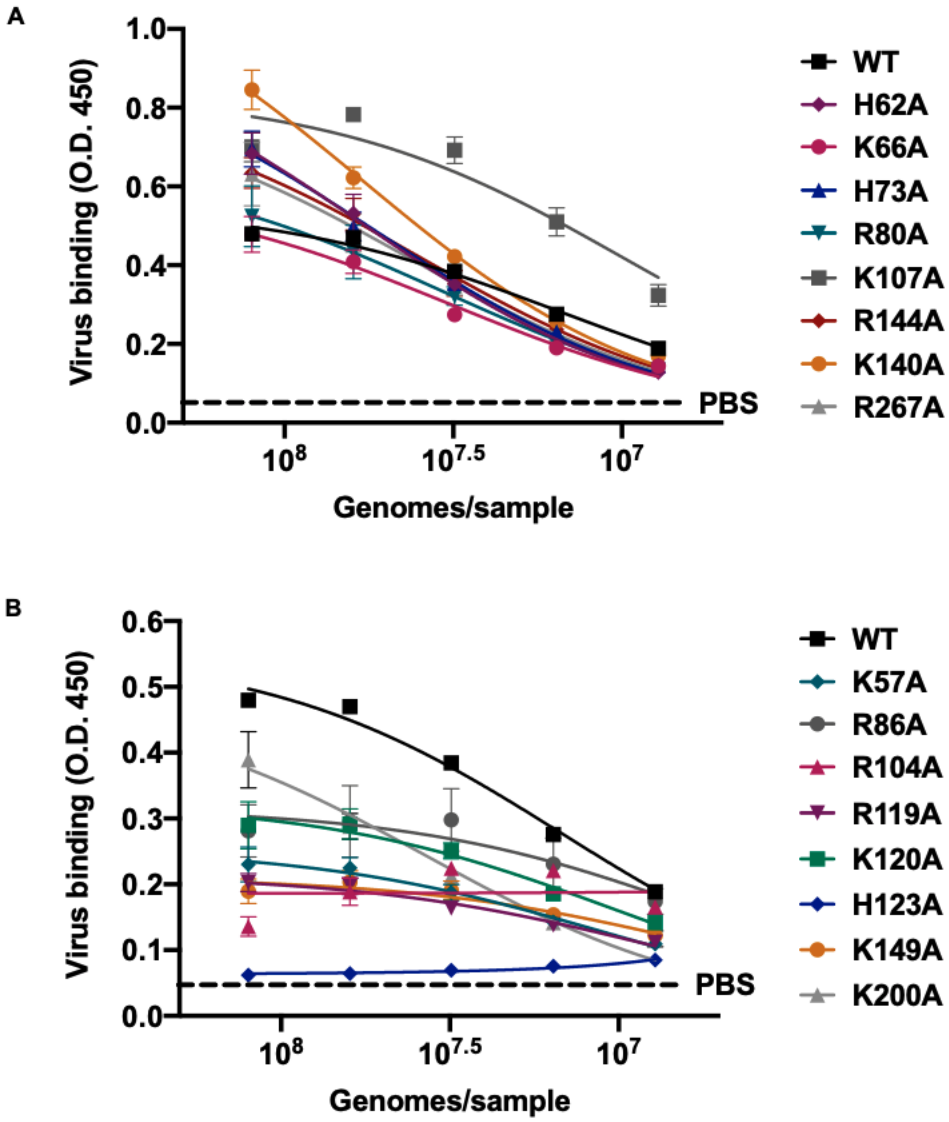

Figure 26. Alanine mutagenesis of eight E2 glycoprotein residues reduce heparin binding capacity.

(A) Mutant viruses with similar or greater heparin-binding capacity relative to WT virus. (B) Mutant viruses with reduced heparin-binding capacity relative to WT. (A and B) Serial dilutions of each virus, quantified by genome number, were adsorbed to wells of avidin-coated ELISA plates bound with biotinylated heparin. PBS was adsorbed to wells coated with heparin and CS as a negative control. Following washes to remove unbound virus, virus binding was detected using mouse monoclonal anti-CHIKV E2 antibody (CHK-187), secondary goat anti-mouse HRP-conjugated antibody, and TMB substrate. Absorbance was quantified at 450 nm for duplicate wells from three independent experiments. The dotted line indicates background levels of binding, as determined using PBS control wells. Error bars indicate SEM. Data were fit using a non-linear regression curve.

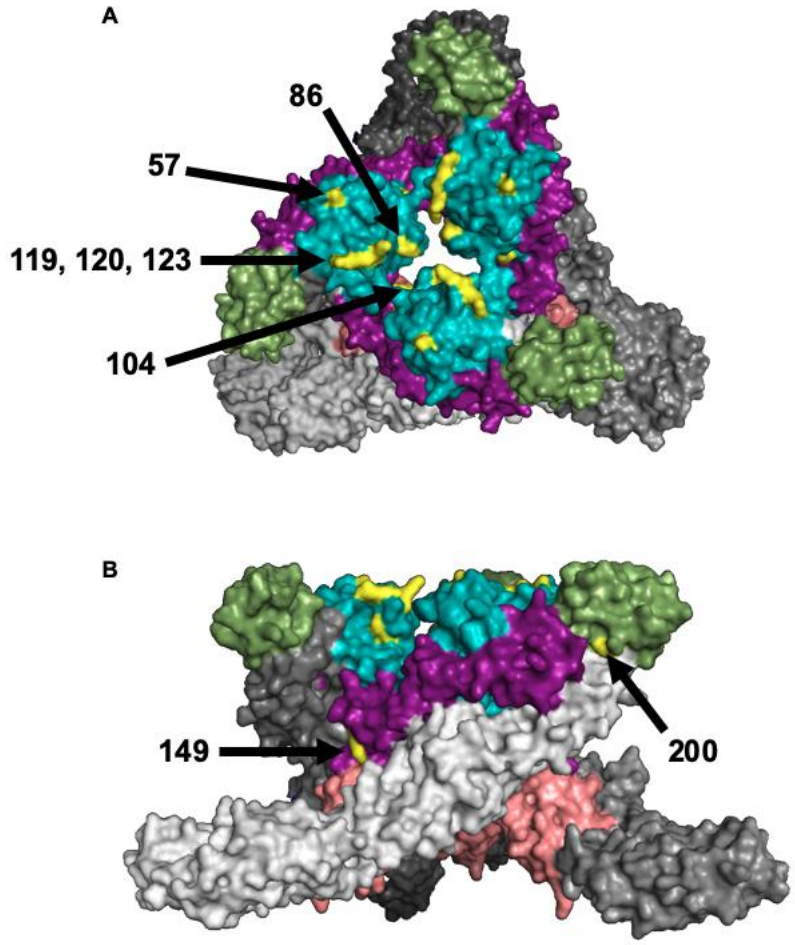

Figure 27. GAG-binding residues in the E2 glycoprotein.

(A) Top and (B) side view of the E1/E2 trimer structure (E1, grey; E2 domain A, blue; E2 domain B, green; E2 arch, purple; E2 domain C, pink). GAG-binding residues in the E2 glycoprotein that were identified using ELISAs are colored in yellow (K57, R86, R119, K120, H123, K149, and K200).

To determine whether the eight putative GAG-binding E2 residues also influence Mxra8 entry receptor engagement, alanine mutant viruses with the lowest heparin binding signals (K57A, R104A, R119A, K120A, H123A, and K149A) were analyzed for Mxra8 binding by ELISA. Serial dilutions of virus were adsorbed to ELISA plates coated with anti-CHIKV antibodies, mouse

Mxra8 protein conjugated to Fc was added to wells, and virus-Mxra8 binding was quantified. Two distinct phenotypes were observed. Three viruses (K57A, K120A, and K149A) displayed similar or slightly higher binding to Mxra8 relative to WT, while the other three viruses (R104A, R119A, and H123A) were diminished in Mxra8 binding (Figure 28). At 1.25E8 genomes/mL, the K120A and K149A Mxra8-binding signals were 1.3 times higher than the WT Mxra8-binding signal. Similarly, the K57A Mxra8-binding signal was 1.5 times higher than the WT Mxra8-binding signal. In contrast, R104A displayed a Mxra8-binding signal that was 2.7 times lower than that of WT. R119A and H123A displayed the largest reduction in Mxra8 binding with ELISA binding signals approximately 5 times lower than that of WT. R119 and K120 are located near the 2H1 and 4N12 epitopes in the E2 sequence (Figure 24), which could affect antibody capture of the mutants to the ELISA plates used to test Mxra8 binding. Collectively, these data indicate that E2 residues (K57, R104, and R119) are required for both GAG and Mxra8 binding, suggesting an overlap in the GAG- and Mxra8-binding sites on the E2 glycoprotein.

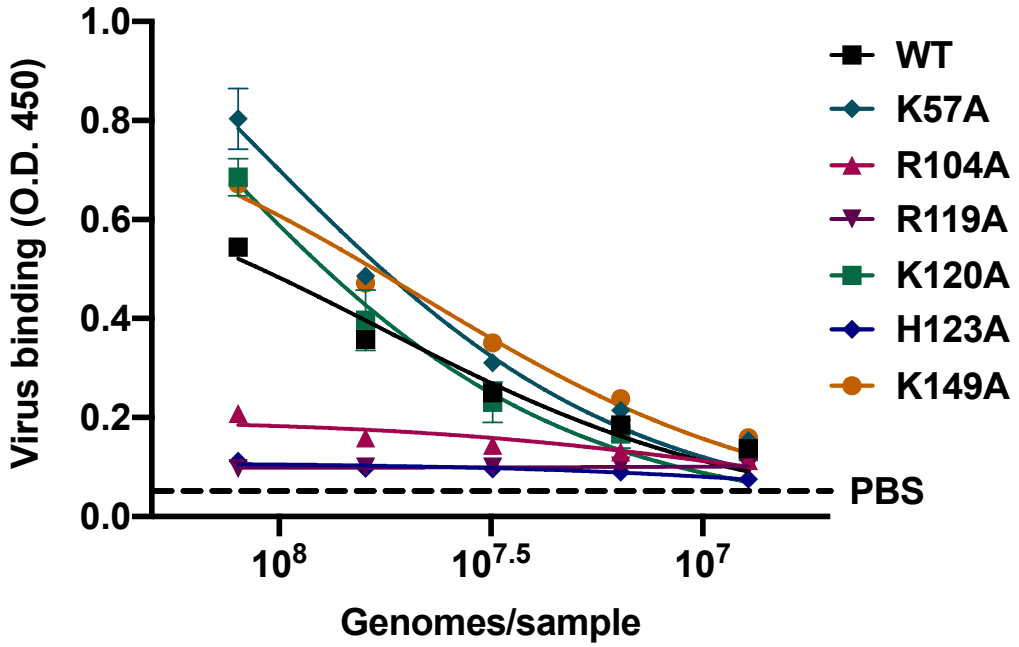

Figure 28. Alanine mutagenesis of three E2 glycoprotein residues reduce Mxra8 binding capacity.

Serial dilutions of each virus, quantified by genome number, were adsorbed to ELISA plates with human CHIKV anti-E2 antibodies (4N12 and 2H1). PBS was adsorbed to wells as a control. Following washes to remove unbound virus, mouse Mxra8-Fc, secondary goat anti-mouse HRP-conjugated antibody, and TMB substrate were added to detect virus binding. Absorbance was quantified at 450 nm for duplicate wells from two independent experiments. The dotted line indicates background levels of binding, as determined using PBS control wells. Error bars indicate SEM. Data were fit using a non-linear regression curve.

To ensure that the alanine mutations were specifically attenuated for GAG binding, mutant viruses with diminished GAG binding were tested for the capacity to bind to WT and *B3GAT3*$^{-/-}$ Hap1 cells. WT Hap1 cells express abundant levels of HS, low levels of CS, and no detectable human Mxra8 (Figures 16 and 17). In contrast, *B3GAT3*$^{-/-}$ cells express little to no HS, CS, or Mxra8 (Figure 21). These features make Hap1 cells suitable to test GAG binding in cultured cells in the absence of the Mxra8 entry receptor. As expected, WT virus bound to *B3GAT3*$^{-/-}$ cells less

efficiently, with an approximately 70% reduction in cell binding observed (Figure 29). Despite the low GAG-binding phenotypes observed using ELISAs (Figure 26), R104A, K120A, and H123A bound to WT GAG-expressing cells to similar or higher levels relative to WT virus with little to no binding to GAG-deficient *B3GAT3*$^{-/-}$ cells observed (Figure 29). In contrast, the binding of K57A, R119A, and K149A to WT cells was reduced relative to that of WT virus (Figure 29), indicating mutagenesis-dependent attenuation. However, R119A and K149A did not bind to GAG-deficient *B3GAT3*$^{-/-}$ cells (Figure 29), suggesting that factors other than GAG-binding are responsible for the diminished cell attachment observed for these alanine mutant viruses. The K57A mutant was the only virus that bound to WT and GAG-deficient *B3GAT3*$^{-/-}$ cells at levels comparable to the binding of WT virus to *B3GAT3*$^{-/-}$ cells (Figure 29), suggesting that the K57A mutation specifically affects GAG-binding capacity. Therefore, K57A is the only mutant virus identified in our studies specifically attenuated for GAG binding, which is an important distinction. Future work will use the K57A virus in mouse models of CHIKV disease to assess the role of virus-GAG interactions in CHIKV pathogenesis.

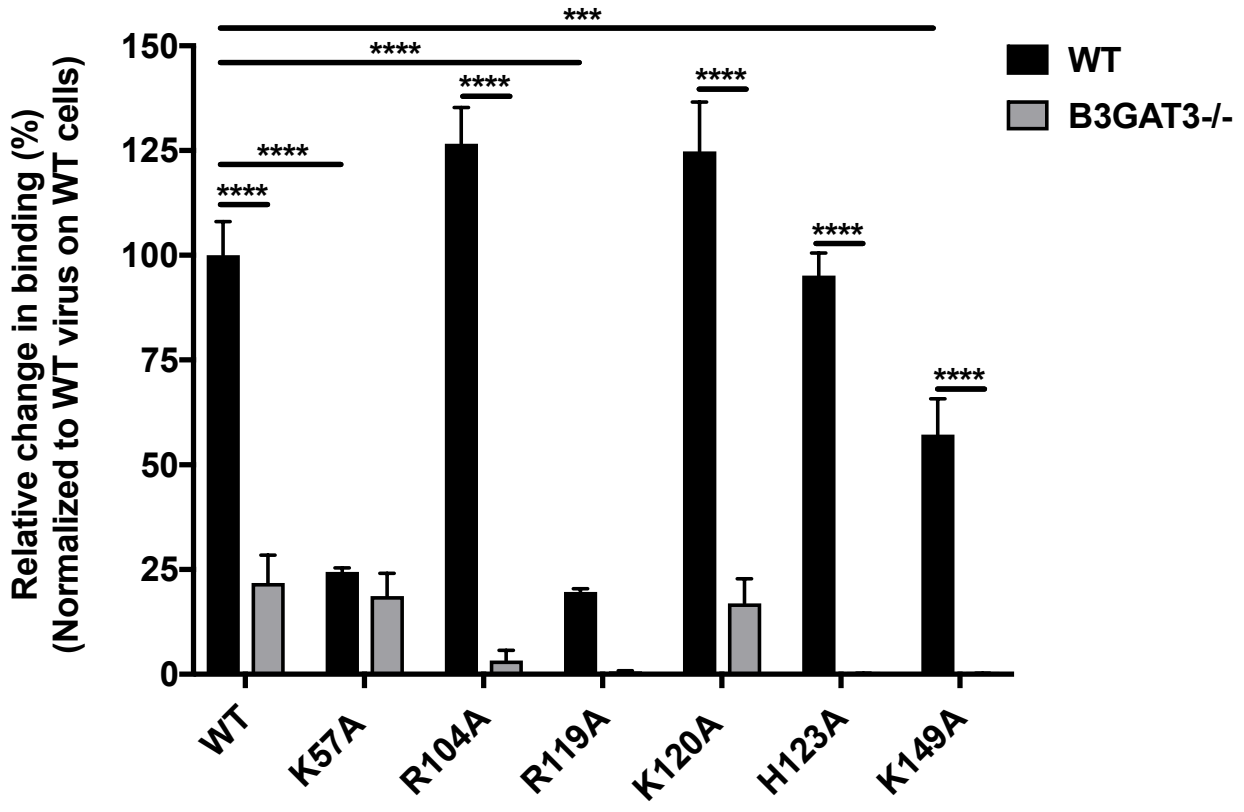

Figure 29. Mutant virus K57A is the only virus specifically attenuated for GAG binding.

WT and *B3GAT3*$^{-/-}$Hap1 cells were adsorbed with 10^8 genomes/sample of virus at 4°C for 2 h and washed three times to remove unbound virus. Total RNA was purified using TRIzol, and CHIKV RNA was quantified using RT-qPCR. Data were normalized to WT virus binding on WT cells. Results are expressed as the mean percentage of binding in triplicate wells from two independent experiments. Error bars indicate SEM. *P* values were determined using one-way ANOVA followed by Tukey's multiple comparison test (***, $P < 0.001$; ****, $P < 0.0001$).

3.3 Discussion

The specific CHIKV residues required for virus-GAG interactions were previously unknown. In the experiments described in this chapter, I recovered and characterized 18 alanine mutant viruses to identify residues in the CHIKV E2 glycoprotein required for GAG binding. The

mutant viruses were assessed for genome/PFU ratio and glycoprotein conformation to determine viral fitness and intact virion structure. I discovered eight E2 residues that when exchanged with alanine decrease heparin-binding capacity. Three of the residues that are required for GAG-binding may also modulate Mxra8 engagement, suggesting that the GAG- and Mxra8-binding sites in E2 overlap. I further identified one mutant virus, K57A, that is specifically attenuated in GAG-binding while maintaining other functions of E2. All other mutant viruses had increased binding to WT cells or decreased binding to GAG-deficient cells compared to WT virus cell binding, making K57A the prime candidate to study in mouse models of CHIKV disease to assess the role of virus-GAG interactions in pathogenesis. Collectively, these data indicate that residues in domain A, domain B, and arch of the CHIKV E2 glycoprotein are required for GAG binding.

Eight E2 residues (K57, R86, R104, R119, K120, H123, K149, and K200) of the 18 residues analyzed are required for virus-GAG interactions. This conclusion is based on heparin binding as assessed by ELISA. However, to fully understand virus-GAG binding, the importance of these residues in HS and CS binding should be tested. On the surface of most cultured cells and *in vivo*, HS and CS are more abundant relative to heparin (231, 235, 236, 239, 242, 314). Heparin also is structurally distinct from HS, containing more sulfation and IdoA residues (231). Furthermore, there is some evidence suggesting that CHIKV strains vary in dependence on HS and CS for attachment (66). In cell-binding assays, a requirement for HS rather than CS is apparent for CHIKV strain 181/25, while the opposite is the case for CHIKV strain SL15649 (66). The work described in Chapter 2 of this dissertation also describes the HS- and CS-binding capacity of SL15649 and other field-isolate CHIKV strains (Figure 15). These data indicate that CHIKV binds to HS and CS on cells, emphasizing the importance of defining the viral binding sites responsible for mediating interactions with HS and CS in addition to heparin. It is possible that the same E2

residues identified in this chapter also function in HS and CS binding. Alternatively, GAG-binding sites might vary according to the type of GAG engaged. GAG types differ structurally by sulfation and disaccharide composition (231), which could influence regions of the virion that are required for GAG binding.

Three residues that influence GAG-binding also were found to be required for Mxra8-binding. Using cryo-electron microscopy, Mxra8 contact sites in CHIKV have been identified in domains A and B of the E2 glycoprotein as well as in the fusion loop and domain II of the E1 glycoprotein (178, 179). Alanine substitutions of two of these Mxra8 contact sites, R119 and H123, decreased Mxra8 engagement as assessed by ELISA (Figure 28), corroborating previous studies of CHIKV-Mxra8 interactions. Although K120 was identified as a Mxra8 contact site (178, 179), I did not observe any Mxra8-binding defects when this residue was exchanged with alanine (Figure 27). Our studies also suggest a role for R104 in Mxra8 binding (Figure 28), although this residue was not previously described as a Mxra8 contact site (178, 179). However, there are important differences between previously published studies and our work, which may explain these discrepancies. Previous research used cryo-electron microscopy to structurally identify putative Mxra8-binding sites in WT virus (178, 179), while we used functional assays that tested Mxra8-binding capacity of alanine mutant viruses. Previous work used VLPs of the 37997 CHIKV strain (178, 179) and human (178) or mouse (179) Mxra8, whereas we investigated interactions between CHIKV strain SL15649 and mouse Mxra8. The CHIKV strains 37997 and SL15649 represent two distinct genetic clades, WA and ECSA, respectively (149, 264). The 37997 and SL15649 E2 protein sequences differ by approximately 6%. While E2 residues 104 and 120 do not differ between the strains, other residues that are predicted to form Mxra8 contact sites do, including residues 72, 74, and 182 (178, 179). Additionally, human and mouse Mxra8 sequences differ by

22%, including regions that are suggested to bind CHIKV (179). These differences in CHIKV strains and Mxra8 orthologs could contribute to the divergent results observed in our research compared with previously published work.

The residues we examined for GAG binding in the CHIKV E2 glycoprotein were primarily in domain A with four residues in the arch and one residue in domain B. Binding of host receptors by CHIKV can be mediated by E2 domain A (27, 218), domain B (27, 99), and arch (27, 218). Molecular docking simulations suggest that HS binding to E2 domain A and arch may trigger a conformational change in domain C, unveiling the E1 glycoprotein fusion loop to promote virus-cell fusion (218). Similarly, structural analyses suggest that ligand binding by domain B initiates glycoprotein conformational changes, which would likewise reveal the E1 glycoprotein fusion loop (27). While these various E2 domains have been implicated in receptor binding, the specific residues required for GAG interactions were previously unknown. Studies using purified E2 domains provide evidence that GAG-binding residues are located in domain B (99). Our studies expand on this finding and suggest that GAG-binding can occur using residues in E2 domain A and arch. Future work from our group will investigate whether other basic, surface-exposed residues in E2 are required for GAG-binding using mutagenesis and cryo-electron microscopy.

In addition to basic, surface-exposed residues in E2, other CHIKV residues also are likely required for GAG binding, including basic, surface-exposed residues in E1 and uncharged, polar residues in E1 and E2. The role of the E1 glycoprotein has yet to be assessed for alphavirus-GAG binding. Like E2, E1 also contains basic residues that are exposed on the virion surface, which could interact with negatively charged GAG chains. Furthermore, the identification of EEEV E2 residues on the periphery of E1/E2 trimeric spikes that mediate heparin binding (221) suggests that GAG chains are engaged (at least partially) between adjacent spikes. E1 residues are more surface-

exposed in the regions between E1/E2 trimeric spikes, which could facilitate GAG binding at the periphery of the E2 glycoprotein between spikes. Preliminary, unpublished work from our lab in collaboration with Dr. Kenneth Stapleford's lab suggests the requirement of residues in the E1 glycoprotein for GAG binding.

Residues in addition to positively charged, basic amino acids also could participate in GAG binding. Uncharged, polar residues, such as asparagine and glutamine, are thought to be important mediators of GAG binding (293, 300). These residues can facilitate non-ionic binding interactions like hydrogen bonding between GAGs and their ligands (242, 293, 300–302). Thus far, the role of asparagine and glutamine have yet to be investigated in alphavirus-GAG interactions.

Attachment factor binding can influence viral tropism and virulence. The contribution of virus-GAG interactions *in vivo* have been assessed for several alphaviruses, including CHIKV (58, 67, 165, 227), EEEV (204), SFV (228), and SINV (219, 229). Following subcutaneous inoculation, strains of EEEV and SINV with increased HS binding are attenuated, cleared rapidly, and disseminate less efficiently (204, 219, 229). Similar findings are observed with CHIKV. CHIKV strains with enhanced HS binding capacity produce attenuated disease characterized by reduced footpad swelling, diminished inflammation and damage to musculoskeletal tissues, reduced viral titers, and rapid viral clearance (58, 67, 165, 227). However, pathogenesis studies of CHIKV strains that lack or have reduced GAG-binding capacity have not been reported. The mutant virus K57A described in this chapter is an ideal candidate for use in studies of CHIKV disease to define the requirement of virus-GAG interactions *in vivo*. K57A has a genome/PFU ratio comparable to that of WT virus (Table 4) and displays correct glycoprotein conformation (Figure 25), reduced GAG binding (Figure 26), intact Mxra8 binding (Figure 28), and is specifically attenuated for

GAG binding as evaluated in cell-binding assays (Figure 29). Future studies will use K57A to clarify the role of GAG binding in viral tropism and virulence in mouse models of CHIKV disease.

Findings reported in this chapter contribute to an understanding of viral determinants of CHIKV-GAG interactions. We targeted 18 amino acids in the E2 glycoprotein to evaluate their contribution to GAG binding. We discovered eight residues in E2 domain A, domain B, and arch that are required for GAG engagement (K57, R86, R104, R119, K120, H123, K149, and K200) and found that three of these residues also are required for Mxra8 binding (R104, R119, and H123). Mutant virus K57A, which is specifically attenuated for GAG-binding capacity, will be used in future studies to further understand the contribution of virus-GAG interactions to CHIKV disease *in vivo*. Overall, findings reported here define residues in domain A, domain B, and arch of the E2 glycoprotein that influence CHIKV binding to GAGs.

4.0 Summary and future directions

4.1 Thesis summary

The cell-surface molecules bound by viruses to attach and enter cells are important determinants of viral tropism and disease. Alphaviruses display broad cell and tissue tropism and, therefore, are thought to mediate interactions with host cells through multiple attachment factors and cell-specific entry receptors. These host molecules have been challenging to identify, and their requirement in virus infection can be difficult to define, especially when multiple receptors are used and their expression varies on different cell types.

CHIKV, an arthritogenic alphavirus, became a global health threat as it spread throughout the world in the early 21st century, emerging in naïve populations and causing millions of cases of severe and debilitating arthritis. Despite the severity of CHIKV disease, there are no licensed therapeutics or vaccines. Since attachment factors and entry receptors are determinants of viral tropism and disease, I sought to better understand these virus-host interactions to enhance knowledge of CHIKV infection and illuminate new possible antiviral drug targets.

Several cell-surface molecules have been identified to facilitate CHIKV attachment and entry. One CHIKV entry receptor, Mxra8, is likely a bona fide entry receptor, but others are yet to be identified. A few putative attachment factors also have been defined for CHIKV, including GAGs, which are expressed ubiquitously in mammals and mosquitoes and likely enhance viral attachment to many cell types. However, the specific GAG types bound by CHIKV and the requirement of these interactions for virus infection is not fully understood. Moreover, the

structural features of GAG chains and the GAG-binding sites on the CHIKV E2 attachment protein are not well defined.

To begin filling these gaps in knowledge, I evaluated CHIKV-GAG binding using glycan microarray technology. In Chapter 2, I report that CHIKV binds specifically to GAGs relative to any of the other 662 glycan tested. CHIKV also preferentially binds to longer (14-mer), sulfated, iduronic-acid containing GAG chains. The highest CHIKV binding signals are observed with heparin, HS, and CS-B (DS). Using ELISAs, I validated the microarray results and determined that CHIKV strains from each genetically distinct clade directly bind to heparin and CS. Strain-specific differences in GAG binding also were observed, with the ECSA (SL15649) strain binding to heparin and CS with the highest avidity and the Asian (H20235) strain binding to heparin and CS with the lowest avidity.

In Chapter 2, I further assessed whether the virus-glycan interactions identified in microarray and ELISA studies contribute to virus binding to and infection of cells. I first characterized several cell lines to identify cells that express HS, CS, and Mxra8, are susceptible to CHIKV infection, and have a haploid or diploid karyotype. Of the eight cell lines tested, I chose to use human osteosarcoma U-2 OS cells, which express high levels of HS, CS, and Mxra8 and human haploid Hap1 cells, which express only HS. I discovered that strains from each CHIKV clade require HS for efficient binding and infection of U-2 OS and Hap1 cells, while an ECSA strain also requires CS for efficient binding to U-2 OS cells. Overall, these data indicate the importance of HS as a CHIKV attachment factor when CS and Mxra8 are present (as for U-2 OS cells) or absent (as for Hap1 cells).

In Chapter 3, I describe my research, defining viral determinants of CHIKV-GAG binding. Following sequence and structural analyses of the CHIKV attachment protein, E2, I identified 18

putative GAG-binding residues in the E2 glycoprotein. I individually exchanged each of these basic, surface-exposed residues with alanine, producing a panel of mutant viruses that was used to define residues in E2 required for GAG interactions. Mutant viruses were quantified to examine genome/PFU ratio as an indicator of viral fitness and tested for glycoprotein conformation to ensure intact virion structure. Using ELISAs, I identified eight E2 residues required for efficient GAG binding, including three of which that also are required for Mxra8 binding. Further analysis showed that one mutant virus, K57A, was specifically attenuated for GAG binding, as determined using cell-binding assays. Therefore, K57A is a low GAG-binding virus candidate to be tested in mouse models of CHIKV disease to determine the role of virus-GAG interactions in viral tropism and disease. Overall, these studies identified residues required for CHIKV-GAG binding in E2 domain A, domain B, and arch, which partially overlap Mxra8-binding sites.

4.2 Future directions

4.2.1 Determine the requirement of CS/DS during CHIKV *in vitro* infection

While my studies in Chapter 2 elucidate the role of HS in cells that express varying levels of GAGs and the Mxra8 entry receptor, the role of CS/DS is not fully understood. In U-2 OS cells, HS is required for all CHIKV strains tested to efficiently bind and infect. However, some dependence on CS for cell binding is observed for the ECSA (SL15649) strain. It is possible that the CS requirement for CHIKV in U-2 OS cells is masked by high HS expression. Therefore, to determine whether CS and DS are required for CHIKV cell binding and infection, cells that express no or low levels of HS and high levels of CS should be evaluated. Of the cells evaluated in Chapter

2, Vero and HFF-1 cells express similar levels of HS and CS. Other cells, such as human chondrocytes (315, 316), human bone marrow cells, and human synovial cells express higher levels of CS compared to HS (316). Mxra8 entry receptor expression also will need to be considered. It is important to understand the requirement of CS/DS in the presence and absence of Mxra8 expression. The chondrocytes, synovial fibroblasts, and HFF-1 cells characterized in Zhang et al. express detectable Mxra8 levels (102). Cells that lack Mxra8 while expressing high levels of CS/DS will have to be identified. Overall, to assess CS/DS dependence in the absence and presence of Mxra8 expression, these cell types that express equal or higher levels of CS compared to HS will be important tools to analyze the binding and entry of CHIKV strains.

To elucidate the requirement of CS/DS during CHIKV infection of cells in culture, cells listed above could be treated with HSase and CSase and assessed for virus binding and infection. Additionally, these cells could be genetically altered using CRISPR-Cas9 technology to ablate genes required for the biosynthesis of HS (EXTL2, EXTL3, EXT1, EXT2) or CS (CSGALNACT1, CSGALNACT2, CHPF, CHSY3, CHSY1) (100, 231). To dissect the requirement of CS or DS (CS-B) during CHIKV *in vitro* infection, cells could be genetically altered to lack the epimerase gene, DSE, which is required for DS chain synthesis (231).

4.2.2 Determine the requirement of GAGs during CHIKV infection of mosquitoes

The research described in this dissertation focuses on CHIKV-GAG interactions in mammalian cultured cells. However, CHIKV also infects mosquitoes (78), and GAG expression has been reported in the tissues of whole mosquitoes (226, 244, 245). Therefore, it would be informative to determine the requirement of GAGs during CHIKV infection of mosquito cells and whole mosquitoes. Several *Aedes aegypti* and *Aedes albopictus* cell lines are commercially

available for use, including A20 (317, 318), Aag2 (317, 319, 320), U4.4 (317, 319), and C6/36 (321). CHIKV infects A20 (322), U4.4 (317, 322), and C6/36 cells (67, 317, 322). However, GAG expression on each of these mosquito cell lines has not been reported. To study CHIKV-GAG binding requirements in mosquito cells, GAG expression profiles must be completed. To determine whether GAGs are required for CHIKV infection of mosquito cells, GAG-expressing mosquito cells could be treated with GAGase or subjected to CRISPR-Cas9 deletion of GAG biosynthesis genes, similar to the approach I used in Chapter 2 to study GAG dependence in mammalian cells. Additionally, the use of genetically altered mosquitoes that do not express HS or CS (if viable) could be used to further investigate the *in vivo* consequences of CHIKV GAG-binding in mosquitoes.

4.2.3 Identify proteoglycans required for CHIKV infection and whether they can facilitate virus entry into cells

Pathogenic strains of CHIKV bind multiple types of GAGs (66, 67, 100, 224). However, the proteoglycans to which these GAGs are covalently attached are unknown. The role of specific proteoglycans during infection of other viruses has been defined. HIV-1 requires syndecan-1 and syndecan-3, both of which contain HS and CS/DS, during infection of cultured cells (279, 323). Hepatitis C virus, hepatitis E virus, and human papillomavirus require syndecan-1 during infection of cultured cells as well (324–326). The HS and CS/DS GAG chains that are bound with the strongest avidity by CHIKV (224) are found covalently attached to core proteins to form proteoglycans at the cell surface (231). All four of the major proteoglycan families are composed of HS, CS/DS, or both: glypicans, lecticans, SLRPs, and syndecans (231, 235, 238). To identify the proteoglycans required for CHIKV infection, an siRNA screen targeting proteoglycan genes

could be conducted in cells confirmed to express those genes. Cells lacking proteoglycans also could be used to overexpress specific genes in CHIKV binding and infection assays to further determine the requirement of specific proteoglycans. These studies could be completed with CHIKV as well as other alphaviruses to better understand the role of specific proteoglycans during alphavirus infection.

In addition to serving as viral attachment factors, proteoglycans are responsible for a variety of functions in the cell, many of which are mediated through the activation of signaling pathways (239, 327–330). This observation begs the question of whether proteoglycans also can function as viral entry receptors, inducing the internalization of virus into the cell. For example, syndecan-4, an HS proteoglycan, activates multiple endocytic pathways, including macropinocytosis and caveolin- and dynamin-dependent endocytosis, to mediate the internalization of various macromolecules (329, 330). CHIKV cell entry is dependent on dynamin for clathrin-mediated endocytosis (92) and can be facilitated by macropinocytosis in muscle cells (331), suggesting that CHIKV could enter cells through proteoglycan-mediated internalization.

Some studies have begun to assess the role of proteoglycans in viral entry. For example, baculoviruses and herpes simplex virus type 1 require syndecan-1, an HS and CS/DS proteoglycan, for virus entry (283, 332, 333). To determine whether proteoglycans are required for CHIKV entry, Mxra8-deficient cells expressing a specific proteoglycan could be ablated for expression of that gene using siRNA or CRISPR-Cas9, infected with virus, treated with ammonium chloride to allow viral entry but not multiple rounds of infection, and quantified for infection by FFU. Additionally, cells deficient in expression of a specific proteoglycan could be transfected to overexpress the proteoglycan of interest, followed by assays of viral infectivity.

4.2.4 Identify the specific GAG moieties required for CHIKV binding

As indicated by my results in Chapter 2, CHIKV-GAG interactions are mediated by chain length, sulfation, and disaccharide composition. I reported that CHIKV bound with higher avidity to longer GAG chains (14-mer) that contained sulfation and IdoA residues. However, the optimal GAG chain length, specific sulfation modifications on GAG chains, and the requirement of IdoA GAG residues has yet to be defined. These specific structural requirements have been determined for some viruses. For example, respiratory syncytial virus (RSV) requires heparin with a minimum 10-mer chain for efficient binding (271), and Zika virus preferentially binds 8- to 18-mer heparin chains (272). While sulfated GAGs are important for the binding of many viruses (269–271, 282–284), specific sulfation modifications on HS chains mediate virus-GAG interactions, such as 3-O sulfation for herpes simplex virus 1 (283, 284) and N-sulfation for RSV (271). Furthermore, the requirement of IdoA has been observed for RSV infection of cultured cells (212).

To identify the specific GAG moieties required for CHIKV binding, a variety of approaches could be taken. Glycan microarrays like the ones described in Chapter 2 could be used. GAG chains of various lengths (2-mer to 20-mer) and sulfation modifications (2-O, 3-O, 4-O, and 6-O sulfation) could be printed on microarray slides and tested for CHIKV binding. Our lab has preliminary, unpublished data that validates this approach and suggests a requirement for specific GAG structures for CHIKV binding. Additionally, CRISPR-Cas9 genetically altered cells deficient in the 2-O, 3-O, 4-O, or 6-O sulfatases could be assessed for CHIKV binding and infection to identify sulfation requirements for virus-GAG interactions. CRISPR-Cas9 genetically-altered cells deficient in the epimerase enzymes GLCE (for HS GlcA to IdoA epimerization) or DSE (for CS/DS GlcA to IdoA epimerization) also could be assessed for CHIKV binding and infection to identify the requirement of IdoA residues on GAG chains to facilitate virus attachment.

4.2.5 Further define GAG binding sites on the CHIKV virion

In Chapter 3, I identify residues in domain A, domain B, and arch of the E2 glycoprotein that are required for CHIKV GAG-binding. This work expands on findings that GAG binding by CHIKV is mediated by domain B of E2 (99) and supports molecular docking studies that suggest CHIKV-GAG interactions occur in the E2 domain A and arch (218). Collectively, these studies coupled with our findings indicate that CHIKV GAG-binding likely occurs by multi-site interactions with the viral E2 glycoprotein. By assessing 18 E2 amino acids, we have only begun to identify the specific GAG-binding residues in E2. Therefore, further investigation is required to assess the contribution of other basic, surface-exposed E2 residues to GAG binding. Additionally, as described in Chapter 3, GAG binding also could be mediated by basic, surface-exposed residues in the E1 glycoprotein as well as uncharged, polar residues like asparagine and glutamine in E1 and E2. While viral mutagenesis studies are informative to identify viral protein residues that are required for GAG binding, these residues may not be actual contact sites. Structural techniques like cryo-electron microscopy should be conducted to define CHIKV residues that contact GAGs. Furthermore, to begin dissecting the binding kinetics of CHIKV to GAGs and Mxra8, surface plasmon resonance and bio-layer interferometry techniques should be used.

4.2.6 Define the contribution of GAG binding during CHIKV *in vivo* infection

Attachment factor binding can be a host determinant for viral tropism and disease. GAG-binding *in vivo* has been assessed for several alphaviruses, including CHIKV (58, 67, 165, 227), EEEV (204), SFV (228), and SINV (219, 229). Like EEEV and SINV (204, 219, 229), infection by CHIKV strains with enhanced HS-binding capacity results in attenuated disease, which is

characterized by reduced footpad swelling, diminished inflammation and pathology in musculoskeletal tissues, reduced viral titers, and rapid viral clearance (58, 67, 165, 227). Studies assessing virus-GAG interactions in mice have used mutant viruses that display altered, usually increased, GAG-binding capacities. To better understand the contribution of GAG binding during CHIKV infection *in vivo*, studies using CHIKV strains that lack or have reduced GAG-binding capacity should be conducted. Future work from our group will assess CHIKV pathogenesis in three-to-four-week-old WT C57BL/6 mice infected with WT virus, high GAG-binding virus (G82R), or low GAG-binding virus (K57A). I hypothesize that a "goldilocks" phenomenon will be observed, in which WT virus, displaying moderate GAG-binding capacity, will cause CHIKV disease in mice, but high and low GAG-binding viruses will be attenuated. Such an observation would suggest that too much or too little GAG-binding capacity alters viral tropism and attenuates virulence.

In addition to using viral mutants, mice with altered GAG expression can be assessed for CHIKV infection and disease to further define the role of CHIKV-GAG interactions *in vivo*. *XYLT1*$^{-/-}$ (334–336) and *XYLT2*$^{-/-}$ (335–337) mice lack a xylosyltransferase gene, which is required to initiate GAG biosynthesis by adding a xylose to a serine residue on a core protein, rendering these animals GAG-deficient (231, 338, 339). *B4GALT7-/-* (335, 336, 340) and *B3GAT3-/-* mice (341, 342) lack a galactosyltransferase gene that also is required to initiate GAG biosynthesis by adding a galactose to the tetrasaccharide linker attached to a core protein, rendering these animals GAG-deficient as well (231). There are several strains of mice that lack CS expression due to deletion of various CS polymerase genes, including CHSY (343), CHPF (343, 344), CSGALNACT1 (343, 345–347), and CSGALNACT2 (347). DS-deficient mice have been genetically altered to lack DS epimerases DSE (348, 349) or DSEL (350), and HS-deficient mice

have been engineered by ablating the following HS polymerase genes: EXT1 (351), EXT2 (352), EXTL2 (353, 354), and EXTL3 (355). Using these mice in pathogenesis studies will help define the requirement of total GAGs and specific GAG types during CHIKV infection *in vivo*. Furthermore, the requirement of specific sulfation modifications on GAG chains can be analyzed using mice that lack particular sulfotransferase genes, such as HS2ST1, which is responsible for HS 2-O sulfation (356–358), HS3ST1, which is responsible for HS 3-O sulfation (359), or HS6ST1, which is responsible for HS 6-O sulfation (360, 361). While studies with these various GAG-altered mouse strains will be informative, it should be noted that multiple, redundant genes are often responsible for a single function like sulfation (231, 362), making it difficult to alter certain GAG characteristics. Furthermore, some of these knockout mice may not breed well or may display disease phenotypes unrelated to CHIKV infection (335). If specific GAG-deficient mice are not viable, engineering conditional, tissue-specific knockout mice using CRISPR-Cas9 could be considered.

4.2.7 Evaluate the use of GAG mimetics during CHIKV infection

The work in this dissertation describes the necessary and specific interactions of CHIKV and GAG attachment factors during binding to and infection of cells in culture. Since attachment factor binding can be a host determinant of alphavirus pathogenesis (67, 165, 203, 204, 219, 220, 227, 228), GAG-based antiviral drugs may be a useful therapeutic approach to combat CHIKV.

Synthetic compounds called GAG mimetics have been designed to mimic the structure of GAGs (276, 363, 364) GAG mimetics have been used for a variety of therapeutic uses, such as anti-coagulation (365–367), tissue repair (368), cancer treatment (369), anti-inflammation (369), and blockade of pathogen cell entry (276, 327, 364, 370). GAG mimetics block attachment to

cultured cells of adenovirus (371), dengue virus (372), and herpes simplex virus (373, 374) and have been used to mitigate dengue virus (288) and Ross River virus (287) infection *in vivo*. Of note, pentosane polysulfate, a heparin-like GAG, reduces CHIKV and Ross River virus disease in mice, resulting in reduced footpad swelling, less joint inflammation, and decreased levels of pro-inflammatory cytokines (287). Studies using pentosane polysulfate provide proof-of-concept that GAG mimetics could function as antiviral therapeutics. Further investigation is required to identify other potential CHIKV-specific GAG mimetic antivirals.

4.3 Conclusions

The research described in this dissertation assesses the importance and specificity of CHIKV-GAG interactions and defines the structural features of GAG chains and CHIKV viral proteins that are required for binding. Studies presented here establish a foundation to further elucidate the contribution of CHIKV-GAG engagement in other cell types like mosquito cells and *in vivo* using mouse models of CHIKV disease. Collectively, this work enhances an understanding of CHIKV attachment factor binding and will help facilitate the development of GAG-based antiviral therapeutics to combat the global health threat posed by CHIKV.

5.0 Materials and methods

5.1 Cells

Baby hamster kidney cells (BHK-21; ATCC CCL-10) were maintained in alpha minimal essential medium (αMEM; Gibco) supplemented to contain 10% fetal bovine serum (FBS; VWR) and 10% tryptose phosphate (Sigma). Vero 81 cells (ATCC CCL-81) were maintained in αMEM supplemented to contain 5% FBS. Human osteosarcoma cells (U-2 OS; ATCC HTB-96) were maintained in McCoy's 5A medium (Gibco) supplemented to contain 10% FBS. Culture media for BHK-21, Vero-81, and U-2 OS cells also were supplemented with 0.29 mg/mL L-glutamine (Gibco), 100 U/mL penicillin (Gibco), 100 μg/mL streptomycin (Gibco), and 25 ng/mL amphotericin B (Sigma). BV2 and HFF-1 (ATCC SCRC-104) cells were maintained in Dulbecco's modified eagle medium (DMEM; Gibco) supplemented to contain 10% FBS. BV2 cells were additionally supplemented to contain 1% HEPES, 100 U/mL penicillin, and 100ug/mL streptomycin. Synovial fibroblasts (ABM T0030) were maintained in Roswell Park Memorial Institute 1640 medium (RPMI; Gibco) supplemented to contain 10% FBS. WT and *B3GAT3*$^{-/-}$ human Hap1 cells (100) were provided by Yusuke Maeda (Osaka University) and Atsushi Tanaka (Thailand-Japan RCC-ERI). Hap1 cells were maintained in Iscove's modified Dulbecco's medium (IMDM; Gibco) supplemented to contain 10% FBS, 100 U/mL penicillin, and 100 μg/mL streptomycin. All cells were cultivated at 37^{o}C in an atmosphere of 5% CO_2.

5.2 VLPs and viruses

Chikungunya VLPs of the 37997 strain were prepared by Emergent BioSolutions as described (108). Suspension-adapted, serum-free human embryonic kidney 293 cells were transfected with an expression plasmid containing strain 37997 structural genes. Supernatants were collected and clarified by centrifugation. VLPs were purified using chromatography and sterile filtration, suspended in 10 mM potassium phosphate, 218 mM sucrose, and 25 mM sodium citrate, and stored at -80°C prior to use.

Virus stocks were recovered from infectious cDNA clone plasmids for each CHIKV strain, including 181/25 (64, 65), SL15649 (149), H20235 (267), 37997 (264), and chimeric Sindbis virus (SINV)-CHIKV in the TR339 and SL15649 strains, respectively (102, 223). CHIKV plasmids were linearized using NotI-HF (NEB), and SINV-CHIKV plasmids were linearized using PvuI-HF (NEB). Viral cDNAs were transcribed *in vitro* using an mMessage mMachine SP6 transcription kit (Ambion). BHK-21 cells (1.19×10^7 cells) were electroporated with *in vitro* transcribed RNA using a Gene Pulser Xcell electroporator (Bio-Rad) and the square wave protocol with 2 pulses at 1000 V for 2.5 ms and 5 s between each pulse. Cells were incubated at 37°C for 48 h. Supernatants were collected and clarified by centrifugation at 1,500 x *g* at 4°C for 10 min to remove cell debris. Remaining supernatant was added to a 20% sucrose cushion in TNE buffer ($PBS^{-/-}$ supplemented to contain 50 mM Tris-HCl pH 7.2, 0.1 M NaCl, and 1 mM EDTA) and centrifuged at ~ 115,000 x *g* for ~ 16 h in a Beckman 32Ti rotor. Pellets containing virus were resuspended in virus dilution buffer (VDB; RPMI medium supplemented to contain 20 mM HEPES [Gibco] and 1% FBS), aliquoted, and stored at -80°C. Titers of virus stocks were determined by plaque assay. Genome copy numbers of virus stocks were determined by RT-qPCR.

5.3 Site-directed mutagenesis

Mutations were introduced into the SINV-CHIKV plasmid using mutagenesis primers designed with the Agilent QuikChange primer design online tool (https://www.agilent.com/store/primerDesignProgram.jsp). QuikChange PCR reactions were conducted using KOD Hot Start DNA polymerase (Sigma-Aldrich), followed by DpnI (NEB) digestion to remove template DNA. Sanger sequencing was used to confirm the fidelity of mutagenesis.

5.4 Viral plaque assays

Confluent monolayers of Vero-81 cells were adsorbed with serial dilutions (10-fold) of virus stocks in VDB at 37ºC for 1 h. Cells were overlaid with 0.5% immunodiffusion agarose (VWR) in αMEM supplemented to contain 10% FBS, 10% tryptose phosphate, 100 U/mL penicillin, and 100 μg/mL streptomycin. Cells were incubated at 37ºC for ~ 48 h. Plaques were visualized following staining with neutral red (Sigma) at 37ºC for 4 to 6 h. Plaques were enumerated in duplicate and averaged to calculate plaque forming units (PFU).

5.5 Viral RT-qPCR

Viral RNA was extracted from 10 μl of purified virus stocks using 490 μl TRIzol reagent (Thermo Fisher Scientific), purified using the PureLink RNA Mini Kit (Invitrogen), and eluted

into a final volume of 100 µl. Viral genomes were quantified using the qScript XLT one-step reverse transcription-quantitative PCR (RT-qPCR) ToughMix kit (Quanta Biosciences). To analyze CHIKV strains, reactions were conducted in 20 µl, containing 5 µl viral RNA, 500 nM forward primer (5'-AGACCAGTCGACGTGTTGTAC-3'), 500 nM reverse primer (5'-GTGCGCATTTTGCCTTCGTA-3'), and 250 nM fluorogenic probe (5'-/56-FAM/ATCTGCACC/ZEN/CAAGTGTACCA/3IABkFQ/-3'), targeting an amplicon in the nonstructural protein 2 (nsp2) coding region. To analyze SINV-CHIKV strains, reactions were conducted in 20 µl, containing 5 µl viral RNA, 500 nM forward primer (5'-CAGCTGATCTCAGCAGTTAATAAACT-3'), 500 nM reverse primer (5'-GCCCGGCTTCTTTTTCTTTTGA-3'), and 250 nM fluorogenic probe (5'-/56-FAM/AATCGGAAG/ZEN/AATAAGAAGCAAAAGCAAAA/3IABkFQ/-3'), targeting an amplicon in the capsid coding region. Standard curves for each virus strain were prepared using *in vitro* transcribed viral RNA. RT-qPCR was conducted using a ViiA 7 Real-Time PCR system (Thermo Fisher Scientific) under the following conditions: 50°C for 10 min, 95°C for 10 min, 40 cycles of 95°C for 15 s, and 60°C for 60 s, with data acquisition in the FAM channel during the 60°C step. RNA concentrations were determined by comparing the C_T values of each sample to an appropriate standard curve. RT-qPCR to determine genome copy numbers of virus stocks (genomes per mL) were conducted in triplicate.

5.6 Glycan microarrays

The binding specificities of the chikungunya 37997 VLPs were analyzed using a neoglycolipid (NGL)-based microarray system (263). Two types of microarrays were used: (1)

glycan microarrays composed of 672 sequence-defined lipid-linked mammalian and non-mammalian glycans as described (375) and (2) GAG-focused microarrays composed of NGL probes of 13 sized-defined glycosaminoglycan (GAG) oligosaccharides and two non-GAG polysaccharide controls. The glycan probes and sequences used in the glycan microarrays are provided in Table S1 of McAllister et al. 2020 (224). The glycan probes and sequences used in the GAG-focused arrays are provided in Figure 14. Information about the preparation of the glycan probes and construction of the microarrays is presented in Table S3 in McAllister et al. 2020 (224) in accordance with the MIRAGE (Minimum Information Required for a Glycomics Experiment) guidelines for reporting of glycan microarray-based data (376).

Multiple analyses were conducted with the chikungunya VLPs and anti-CHIKV antibodies (Table S3 in McAllister et al. 2020 (224)). Slides were blocked at room temperature (RT) for 1 h with HBS buffer (10 mM HEPES at pH 7.4 with 150 mM NaCl and 5mM $CaCl_2$) supplemented to contain 0.02% (w/v) casein (Pierce) and 1% (w/v) BSA (Sigma). Microarrays were overlaid with VLP solution (50 μg/ml used in most analyses) at 4°C for 1.5 h and fixed with 4% paraformaldehyde (PFA) diluted in HPLC-grade water at 4°C for 30 min. VLP binding was detected following incubation with anti-CHIKV E2 antibody (CHK-152 (60); 1:300) or ascites fluid (ATCC VR-1241AF; 1:300) at RT for 1 h, biotinylated goat anti-mouse IgG (Sigma; 2 μg/ml) at RT for 1 h, and Alexa Fluor 647-labelled streptavidin (Molecular Probes;1 μg/ml) at RT for 30 min. Imaging and data analysis are described in the supplementary MIRAGE document (Table S3 in McAllister et al. 2020 (224)).

5.7 GAG ELISAs and RBS calculations

Pierce NeutrAvidin-coated ELISA plates (Thermo Fisher Scientific 15123B) were adsorbed with 4 ng/µl of heparin conjugated to biotin (Creative PEGWorks HP-207) or 15 ng/µl of chondroitin sulfate conjugated to biotin (Creative PEGWorks CS-106, mixture of CS-A, CS-B, and CS-C) at RT for 2 h. Wells were washed three times with wash buffer ($PBS^{-/-}$ supplemented to contain 0.05% Tween 20). ELISA plates were adsorbed with serial dilutions (1:2) of virus in VDB at RT for 1 h. As a negative control, PBS was adsorbed to ELISA plates coated with heparin and CS. Wells were washed with wash buffer three times to remove unbound virus. Bound virus was detected following incubation with a mouse monoclonal anti-CHIKV E2 antibody (CHK-187 (60); 1 ug/mL) at RT for 1 h, a horseradish peroxidase-conjugated goat anti-mouse Ig (1:10,000; SouthernBiotech 1010-05) at RT for 1 h, and TMB substrate (Thermo Fisher Scientific) for up to 5 min. Absorbance at 450 nm was quantified using a Synergy H1 microplate reader (BioTek). Data were used to prepare a non-linear regression curve assuming one-site specific binding, and relative binding strength (RBS) values were calculated for each virus. RBS values refer to the concentration in genomes/mL of virus at which 50% of GAG-binding sites are occupied.

5.8 Conformational ELISAs

ELISA plates (Immulon 2HB; Thermo Fisher Scientific 62402-972) were adsorbed with 1 µg/mL mouse monoclonal CHIKV E2-specific antibody CHK-152 (60) at 4ºC overnight. Wells were washed three times with wash buffer ($PBS^{-/-}$ supplemented to contain 0.05% Tween 20). ELISA plates were adsorbed with blocking buffer ($PBS^{-/-}$ supplemented to contain 0.05% Tween

20 and 1% FBS) at RT for 1 h. Wells were washed three times with wash buffer and adsorbed with serial dilutions (1:2) of virus in VDB at RT for 1 h. As a negative control, PBS was adsorbed to ELISA plates. Wells were washed with wash buffer three times to remove unbound virus. Bound virus was detected following incubation with human monoclonal CHIKV-specific antibodies (4N12 and 2H1 (312); 1 µg/mL) at RT for 1 h, a horseradish peroxidase-conjugated goat anti-human immunoglobulin (1:10,000; SouthernBiotech 2040-05) at RT for 1 h, and TMB substrate (Thermo Fisher Scientific) for 5 min. Absorbance at 450 nm was quantified using a Synergy H1 microplate reader (BioTek). Data were used to prepare a non-linear regression curve assuming one-site specific binding.

5.9 Mxra8 ELISAs

ELISA plates (Immulon 2HB; Thermo Fisher Scientific 62402-972) were adsorbed with 1 µg/mL human monoclonal CHIKV-specific antibodies, 4N12 and 2H1 (312), at 4ºC overnight. Wells were washed three times with wash buffer ($PBS^{-/-}$ supplemented to contain 0.05% Tween 20). ELISA plates were adsorbed with blocking buffer ($PBS^{-/-}$ supplemented to contain 0.05% Tween 20 and 1% FBS) at RT for 1 h. Wells were washed three times with wash buffer and adsorbed with serial dilutions (1:2) of virus in VDB at RT for 1 h. As a negative control, PBS was adsorbed to ELISA plates. Wells were washed with wash buffer three times to remove unbound virus. Virus was evaluated for Mxra8 binding by incubation with 1 µg/mL Fc fusion protein conjugated to the extracellular domain of mouse Mxra8 (Mxra8-Fc) (102) at RT for 1h. Wells were washed three times with wash buffer and adsorbed with a horseradish peroxidase-conjugated goat anti-mouse immunoglobulin (1:10,000; SouthernBiotech 1010-05) at RT for 1 h and TMB

substrate (Thermo Fisher Scientific) for 5 min. Absorbance at 450 nm was quantified using a Synergy H1 microplate reader (BioTek). Data were used to prepare a non-linear regression curve assuming one-site specific binding.

5.10 Cell-surface glycan and protein expression

Cells were detached from tissue-culture flasks using CellStripper Dissociation Reagent (Corning), quenched with $PBS^{+/+}$ supplemented to contain 2% FBS, and centrifuged at 1500 x *g* at 4°C for 5 min. Cells (5 x 10^5 cells per sample) were stained with human anti-HS (1:750; Amsbio 370255-S), human anti-CS (1:750; Sigma C8035), human anti-Mxra8 (1 μg/mL; MBL International W040-3), or mouse anti-Mxra8 (1 μg/mL; 4E7.D10 (102)) antibodies at 4°C for 1 h. Cells were incubated with Alexa Fluor 647 antibody (1:1000; Thermo Fischer Scientific) at 4°C for 1 h. Samples were washed twice with VDB between incubations. Samples were fixed with 1% PFA at 4°C for 5 min and analyzed by flow cytometry (LSRII flow cytometer; BD Biosciences). Binding events were gated using secondary antibody-only control samples as the no-binding controls, and median fluorescent intensity (MFI) was determined using FlowJo V10 software.

5.11 Virus binding to cells

Cells were detached from tissue-culture flasks using CellStripper Dissociation Reagent, quenched with $PBS^{+/+}$ supplemented to contain 2% FBS, and centrifuged at 1500 x *g* at 4°C for 5 min. Cells (5 x 10^5 cells per sample) were adsorbed with virus at 10^8 genomes per sample at 4°C

for 2 h and washed three times with VDB. Cells were centrifuged at 1500 x *g* for 5 min, and pellets were resuspended in 750 μl of TRIzol. RNA was purified, and viral genomes per sample were quantified using RT-qPCR.

5.12 Focus-forming unit (FFU) assays

Virus was adsorbed to monolayers of U-2 OS or Hap1 cells at the MOIs indicated in the figure legends. Following incubation at 37°C for 1 h, the inoculum was removed, and cells were incubated at 37°C for 18 h in medium supplemented to contain 20 mM NH_4Cl unless otherwise noted. Cells were fixed with ice-cold methanol for 30 min and washed three times with $PBS^{-/-}$. Blocking buffer ($PBS^{+/+}$ supplemented to contain 5% FBS and 0.1% TX-100) was added to the plate at RT for 1 h. Cells were stained with anti-CHIKV ascites fluid (1:1500; ATCC VR-1241AF) at RT for 1 h and goat anti-mouse Alexa Fluor 488 IgG (1:1000; Invitrogen A11029) with 4',6-diamidino-2-phenylindole (DAPI; 1:1000; Thermo Fisher Scientific) at RT for 1 h. Cells were washed with $PBS^{-/-}$ three times at RT for 5 min per wash between each staining step. Infectivity was quantified by indirect immunofluorescence using the Lionheart FX automated microscope and Gen5 software (BioTek).

5.13 GAG cleavage assays

U-2 OS cells were adsorbed with heparinases (HSase I, II, III; Sigma H2519, H6512, H8891, respectively) or chondroitinases (CSase ABC; Sigma C3667) at a final concentration of 2

mIU/mL diluted in digestion buffer (MilliQ water supplemented to contain 20 mM HEPES pH 7.5, 150 mM NaCl, 4 mM $CaCl_2$, and 0.1% BSA) at 37°C for 1 h. Cells were washed with $PBS^{-/-}$ three times. Cell-surface GAG expression was quantified by flow cytometry, virus binding by RT-qPCR, and virus infectivity by FFU.

5.14 Transient complementation of KO cells

Hap1 *B3GAT3*$^{-/-}$ cells were transfected with pcDNA3.1(+)-N-eGFP containing human *B3GAT3* (GenScript OHu21110C) using Lipofectamine 3000 (Thermo Fisher Scientific L3000015) at a 3:1 transfection reagent to DNA ratio. Medium was changed at 24 h post-transfection. At 36 h post-transfection, cell-surface GAG expression was quantified by flow cytometry, virus binding by RT-qPCR, and virus infectivity by FFU assay.

5.15 Statistical analysis

Statistical tests were conducted using GraphPad PRISM 7 software. *P* values less than 0.05 were considered to be statistically significant. Descriptions of the specific statistical tests are provided in figure legends.

5.16 Biosafety

All studies using VLPs and SINV-CHIKV chimeras were conducted using biosafety level 2 conditions, and all studies using viable virus were conducted in a certified biosafety level 3 facility. Protocols used were approved by the University of Pittsburgh Department of Environment, Health, and Safety and the University of Pittsburgh Institutional Biosafety Committee.

Appendix A Copyright permissions

Figures in Chapter 1 and 2 and text from Chapter 2 were previously published and presented herein in a modified form with permission of the copyright holder.

Weaver SC, Klimstra WB, Ryman KD. 2008. Togaviruses: General Features, p. 107–116. *In* Encyclopedia of Virology. Elsevier.

Natrajan MS, Rojas A, Waggoner JJ. 2019. Beyond fever and pain: diagnostic methods for chikungunya virus. J Clin Microbiol 57.

Suhrbier A, Jaffar-Bandjee M-C, Gasque P. 2012. Arthritogenic alphaviruses--an overview. Nat Rev Rheumatol 8:420–429.

Lentscher A. 2020. Tissue-Restricted Chikungunya Virus Is Attenuated in Mice and Protective Against Virulent Virus Challenge. Doctor, University of Pittsburgh.

Silva LA, Dermody TS. 2017. Chikungunya virus: epidemiology, replication, disease mechanisms, and prospective intervention strategies. J Clin Invest 127:737–749.

Holmes AC, Basore K, Fremont DH, Diamond MS. 2020. A molecular understanding of alphavirus entry. PLoS Pathog 16:e1008876.

McAllister N, Liu Y, Silva LM, Lentscher AJ, Chai W, Wu N, Griswold KA, Raghunathan K, Vang L, Alexander J, Warfield KL, Diamond MS, Feizi T, Silva LA, Dermody TS. 2020. Chikungunya virus strains from each genetic clade bind sulfated glycosaminoglycans as attachment factors. J Virol 94:e01500-20.

Appendix B Abbreviations glossary

αMEM	Minimum essential medium alpha
ANOVA	Analysis of variance
ATPS-beta	ATP synthetase beta subunit 1
BHK	Baby hamster kidney
BSA	Bovine serum albumin
BSL	Biological safety level
B3GAT3	Beta-1,3-glucuronyltransferase 3
Cas9	CRISPR-associated protein 9
CCL	Chemokine (C-C motif) ligand
cDNA	Complementary deoxyribonucleic acid
CHIKF	Chikungunya virus fever
CHIKV	Chikungunya virus
CHO	Chinese hamster ovary
CI	Confidence interval
CPC motif	Cation-polar-cation motif
CPV	Cytopathic vesicle
CRISPR	Clustered regularly interspaced short palindromic repeats
cryo-EM	Cryo-electron microscopy
CS	Chondroitin sulfate
CSase	Chondroitinase

CW motif	Cardin and Weintraub motif
CXCL	Chemokine (C-X-C motif) ligand
DAPI	4’,6’-diamidino-2-phenylindole
DENV	Dengue virus
DMEM	Dulbecco’s Modified Eagle Medium
DNA	Deoxyribonucleic acid
dNTPs	Deoxynucleoside triphosphates
DS	Dermatan sulfate
DC-SIGN	Dendritic cell-specific intracellular adhesion molecule-3-grabbing non-integrin
DHPE	1,2-dihexadecyl-sn-glycero-3-phosphoethanolamine
DMARDs	Disease-modifying anti-rheumatic drugs
dUA	4,5-unsaturated hexuronic acid
ECSA	Eastern, central, southern African
EDTA	Ethylenediaminetetraacetic acid
EEEV	Eastern equine encephalitis virus
ELISA	Enzyme-linked immunosorbent assay
FACS	Fluorescence-activated cell sorting
FBS	Fetal bovine serum
FDA	Food and drug administration
GAG	Glycosaminoglycan
Gal	Galactose
GalNAc	N-acetylgalactosamine

Gas6	Growth arrest-specific gene 6
Glc	Glucose
GlcA	Glucuronic acid
GlcNAc	N-acetylglucosamine
GMK	Green monkey kidney
GPI	Glycosylphosphatidylinositol
h	Hour
HEPES	4-(2-hydroxyethyl)-1-piperazineethanesulfonic acid
HFF	Human foreskin fibroblast
HS	Heparan sulfate
HSase	Heparinase
IdoA	Iduronic acid
IFN	Interferon
IFNAR	Interferon α/β receptor
Ifnlr	Interferon lambda receptor
Ig	Immunoglobulin
IL	Interleukin
IOL	Indian Ocean lineage
IMDM	Iscove modified Dulbecco media
IRES	Internal ribosome entry site
Kb	Kilobase
kDa	Kilodalton
KO	Knock-out

KS	Keratan sulfate
LAV	Live attenuated vaccine
LDLRAD3	Low-density lipoprotein receptor class A domain-containing 3
LR	La Réunion
L-SIGN	Liver-specific intracellular adhesion molecule-3-grabbing non-integrin
mAB	Monoclonal antibody
ManA	2,5-anhydro-mannose
MAYV	Mayaro virus
MEF	Murine embryonic fibroblasts
MFG-E8	Milk fat globule-epidermal growth factor-factor 8
MFI	Median fluorescence intensity
Min	Minute
mM	Millimolar
MOI	Multiplicity of infection
mRNA	Messenger RNA
Mxra8	Matrix remodeling associated protein 8
ND	Not determined
NGL	Neoglycolipid
NH_4Cl	Ammonium chloride
NK cells	Natural killer cells
nm	Nanometer
nM	Nanomolar
NRAMP2	Natural resistance-associated macrophage protein

NS	Not shown
NSAID	Non-steroidal anti-inflammatory drug
nsP	Nonstructural protein
ONNV	O'nyong-nyong virus
ORF	Open reading frame
PAGE	Polyacrylamide gel electrophoresis
PBS	Phosphate-buffered saline
PBS-T	Phosphate-buffered saline with Tween 20
PCR	Polymerase chain reaction
PDB	Protein data bank
PFA	Paraformaldehyde
PFU	Plaque forming unit
PG	Proteoglycan
PHB1	Prohibitin 1
p.i.	Postinfection
PRR	Pattern recognition receptor
PS	Phosphatidylserine
qRT-PCR	Quantitative real time PCR
RANTES	Regulated on activation, normal T cell expressed and secreted
RBS	Relative binding strength
RdRp	RNA dependent RNA polymerase
RNA	Ribonucleic acid
RPMI	Roswell Park Memorial Institute

RRV	Ross River virus
RSV	Respiratory syncytial virus
s	Second
SEM	Standard error of the mean
SFV	Semliki Forest virus
SINV	Sindbis virus
siRNA	Small-interfering RNA
SLRP	Small leucine-rich family of proteoglycans
ssRNA	Single-stranded RNA
TIM-1	T cell immunoglobulin mucin 1
UTR	Untranslated region
VDB	Virus dilution buffer
VEEV	Venezuelan equine encephalitis virus
VLP	Virus-like particle
WA	West African
WEEV	Western equine encephalitis virus
WT	Wildtype
μl	Microliter
USAMRIID	United States Army Medical Institute of Infectious Diseases

Appendix C Collaborative studies on chikungunya virus

Lentscher AJ, McCarthy MK, May NA, Davenport BJ, Montgomery SA, Raghunathan K, **McAllister N**, Silva LA, Morrison TE, Dermody TS. 2020. Chikungunya virus replication in skeletal muscle cells is required for disease development. J Clin Invest. 30(3):1466-1478.

Lentscher AJ*, **McAllister N***, Welsh O, Sutherland D, Griswold K, Silva LA, Dermody TS. Vaccine candidate with increased GAG binding and restricted replication in skeletal muscle protects against challenge with virulent CHIKV. *Manuscript in preparation*.

*, Authors contributed equally.

Appendix D Collaborative studies on reovirus

Brown J, Short S, Stencel-Baerenwald J, Urbanek K, Pruijssers A, **McAllister N**, Taylor G, Aravamudhan P, Khomandiak S, Jabri B, Williams C, Dermody TS. 2018. Reovirus-induced apoptosis in the intestine limits establishment of enteric infection. J Virol 92(10).

Bouziat R*, Hinterleitner R*, Brown JJ*, Stencel-Baerenwald JE, Ikizler M, Discepolo V, Meisel M, Kim SM, Pruijssers AJ, Iskarpatyoti JA, Costes LMM, Lawrence I, Varma M, Zurenski MA, Khomandiak S, Ernest JD, **McAllister N**, Aravamudhan P, Boehme KW, Hu F, Samsom JN, Reinecker HC, Kupfer SS, Guandalini S, Semrad C, Barreiro LB, Xavier RJ, Ng A, Dermody TS, Jabri B. 2017. Reovirus infection breaks tolerance to dietary antigens and promotes development of celiac disease. Science 356(6333): 44-50.

Baldridge MT*, Lee S*, Brown JJ, **McAllister N**, Urbanek K, Dermody TS, Nice TJ, Virgin HW 2017. Expression of *Ifnlr1* on intestinal epithelial cells required for the antiviral effects of IFN-lambda against norovirus and reovirus. J Virol 91(7).

*, Authors contributed equally.

Bibliography

1. Mercer J, Schelhaas M, Helenius A. 2010. Virus entry by endocytosis. Annu Rev Biochem 79:803–833.

2. Marsh M, Helenius A. 2006. Virus entry: open sesame. Cell 124:729–740.

3. Casasnovas JM. 2013. Virus-receptor interactions and receptor-mediated virus entry into host cells. Subcell Biochem 68:441–466.

4. Halstead SB. 2015. Reappearance of chikungunya, formerly called dengue, in the Americas. Emerging Infect Dis 21:557–561.

5. Thiberville S-D, Moyen N, Dupuis-Maguiraga L, Nougairede A, Gould EA, Roques P, de Lamballerie X. 2013. Chikungunya fever: epidemiology, clinical syndrome, pathogenesis and therapy. Antiviral Res 99:345–370.

6. Powers AM, Logue CH. 2007. Changing patterns of chikungunya virus: re-emergence of a zoonotic arbovirus. J Gen Virol 88:2363–2377.

7. Staples JE, Breiman RF, Powers AM. 2009. Chikungunya fever: an epidemiological review of a re-emerging infectious disease. Clin Infect Dis 49:942–948.

8. Schwartz O, Albert ML. 2010. Biology and pathogenesis of chikungunya virus. Nat Rev Microbiol 8:491–500.

9. Gibney KB, Fischer M, Prince HE, Kramer LD, St George K, Kosoy OL, Laven JJ, Staples JE. 2011. Chikungunya fever in the United States: a fifteen year review of cases. Clin Infect Dis 52:e121-6.

10. PAHO. 2018. Geographic Spread of Chikungunya in the Americas December 2013 - December 2017.

11. Silva LA, Dermody TS. 2017. Chikungunya virus: epidemiology, replication, disease mechanisms, and prospective intervention strategies. J Clin Invest 127:737–749.

12. Dupuis-Maguiraga L, Noret M, Brun S, Le Grand R, Gras G, Roques P. 2012. Chikungunya disease: infection-associated markers from the acute to the chronic phase of arbovirus-induced arthralgia. PLoS Negl Trop Dis 6:e1446.

13. Ayu SM, Lai LR, Chan YF, Hatim A, Hairi NN, Ayob A, Sam I-C. 2010. Seroprevalence survey of Chikungunya virus in Bagan Panchor, Malaysia. Am J Trop Med Hyg 83:1245–1248.

14. Schilte C, Staikowsky F, Couderc T, Madec Y, Carpentier F, Kassab S, Albert ML, Lecuit M, Michault A. 2013. Chikungunya virus-associated long-term arthralgia: a 36-month prospective longitudinal study. PLoS Negl Trop Dis 7:e2137.

15. Lemant J, Boisson V, Winer A, Thibault L, André H, Tixier F, Lemercier M, Antok E, Cresta MP, Grivard P, Besnard M, Rollot O, Favier F, Huerre M, Campinos JL, Michault A. 2008. Serious acute chikungunya virus infection requiring intensive care during the Reunion Island outbreak in 2005-2006. Crit Care Med 36:2536–2541.

16. Borgherini G, Poubeau P, Jossaume A, Gouix A, Cotte L, Michault A, Arvin-Berod C, Paganin F. 2008. Persistent arthralgia associated with chikungunya virus: a study of 88 adult patients on Reunion Island. Clin Infect Dis 47:469–475.

17. Soumahoro M-K, Boelle P-Y, Gaüzere B-A, Atsou K, Pelat C, Lambert B, La Ruche G, Gastellu-Etchegorry M, Renault P, Sarazin M, Yazdanpanah Y, Flahault A, Malvy D, Hanslik T. 2011. The Chikungunya epidemic on La Réunion Island in 2005-2006: a cost-of-illness study. PLoS Negl Trop Dis 5:e1197.

18. Chen R, Mukhopadhyay S, Merits A, Bolling B, Nasar F, Coffey LL, Powers A, Weaver SC, Ictv Report Consortium. 2018. ICTV virus taxonomy profile: togaviridae. J Gen Virol 99:761–762.

19. Jose J, Snyder JE, Kuhn RJ. 2009. A structural and functional perspective of alphavirus replication and assembly. Future Microbiol 4:837–856.

20. Brown CR, Moore AT, Young GR, Padhi A, Komar N. 2009. Isolation of Buggy Creek virus (Togaviridae: Alphavirus) from field-collected eggs of Oeciacus vicarius (Hemiptera: Cimicidae). J Med Entomol 46:375–379.

21. Lwande OW, Lutomiah J, Obanda V, Gakuya F, Mutisya J, Mulwa F, Michuki G, Chepkorir E, Fischer A, Venter M, Sang R. 2013. Isolation of tick and mosquito-borne arboviruses from ticks sampled from livestock and wild animal hosts in Ijara District, Kenya. Vector Borne Zoonotic Dis 13:637–642.

22. Weaver SC, Reisen WK. 2010. Present and future arboviral threats. Antiviral Res 85:328–345.

23. Weaver SC, Klimstra WB, Ryman KD. 2008. Togaviruses: General Features, p. 107–116. *In* Encyclopedia of Virology. Elsevier.

24. Jupp PG, McIntosh BM. 1990. Aedes furcifer and other mosquitoes as vectors of chikungunya virus at Mica, northeastern Transvaal, South Africa. J Am Mosq Control Assoc 6:415–420.

25. Carey DE. 1971. Chikungunya and dengue: a case of mistaken identity? J Hist Med Allied Sci 26:243–262.

26. Robinson MC. 1955. An epidemic of virus disease in Southern Province, Tanganyika territory, in 1952-1953. Clinical Features. Trans R Soc Trop Med Hyg 49:28–32.

27. Voss JE, Vaney M-C, Duquerroy S, Vonrhein C, Girard-Blanc C, Crublet E, Thompson A, Bricogne G, Rey FA. 2010. Glycoprotein organization of Chikungunya virus particles revealed by X-ray crystallography. Nature 468:709–712.

28. Khan AH, Morita K, Parquet MDC, Hasebe F, Mathenge EGM, Igarashi A. 2002. Complete nucleotide sequence of chikungunya virus and evidence for an internal polyadenylation site. J Gen Virol 83:3075–3084.

29. Solignat M, Gay B, Higgs S, Briant L, Devaux C. 2009. Replication cycle of chikungunya: a re-emerging arbovirus. Virology 393:183–197.

30. Kuhn RJ. 2013. Togaviridae, p. 629–650. *In* Knipe, DM, Howley, PM (eds.), Fields Virology. Lippincott, Williams, and Wilkins, Philadelphia, Pennsylvania, USA.

31. Natrajan MS, Rojas A, Waggoner JJ. 2019. Beyond fever and pain: diagnostic methods for chikungunya virus. J Clin Microbiol 57.

32. Rudolph KE, Lessler J, Moloney RM, Kmush B, Cummings DAT. 2014. Incubation periods of mosquito-borne viral infections: a systematic review. Am J Trop Med Hyg 90:882–891.

33. Kumar NP, Suresh A, Vanamail P, Sabesan S, Krishnamoorthy KG, Mathew J, Jose VT, Jumbulingam P. 2011. Chikungunya virus outbreak in Kerala, India, 2007: a seroprevalence survey. Mem Inst Oswaldo Cruz 106:912–916.

34. Sissoko D, Ezzedine K, Moendandzé A, Giry C, Renault P, Malvy D. 2010. Field evaluation of clinical features during chikungunya outbreak in Mayotte, 2005-2006. Trop Med Int Health 15:600–607.

35. Gérardin P, Fianu A, Michault A, Mussard C, Boussaïd K, Rollot O, Grivard P, Kassab S, Bouquillard E, Borgherini G, Gaüzère B-A, Malvy D, Bréart G, Favier F. 2013. Predictors of Chikungunya rheumatism: a prognostic survey ancillary to the TELECHIK cohort study. Arthritis Res Ther 15:R9.

36. Thiberville S-D, Boisson V, Gaudart J, Simon F, Flahault A, de Lamballerie X. 2013. Chikungunya fever: a clinical and virological investigation of outpatients on Reunion Island, South-West Indian Ocean. PLoS Negl Trop Dis 7:e2004.

37. Javelle E, Ribera A, Degasne I, Gaüzère B-A, Marimoutou C, Simon F. 2015. Specific management of post-chikungunya rheumatic disorders: a retrospective study of 159 cases in Reunion Island from 2006-2012. PLoS Negl Trop Dis 9:e0003603.

38. Suhrbier A, Jaffar-Bandjee M-C, Gasque P. 2012. Arthritogenic alphaviruses--an overview. Nat Rev Rheumatol 8:420–429.

39. Economopoulou A, Dominguez M, Helynck B, Sissoko D, Wichmann O, Quenel P, Germonneau P, Quatresous I. 2009. Atypical Chikungunya virus infections: clinical manifestations, mortality and risk factors for severe disease during the 2005-2006 outbreak on Réunion. Epidemiol Infect 137:534–541.

40. Tandale BV, Sathe PS, Arankalle VA, Wadia RS, Kulkarni R, Shah SV, Shah SK, Sheth JK, Sudeep AB, Tripathy AS, Mishra AC. 2009. Systemic involvements and fatalities during Chikungunya epidemic in India, 2006. J Clin Virol 46:145–149.

41. Borgherini G, Poubeau P, Staikowsky F, Lory M, Le Moullec N, Becquart JP, Wengling C, Michault A, Paganin F. 2007. Outbreak of chikungunya on Reunion Island: early clinical and laboratory features in 157 adult patients. Clin Infect Dis 44:1401–1407.

42. Das T, Jaffar-Bandjee MC, Hoarau JJ, Krejbich Trotot P, Denizot M, Lee-Pat-Yuen G, Sahoo R, Guiraud P, Ramful D, Robin S, Alessandri JL, Gauzere BA, Gasque P. 2010. Chikungunya fever: CNS infection and pathologies of a re-emerging arbovirus. Prog Neurobiol 91:121–129.

43. Bouquillard E, Combe B. 2009. A report of 21 cases of rheumatoid arthritis following Chikungunya fever. A mean follow-up of two years. Joint Bone Spine 76:654–657.

44. Ribéra A, Degasne I, Jaffar Bandjee MC, Gasque P. 2012. [Chronic rheumatic manifestations following chikungunya virus infection: clinical description and therapeutic considerations]. Med Trop (Mars) 72 Spec No:83–85.

45. Abdelnabi R, Neyts J, Delang L. 2015. Towards antivirals against chikungunya virus. Antiviral Res 121:59–68.

46. Ashbrook AW, Lentscher AJ, Zamora PF, Silva LA, May NA, Bauer JA, Morrison TE, Dermody TS. 2016. Antagonism of the Sodium-Potassium ATPase Impairs Chikungunya Virus Infection. MBio 7.

47. Gigante A, Canela M-D, Delang L, Priego E-M, Camarasa M-J, Querat G, Neyts J, Leyssen P, Pérez-Pérez M-J. 2014. Identification of [1,2,3]triazolo[4,5-d]pyrimidin-7(6H)-ones as novel inhibitors of Chikungunya virus replication. J Med Chem 57:4000–4008.

48. Kaur P, Thiruchelvan M, Lee RCH, Chen H, Chen KC, Ng ML, Chu JJH. 2013. Inhibition of chikungunya virus replication by harringtonine, a novel antiviral that suppresses viral protein expression. Antimicrob Agents Chemother 57:155–167.

49. Lucas-Hourani M, Lupan A, Desprès P, Thoret S, Pamlard O, Dubois J, Guillou C, Tangy F, Vidalain P-O, Munier-Lehmann H. 2013. A phenotypic assay to identify Chikungunya virus inhibitors targeting the nonstructural protein nsP2. J Biomol Screen 18:172–179.

50. Bassetto M, De Burghgraeve T, Delang L, Massarotti A, Coluccia A, Zonta N, Gatti V, Colombano G, Sorba G, Silvestri R, Tron GC, Neyts J, Leyssen P, Brancale A. 2013. Computer-aided identification, design and synthesis of a novel series of compounds with selective antiviral activity against chikungunya virus. Antiviral Res 98:12–18.

51. Das PK, Puusepp L, Varghese FS, Utt A, Ahola T, Kananovich DG, Lopp M, Merits A, Karelson M. 2016. Design and validation of novel chikungunya virus protease inhibitors. Antimicrob Agents Chemother 60:7382–7395.

52. Delang L, Segura Guerrero N, Tas A, Quérat G, Pastorino B, Froeyen M, Dallmeier K, Jochmans D, Herdewijn P, Bello F, Snijder EJ, de Lamballerie X, Martina B, Neyts J, van Hemert MJ, Leyssen P. 2014. Mutations in the chikungunya virus non-structural proteins cause resistance to favipiravir (T-705), a broad-spectrum antiviral. J Antimicrob Chemother 69:2770–2784.

53. Briolant S, Garin D, Scaramozzino N, Jouan A, Crance JM. 2004. In vitro inhibition of Chikungunya and Semliki Forest viruses replication by antiviral compounds: synergistic effect of interferon-α and ribavirin combination. Antiviral Res 61:111–117.

54. Albulescu IC, van Hoolwerff M, Wolters LA, Bottaro E, Nastruzzi C, Yang SC, Tsay S-C, Hwu JR, Snijder EJ, van Hemert MJ. 2015. Suramin inhibits chikungunya virus replication through multiple mechanisms. Antiviral Res 121:39–46.

55. Ravichandran R, Manian M. 2008. Ribavirin therapy for Chikungunya arthritis. J Infect Dev Ctries 2:140–142.

56. Couderc T, Chrétien F, Schilte C, Disson O, Brigitte M, Guivel-Benhassine F, Touret Y, Barau G, Cayet N, Schuffenecker I, Desprès P, Arenzana-Seisdedos F, Michault A, Albert ML, Lecuit M. 2008. A mouse model for Chikungunya: young age and inefficient type-I interferon signaling are risk factors for severe disease. PLoS Pathog 4:e29.

57. Lum F-M, Teo T-H, Lee WWL, Kam Y-W, Rénia L, Ng LFP. 2013. An essential role of antibodies in the control of Chikungunya virus infection. J Immunol 190:6295–6302.

58. Hawman DW, Fox JM, Ashbrook AW, May NA, Schroeder KMS, Torres RM, Crowe JE, Dermody TS, Diamond MS, Morrison TE. 2016. Pathogenic chikungunya virus evades B cell responses to establish persistence. Cell Rep 16:1326–1338.

59. Hawman DW, Stoermer KA, Montgomery SA, Pal P, Oko L, Diamond MS, Morrison TE. 2013. Chronic joint disease caused by persistent Chikungunya virus infection is controlled by the adaptive immune response. J Virol 87:13878–13888.

60. Pal P, Dowd KA, Brien JD, Edeling MA, Gorlatov S, Johnson S, Lee I, Akahata W, Nabel GJ, Richter MKS, Smit JM, Fremont DH, Pierson TC, Heise MT, Diamond MS. 2013. Development of a highly protective combination monoclonal antibody therapy against Chikungunya virus. PLoS Pathog 9:e1003312.

61. Goh LYH, Hobson-Peters J, Prow NA, Gardner J, Bielefeldt-Ohmann H, Pyke AT, Suhrbier A, Hall RA. 2013. Neutralizing monoclonal antibodies to the E2 protein of chikungunya virus protects against disease in a mouse model. Clin Immunol 149:487–497.

62. Fric J, Bertin-Maghit S, Wang C-I, Nardin A, Warter L. 2013. Use of human monoclonal antibodies to treat Chikungunya virus infection. J Infect Dis 207:319–322.

63. Broeckel R, Fox JM, Haese N, Kreklywich CN, Sukulpovi-Petty S, Legasse A, Smith PP, Denton M, Corvey C, Krishnan S, Colgin LMA, Ducore RM, Lewis AD, Axthelm MK, Mandron M, Cortez P, Rothblatt J, Rao E, Focken I, Carter K, Sapparapau G, Crowe JE, Diamond MS, Streblow DN. 2017. Therapeutic administration of a recombinant human monoclonal antibody reduces the severity of chikungunya virus disease in rhesus macaques. PLoS Negl Trop Dis 11:e0005637.

64. Harrison VR, Eckels KH, Bartelloni PJ, Hampton C. 1971. Production and evaluation of a formalin-killed Chikungunya vaccine. J Immunol 107:643–647.

65. Levitt NH, Ramsburg HH, Hasty SE, Repik PM, Cole FE, Lupton HW. 1986. Development of an attenuated strain of chikungunya virus for use in vaccine production. Vaccine 4:157–162.

66. Silva LA, Khomandiak S, Ashbrook AW, Weller R, Heise MT, Morrison TE, Dermody TS. 2014. A single-amino-acid polymorphism in Chikungunya virus E2 glycoprotein influences glycosaminoglycan utilization. J Virol 88:2385–2397.

67. Ashbrook AW, Burrack KS, Silva LA, Montgomery SA, Heise MT, Morrison TE, Dermody TS. 2014. Residue 82 of the Chikungunya virus E2 attachment protein modulates viral dissemination and arthritis in mice. J Virol 88:12180–12192.

68. Gorchakov R, Wang E, Leal G, Forrester NL, Plante K, Rossi SL, Partidos CD, Adams AP, Seymour RL, Weger J, Borland EM, Sherman MB, Powers AM, Osorio JE, Weaver SC. 2012. Attenuation of Chikungunya virus vaccine strain 181/clone 25 is determined by two amino acid substitutions in the E2 envelope glycoprotein. J Virol 86:6084–6096.

69. Edelman R, Tacket CO, Wasserman SS, Bodison SA, Perry JG, Mangiafico JA. 2000. Phase II safety and immunogenicity study of live chikungunya virus vaccine TSI-GSD-218. Am J Trop Med Hyg 62:681–685.

70. Schwameis M, Buchtele N, Wadowski PP, Schoergenhofer C, Jilma B. 2016. Chikungunya vaccines in development. Hum Vaccin Immunother 12:716–731.

71. Plante K, Wang E, Partidos CD, Weger J, Gorchakov R, Tsetsarkin K, Borland EM, Powers AM, Seymour R, Stinchcomb DT, Osorio JE, Frolov I, Weaver SC. 2011. Novel chikungunya vaccine candidate with an IRES-based attenuation and host range alteration mechanism. PLoS Pathog 7:e1002142.

72. Roy CJ, Adams AP, Wang E, Plante K, Gorchakov R, Seymour RL, Vinet-Oliphant H, Weaver SC. 2014. Chikungunya vaccine candidate is highly attenuated and protects nonhuman primates against telemetrically monitored disease following a single dose. J Infect Dis 209:1891–1899.

73. Chen GL, Coates EE, Plummer SH, Carter CA, Berkowitz N, Conan-Cibotti M, Cox JH, Beck A, O'Callahan M, Andrews C, Gordon IJ, Larkin B, Lampley R, Kaltovich F, Gall J, Carlton K, Mendy J, Haney D, May J, Bray A, Bailer RT, Dowd KA, Brockett B, Gordon D, Koup RA, Schwartz R, Mascola JR, Graham BS, Pierson TC, Donastorg Y, Rosario N,

Pape JW, Hoen B, Cabié A, Diaz C, Ledgerwood JE, VRC 704 Study Team. 2020. Effect of a Chikungunya Virus-Like Particle Vaccine on Safety and Tolerability Outcomes: A Randomized Clinical Trial. JAMA 323:1369–1377.

74. Akahata W, Yang Z-Y, Andersen H, Sun S, Holdaway HA, Kong W-P, Lewis MG, Higgs S, Rossmann MG, Rao S, Nabel GJ. 2010. A virus-like particle vaccine for epidemic Chikungunya virus protects nonhuman primates against infection. Nat Med 16:334–338.

75. Chang L-J, Dowd KA, Mendoza FH, Saunders JG, Sitar S, Plummer SH, Yamshchikov G, Sarwar UN, Hu Z, Enama ME, Bailer RT, Koup RA, Schwartz RM, Akahata W, Nabel GJ, Mascola JR, Pierson TC, Graham BS, Ledgerwood JE, VRC 311 Study Team. 2014. Safety and tolerability of chikungunya virus-like particle vaccine in healthy adults: a phase 1 dose-escalation trial. Lancet 384:2046–2052.

76. Gao S, Song S, Zhang L. 2019. Recent progress in vaccine development against chikungunya virus. Front Microbiol 10:2881.

77. Volk SM, Chen R, Tsetsarkin KA, Adams AP, Garcia TI, Sall AA, Nasar F, Schuh AJ, Holmes EC, Higgs S, Maharaj PD, Brault AC, Weaver SC. 2010. Genome-scale phylogenetic analyses of chikungunya virus reveal independent emergences of recent epidemics and various evolutionary rates. J Virol 84:6497–6504.

78. Diallo D, Sall AA, Buenemann M, Chen R, Faye O, Diagne CT, Faye O, Ba Y, Dia I, Watts D, Weaver SC, Hanley KA, Diallo M. 2012. Landscape ecology of sylvatic chikungunya virus and mosquito vectors in Souteastern Senegal. PLoS Negl Trop Dis 6:e1649.

79. Diallo M, Thonnon J, Traore-Lamizana M, Fontenille D. 1999. Vectors of Chikungunya virus in Senegal: current data and transmission cycles. Am J Trop Med Hyg 60:281–286.

80. Weaver SC. 2006. Evolutionary influences in arboviral disease. Curr Top Microbiol Immunol 299:285–314.

81. Hammon WM, Rundnick A, Sather GE. 1960. Viruses associated with epidemic hemorrhagic fevers of the Philippines and Thailand. Science 131:1102–1103.

82. Powers AM, Brault AC, Tesh RB, Weaver SC. 2000. Re-emergence of Chikungunya and O'nyong-nyong viruses: evidence for distinct geographical lineages and distant evolutionary relationships. J Gen Virol 81:471–479.

83. Lentscher A. Tissue-Restricted Chikungunya Virus Is Attenuated in Mice and Protective Against Virulent Virus Challenge.

84. de Lamballerie X, Leroy E, Charrel RN, Ttsetsarkin K, Higgs S, Gould EA. 2008. Chikungunya virus adapts to tiger mosquito via evolutionary convergence: a sign of things to come? Virol J 5:33.

85. Rezza G, Nicoletti L, Angelini R, Romi R, Finarelli AC, Panning M, Cordioli P, Fortuna C, Boros S, Magurano F, Silvi G, Angelini P, Dottori M, Ciufolini MG, Majori GC,

Cassone A, CHIKV study group. 2007. Infection with chikungunya virus in Italy: an outbreak in a temperate region. Lancet 370:1840–1846.

86. Grandadam M, Caro V, Plumet S, Thiberge JM, Souarès Y, Failloux A-B, Tolou HJ, Budelot M, Cosserat D, Leparc-Goffart I, Desprès P. 2011. Chikungunya virus, southeastern France. Emerging Infect Dis 17:910–913.

87. Tsetsarkin KA, Vanlandingham DL, McGee CE, Higgs S. 2007. A single mutation in chikungunya virus affects vector specificity and epidemic potential. PLoS Pathog 3:e201.

88. Tsetsarkin KA, Chen R, Leal G, Forrester N, Higgs S, Huang J, Weaver SC. 2011. Chikungunya virus emergence is constrained in Asia by lineage-specific adaptive landscapes. Proc Natl Acad Sci USA 108:7872–7877.

89. Cassadou S, Boucau S, Petit-Sinturel M, Huc P, Leparc-Goffart I, Ledrans M. 2014. Emergence of chikungunya fever on the French side of Saint Martin Island, October to December 2013. Euro Surveill 19.

90. Geographic Distribution | Chikungunya virus | CDC.

91. Kraemer MUG, Sinka ME, Duda KA, Mylne AQN, Shearer FM, Barker CM, Moore CG, Carvalho RG, Coelho GE, Van Bortel W, Hendrickx G, Schaffner F, Elyazar IRF, Teng H-J, Brady OJ, Messina JP, Pigott DM, Scott TW, Smith DL, Wint GRW, Golding N, Hay SI. 2015. The global distribution of the arbovirus vectors Aedes aegypti and Ae. albopictus. Elife 4:e08347.

92. Sourisseau M, Schilte C, Casartelli N, Trouillet C, Guivel-Benhassine F, Rudnicka D, Sol-Foulon N, Le Roux K, Prevost M-C, Fsihi H, Frenkiel M-P, Blanchet F, Afonso PV, Ceccaldi P-E, Ozden S, Gessain A, Schuffenecker I, Verhasselt B, Zamborlini A, Saïb A, Rey FA, Arenzana-Seisdedos F, Desprès P, Michault A, Albert ML, Schwartz O. 2007. Characterization of reemerging chikungunya virus. PLoS Pathog 3:e89.

93. van Duijl-Richter MKS, Hoornweg TE, Rodenhuis-Zybert IA, Smit JM. 2015. Early Events in Chikungunya Virus Infection-From Virus Cell Binding to Membrane Fusion. Viruses 7:3647–3674.

94. Wintachai P, Wikan N, Kuadkitkan A, Jaimipuk T, Ubol S, Pulmanausahakul R, Auewarakul P, Kasinrerk W, Weng W-Y, Panyasrivanit M, Paemanee A, Kittisenachai S, Roytrakul S, Smith DR. 2012. Identification of prohibitin as a Chikungunya virus receptor protein. J Med Virol 84:1757–1770.

95. Moller-Tank S, Kondratowicz AS, Davey RA, Rennert PD, Maury W. 2013. Role of the phosphatidylserine receptor TIM-1 in enveloped-virus entry. J Virol 87:8327–8341.

96. Fongsaran C, Jirakanwisal K, Kuadkitkan A, Wikan N, Wintachai P, Thepparit C, Ubol S, Phaonakrop N, Roytrakul S, Smith DR. 2014. Involvement of ATP synthase β subunit in chikungunya virus entry into insect cells. Arch Virol 159:3353–3364.

97. Klimstra WB, Nangle EM, Smith MS, Yurochko AD, Ryman KD. 2003. DC-SIGN and L-SIGN can act as attachment receptors for alphaviruses and distinguish between mosquito cell- and mammalian cell-derived viruses. J Virol 77:12022–12032.

98. Carnec X, Meertens L, Dejarnac O, Perera-Lecoin M, Hafirassou ML, Kitaura J, Ramdasi R, Schwartz O, Amara A. 2016. The phosphatidylserine and phosphatidylethanolamine receptor cd300a binds dengue virus and enhances infection. J Virol 90:92–102.

99. Weber C, Berberich E, von Rhein C, Henß L, Hildt E, Schnierle BS. 2017. Identification of functional determinants in the chikungunya virus E2 protein. PLoS Negl Trop Dis 11:e0005318.

100. Tanaka A, Tumkosit U, Nakamura S, Motooka D, Kishishita N, Priengprom T, Sa-Ngasang A, Kinoshita T, Takeda N, Maeda Y. 2017. Genome-Wide Screening Uncovers the Significance of N-Sulfation of Heparan Sulfate as a Host Cell Factor for Chikungunya Virus Infection. J Virol 91.

101. Koehler M, Delguste M, Sieben C, Gillet L, Alsteens D. 2020. Initial Step of Virus Entry: Virion Binding to Cell-Surface Glycans. Annu Rev Virol.

102. Zhang R, Kim AS, Fox JM, Nair S, Basore K, Klimstra WB, Rimkunas R, Fong RH, Lin H, Poddar S, Crowe JE, Doranz BJ, Fremont DH, Diamond MS. 2018. Mxra8 is a receptor for multiple arthritogenic alphaviruses. Nature 557:570–574.

103. Bernard E, Solignat M, Gay B, Chazal N, Higgs S, Devaux C, Briant L. 2010. Endocytosis of chikungunya virus into mammalian cells: role of clathrin and early endosomal compartments. PLoS One 5:e11479.

104. Hoornweg TE, van Duijl-Richter MKS, Ayala Nuñez NV, Albulescu IC, van Hemert MJ, Smit JM. 2016. Dynamics of Chikungunya Virus Cell Entry Unraveled by Single-Virus Tracking in Living Cells. J Virol 90:4745–4756.

105. Strauss EG, Rice CM, Strauss JH. 1983. Sequence coding for the alphavirus nonstructural proteins is interrupted by an opal termination codon. Proc Natl Acad Sci USA 80:5271–5275.

106. Lemm JA, Rümenapf T, Strauss EG, Strauss JH, Rice CM. 1994. Polypeptide requirements for assembly of functional Sindbis virus replication complexes: a model for the temporal regulation of minus- and plus-strand RNA synthesis. EMBO J 13:2925–2934.

107. Shirako Y, Strauss JH. 1994. Regulation of Sindbis virus RNA repliation: uncleaved P123 and nsP4 function in minus-strand RNA synthesis, whereas cleaved products from P123 are required for efficient plus-strand RNA synthesis. J Virol 68:1874–1885.

108. Frolova EI, Gorchakov R, Pereboeva L, Atasheva S, Frolov I. 2010. Functional Sindbis virus replicative complexes are formed at the plasma membrane. J Virol 84:11679–11695.

109. Kujala P, Ikaheimonen A, Ehsani N, Vihinen H, Auvinien P, Kaariainen L. 2001. Biogenesis of Semliki Forest virus RNA replication complex. J Virol 75:3873–3884.

110. Hardy WR, Strauss JH. 1989. Processing of the nonstructural proteins of Sindbis virus: nonstructural proteinase is in the C-terminal half of nsP2 and functions both in. J Virol 63:4653–4664.

111. Liljeström P, Garoff H. 1991. Internally located cleavable signal sequences direct the formation of Semliki Forest virus membrane proteins from a polyprotein precursor. J Virol 65:147–154.

112. Aliperti G, Schlesinger MJ. 1978. Evidence for an autoprotease activity of Sindbis virus capsid protein. Virology 90:366–369.

113. de Curtis I, Simons K. 1988. Dissection of Semliki Forest virus glycoprotein delivery from the trans-Golgi network to the cell surface in permeabilized BHK cells. Proc Natl Acad Sci USA 85:8052–8056.

114. Moehring JM, Inocencio NM, Robertson BJ, Moehring TJ. 1993. Expression of mouse furin in a Chinese hamster cell resistant to. J Biol Chem 268:2590–2594.

115. Ryan C, Ivanova L, Schlesinger MJ. 1998. Effects of site-directed mutations of transmembrane cysteines in Sindbis virus E1 and E2 glycoproteins on palmitylation and virus replication. Virology 249:62–67.

116. Ivanova L, Schlesinger MJ. 1993. Site-directed mutations in the Sindbis virus E2 glycoprotein identify palmitoylation sites and affect virus budding. J Virol 67:2546–2551.

117. Firth AE, Chung BY, Fleeton MN, Atkins JF. 2008. Discovery of frameshifting in Alphavirus 6K resolves a 20-year enigma. Virol J 5:108.

118. Soonsawad P, Xing L, Milla E, Espinoza JM, Kawano M, Marko M, Hsieh C, Furukawa H, Kawasaki M, Weerachatyanukul W, Srivastava R, Barnett SW, Srivastava IK, Cheng RH. 2010. Structural evidence of glycoprotein assembly in cellular membrane compartments prior to Alphavirus budding. J Virol 84:11145–11151.

119. Sjöberg M, Garoff H. 2003. Interactions between the transmembrane segments of the alphavirus E1 and E2 proteins play a role in virus budding and fusion. J Virol 77:3441–3450.

120. Chen KC, Kam Y-W, Lin RTP, Ng MM-L, Ng LF, Chu JJH. 2013. Comparative analysis of the genome sequences and replication profiles of chikungunya virus isolates within the East, Central and South African (ECSA) lineage. Virol J 10:169.

121. Bosco-Lauth AM, Nemeth NM, Kohler DJ, Bowen RA. 2016. Viremia in North American Mammals and Birds After Experimental Infection with Chikungunya Viruses. Am J Trop Med Hyg 94:504–506.

122. Guilherme JM, Gonella-Legall C, Legall F, Nakoume E, Vincent J. 1996. Seroprevalence of five arboviruses in Zebu cattle in the Central African Republic. Trans R Soc Trop Med Hyg 90:31–33.

123. McCrae AW, Henderson BE, Kirya BG, Sempala SD. 1971. Chikungunya virus in the Entebbe area of Uganda: isolations and epidemiology. Trans R Soc Trop Med Hyg 65:152–168.

124. Acharya D, Paul AM, Anderson JF, Huang F, Bai F. 2015. Loss of Glycosaminoglycan Receptor Binding after Mosquito Cell Passage Reduces Chikungunya Virus Infectivity. PLoS Negl Trop Dis 9:e0004139.

125. Fredericks AC, Russell TA, Wallace LE, Davidson AD, Fernandez-Sesma A, Maringer K. 2019. Aedes aegypti (Aag2)-derived clonal mosquito cell lines reveal the effects of pre-existing persistent infection with the insect-specific bunyavirus Phasi Charoen-like virus on arbovirus replication. PLoS Negl Trop Dis 13:e0007346.

126. Vedururu RK, Neave MJ, Sundaramoorthy V, Green D, Harper JA, Gorry PR, Duchemin J-B, Paradkar PN. 2019. Whole Transcriptome Analysis of Aedes albopictus Mosquito Head and Thorax Post-Chikungunya Virus Infection. Pathogens 8.

127. Vedururu RK, Neave MJ, Tachedjian M, Klein MJ, Gorry PR, Duchemin J-B, Paradkar PN. 2019. RNASeq Analysis of Aedes albopictus Mosquito Midguts after Chikungunya Virus Infection. Viruses 11.

128. Sudeep AB, Vyas PB, Parashar D, Shil P. 2019. Differential susceptibility & replication potential of Vero E6, BHK-21, RD, A-549, C6/36 cells & Aedes aegypti mosquitoes to three strains of chikungunya virus. Indian J Med Res 149:771–777.

129. Pal P, Fox JM, Hawman DW, Huang Y-JS, Messaoudi I, Kreklywich C, Denton M, Legasse AW, Smith PP, Johnson S, Axthelm MK, Vanlandingham DL, Streblow DN, Higgs S, Morrison TE, Diamond MS. 2014. Chikungunya viruses that escape monoclonal antibody therapy are clinically attenuated, stable, and not purified in mosquitoes. J Virol 88:8213–8226.

130. Dong S, Balaraman V, Kantor AM, Lin J, Grant DG, Held NL, Franz AWE. 2017. Chikungunya virus dissemination from the midgut of *Aedes aegypti* is associated with temporal basal lamina degradation during bloodmeal digestion. PLoS Negl Trop Dis 11:e0005976.

131. Merwaiss F, Filomatori CV, Susuki Y, Bardossy ES, Alvarez DE, Saleh M-C. 2020. “Chikungunya virus replication rate determines the capacity of crossing tissue barriers in mosquitoes”. J Virol.

132. Zhang R, Earnest JT, Kim AS, Winkler ES, Desai P, Adams LJ, Hu G, Bullock C, Gold B, Cherry S, Diamond MS. 2019. Expression of the mxra8 receptor promotes alphavirus infection and pathogenesis in mice and drosophila. Cell Rep 28:2647–2658.e5.

133. Matusali G, Colavita F, Bordi L, Lalle E, Ippolito G, Capobianchi MR, Castilletti C. 2019. Tropism of the chikungunya virus. Viruses 11.

134. Franz AWE, Kantor AM, Passarelli AL, Clem RJ. 2015. Tissue barriers to arbovirus infection in mosquitoes. Viruses 7:3741–3767.

135. McFarlane M, Arias-Goeta C, Martin E, O'Hara Z, Lulla A, Mousson L, Rainey SM, Misbah S, Schnettler E, Donald CL, Merits A, Kohl A, Failloux A-B. 2014. Characterization of *Aedes aegypti* innate-immune pathways that limit chikungunya virus replication. PLoS Negl Trop Dis 8:e2994.

136. Sirisena PDNN, Kumar A, Sunil S. 2018. Evaluation of Aedes aegypti (Diptera: Culicidae) Life Table Attributes Upon Chikungunya Virus Replication Reveals Impact on Egg-Laying Pathways. J Med Entomol 55:1580–1587.

137. Wong HV, Chan YF, Sam I-C, Sulaiman WYW, Vythilingam I. 2016. Chikungunya virus infection of aedes mosquitoes. Methods Mol Biol 1426:119–128.

138. Vega-Rúa A, Schmitt C, Bonne I, Krijnse Locker J, Failloux A-B. 2015. Chikungunya virus replication in salivary glands of the mosquito *Aedes albopictus*. Viruses 7:5902–5907.

139. Haese NN, Broeckel RM, Hawman DW, Heise MT, Morrison TE, Streblow DN. 2016. Animal models of chikungunya virus infection and disease. J Infect Dis 214:S482–S487.

140. Broeckel RM, Haese NN, Messaoudi I, Streblow DN. 2015. Nonhuman primate models of chikungunya virus infection and disease. Pathogens 4:662–681.

141. Schilte C, Couderc T, Chretien F, Sourisseau M, Gangneux N, Guivel-Benhassine F, Kraxner A, Tschopp J, Higgs S, Michault A, Arenzana-Seisdedos F, Colonna M, Peduto L, Schwartz O, Lecuit M, Albert ML. 2010. Type I IFN controls chikungunya virus via its action on nonhematopoietic cells. J Exp Med 207:429–442.

142. Young AR, Locke MC, Cook LE, Hiller BE, Zhang R, Hedberg ML, Monte KJ, Veis DJ, Diamond MS, Lenschow DJ. 2019. Dermal and muscle fibroblasts and skeletal myofibers survive chikungunya virus infection and harbor persistent RNA. PLoS Pathog 15:e1007993.

143. Puiprom O, Morales Vargas RE, Potiwat R, Chaichana P, Ikuta K, Ramasoota P, Okabayashi T. 2013. Characterization of chikungunya virus infection of a human keratinocyte cell line: role of mosquito salivary gland protein in suppressing the host immune response. Infect Genet Evol 17:210–215.

144. Bernard E, Hamel R, Neyret A, Ekchariyawat P, Molès J-P, Simmons G, Chazal N, Desprès P, Missé D, Briant L. 2015. Human keratinocytes restrict chikungunya virus replication at a post-fusion step. Virology 476:1–10.

145. Rudd PA, Wilson J, Gardner J, Larcher T, Babarit C, Le TT, Anraku I, Kumagai Y, Loo Y-M, Gale M, Akira S, Khromykh AA, Suhrbier A. 2012. Interferon response factors 3 and 7 protect agianst chikungunya virus hemorrhagic fever and shock. J Virol 86:9888–9898.

146. Her Z, Malleret B, Chan M, Ong EKS, Wong S-C, Kwek DJC, Tolou H, Lin RTP, Tambyah PA, Rénia L, Ng LFP. 2010. Active infection of human blood monocytes by Chikungunya virus triggers an innate immune response. J Immunol 184:5903–5913.

147. Labadie K, Larcher T, Joubert C, Mannioui A, Delache B, Brochard P, Guigand L, Dubreil L, Lebon P, Verrier B, de Lamballerie X, Suhrbier A, Cherel Y, Le Grand R, Roques P. 2010. Chikungunya disease in nonhuman primates involves long-term viral persistence in macrophages. J Clin Invest 120:894–906.

148. Gardner J, Anraku I, Le TT, Larcher T, Major L, Roques P, Schroder WA, Higgs S, Suhrbier A. 2010. Chikungunya virus arthritis in adult wild-type mice. J Virol 84:8021–8032.

149. Morrison TE, Oko L, Montgomery SA, Whitmore AC, Lotstein AR, Gunn BM, Elmore SA, Heise MT. 2011. A mouse model of chikungunya virus-induced musculoskeletal inflammatory disease: evidence of arthritis, tenosynovitis, myositis, and persistence. Am J Pathol 178:32–40.

150. Panning M, Grywna K, van Esbroeck M, Emmerich P, Drosten C. 2008. Chikungunya fever in travelers returning to Europe from the Indian Ocean region, 2006. Emerging Infect Dis 14:416–422.

151. Hoarau J-J, Jaffar Bandjee M-C, Krejbich Trotot P, Das T, Li-Pat-Yuen G, Dassa B, Denizot M, Guichard E, Ribera A, Henni T, Tallet F, Moiton MP, Gauzère BA, Bruniquet S, Jaffar Bandjee Z, Morbidelli P, Martigny G, Jolivet M, Gay F, Grandadam M, Tolou H, Vieillard V, Debré P, Autran B, Gasque P. 2010. Persistent chronic inflammation and infection by Chikungunya arthritogenic alphavirus in spite of a robust host immune response. J Immunol 184:5914–5927.

152. Phuklia W, Kasisith J, Modhiran N, Rodpai E, Thannagith M, Thongsakulprasert T, Smith DR, Ubol S. 2013. Osteoclastogenesis induced by CHIKV-infected fibroblast-like synoviocytes: a possible interplay between synoviocytes and monocytes/macrophages in CHIKV-induced arthralgia/arthritis. Virus Res 177:179–188.

153. Noret M, Herrero L, Rulli N, Rolph M, Smith PN, Li RW, Roques P, Gras G, Mahalingam S. 2012. Interleukin 6, RANKL, and osteoprotegerin expression by chikungunya virus-infected human osteoblasts. J Infect Dis 206:455–7: 457.

154. Ozden S, Huerre M, Riviere J-P, Coffey LL, Afonso PV, Mouly V, de Monredon J, Roger J-C, El Amrani M, Yvin J-L, Jaffar M-C, Frenkiel M-P, Sourisseau M, Schwartz O, Butler-Browne G, Desprès P, Gessain A, Ceccaldi P-E. 2007. Human muscle satellite cells as targets of Chikungunya virus infection. PLoS One 2:e527.

155. Dhanwani R, Khan M, Bhaskar ASB, Singh R, Patro IK, Rao PVL, Parida MM. 2012. Characterization of Chikungunya virus infection in human neuroblastoma SH-SY5Y cells: role of apoptosis in neuronal cell death. Virus Res 163:563–572.

156. Abraham R, Mudaliar P, Padmanabhan A, Sreekumar E. 2013. Induction of cytopathogenicity in human glioblastoma cells by chikungunya virus. PLoS One 8:e75854.

157. Abraham R, Singh S, Nair SR, Hulyalkar NV, Surendran A, Jaleel A, Sreekumar E. 2017. Nucleophosmin (NPM1)/B23 in the proteome of human astrocytic cells restricts chikungunya virus replication. J Proteome Res 16:4144–4155.

158. Abere B, Wikan N, Ubol S, Auewarakul P, Paemanee A, Kittisenachai S, Roytrakul S, Smith DR. 2012. Proteomic analysis of chikungunya virus infected microglial cells. PLoS One 7.

159. Wei Chiam C, Fun Chan Y, Chai Ong K, Thong Wong K, Sam I-C. 2015. Neurovirulence comparison of chikungunya virus isolates of the Asian and East/Central/South African genotypes from Malaysia. J Gen Virol 96:3243–3254.

160. Couderc T, Gangneux N, Chrétien F, Caro V, Le Luong T, Ducloux B, Tolou H, Lecuit M, Grandadam M. 2012. Chikungunya virus infection of corneal grafts. J Infect Dis 206:851–859.

161. Lisa F. P. Ng, Angela Chow, Yong-Jiang Sun, Dyan J. C. Kwek, Poh-Lian Lim, Frederico Dimatatac, Lee-Ching Ng, Eng-Eong Ooi, Khar-Heng Choo, Zhisheng Her, Philippe Kourilsky, Yee-Sin Leo. 2009. IL-1β, IL-6, and RANTES as biomarkers of chikungunya severity. PLos One.

162. Kelvin AA, Banner D, Silvi G, Moro ML, Spataro N, Gaibani P, Cavrini F, Pierro A, Rossini G, Cameron MJ, Bermejo-Martin JF, Paquette SG, Xu L, Danesh A, Farooqui A, Borghetto I, Kelvin DJ, Sambri V, Rubino S. 2011. Inflammatory cytokine expression is associated with chikungunya virus resolution and symptom severity. PLoS Negl Trop Dis 5:e1279.

163. Chow A, Her Z, Ong EKS, Chen J, Dimatatac F, Kwek DJC, Barkham T, Yang H, Rénia L, Leo Y-S, Ng LFP. 2011. Persistent arthralgia induced by Chikungunya virus infection is associated with interleukin-6 and granulocyte macrophage colony-stimulating factor. J Infect Dis 203:149–157.

164. Wauquier N, Becquart P, Nkoghe D, Padilla C, Ndjoyi-Mbiguino A, Leroy EM. 2011. The acute phase of Chikungunya virus infection in humans is associated with strong innate immunity and T CD8 cell activation. J Infect Dis 204:115–123.

165. Gardner CL, Hritz J, Sun C, Vanlandingham DL, Song TY, Ghedin E, Higgs S, Klimstra WB, Ryman KD. 2014. Deliberate attenuation of chikungunya virus by adaptation to heparan sulfate-dependent infectivity: a model for rational arboviral vaccine design. PLoS Negl Trop Dis 8:e2719.

166. Rulli NE, Rolph MS, Srikiatkhachorn A, Anantapreecha S, Guglielmotti A, Mahalingam S. 2011. Protection from arthritis and myositis in a mouse model of acute chikungunya virus disease by bindarit, an inhibitor of monocyte chemotactic protein-1 synthesis. J Infect Dis 204:1026–1030.

167. Chen W, Foo S-S, Taylor A, Lulla A, Merits A, Hueston L, Forwood MR, Walsh NC, Sims NA, Herrero LJ, Mahalingam S. 2015. Bindarit, an inhibitor of monocyte chemotactic protein synthesis, protects against bone loss induced by chikungunya virus infection. J Virol 89:581–593.

168. Poo YS, Nakaya H, Gardner J, Larcher T, Schroder WA, Le TT, Major LD, Suhrbier A. 2014. CCR2 deficiency promotes exacerbated chronic erosive neutrophil-dominated chikungunya virus arthritis. J Virol 88:6862–6872.

169. Stoermer KA, Burrack A, Oko L, Montgomery SA, Borst LB, Gill RG, Morrison TE. 2012. Genetic ablation of arginase 1 in macrophages and neutrophils enhances clearance of an arthritogenic alphavirus. J Immunol 189:4047–4059.

170. Petitdemange C, Becquart P, Wauquier N, Béziat V, Debré P, Leroy EM, Vieillard V. 2011. Unconventional repertoire profile is imprinted during acute chikungunya infection for natural killer cells polarization toward cytotoxicity. PLoS Pathog 7:e1002268.

171. Teo T-H, Lum F-M, Claser C, Lulla V, Lulla A, Merits A, Rénia L, Ng LFP. 2013. A pathogenic role for CD4+ T cells during Chikungunya virus infection in mice. J Immunol 190:259–269.

172. Teo T-H, Lum F-M, Lee WWL, Ng LFP. 2012. Mouse models for Chikungunya virus: deciphering immune mechanisms responsible for disease and pathology. Immunol Res 53:136–147.

173. Davenport BJ, Bullock C, McCarthy MK, Hawman DW, Murphy KM, Kedl RM, Diamond MS, Morrison TE. 2020. Chikungunya Virus Evades Antiviral CD8+ T Cell Responses To Establish Persistent Infection in Joint-Associated Tissues. J Virol 94.

174. Holmes AC, Basore K, Fremont DH, Diamond MS. 2020. A molecular understanding of alphavirus entry. PLoS Pathog 16:e1008876.

175. Vancini R, Hernandez R, Brown D. 2015. Alphavirus entry into host cells. Prog Mol Biol Transl Sci 129:33–62.

176. Rose PP, Hanna SL, Spiridigliozzi A, Wannissorn N, Beiting DP, Ross SR, Hardy RW, Bambina SA, Heise MT, Cherry S. 2011. Natural resistance-associated macrophage protein is a cellular receptor for sindbis virus in both insect and mammalian hosts. Cell Host Microbe 10:97–104.

177. Ma H, Kim AS, Kafai NM, Earnest JT, Shah AP, Case JB, Basore K, Gilliland TC, Sun C, Nelson CA, Thackray LB, Klimstra WB, Fremont DH, Diamond MS. 2020. LDLRAD3 is a receptor for Venezuelan equine encephalitis virus. Nature 588:308–314.

178. Song H, Zhao Z, Chai Y, Jin X, Li C, Yuan F, Liu S, Gao Z, Wang H, Song J, Vazquez L, Zhang Y, Tan S, Morel CM, Yan J, Shi Y, Qi J, Gao F, Gao GF. 2019. Molecular basis of arthritogenic alphavirus receptor MXRA8 binding to chikungunya virus envelope protein. Cell 177:1714–1724.e12.

179. Basore K, Kim AS, Nelson CA, Zhang R, Smith BK, Uranga C, Vang L, Cheng M, Gross ML, Smith J, Diamond MS, Fremont DH. 2019. Cryo-EM Structure of Chikungunya Virus in Complex with the Mxra8 Receptor. Cell 177:1725–1737.e16.

180. Kim AS, Zimmerman O, Fox JM, Nelson CA, Basore K, Zhang R, Durnell L, Desai C, Bullock C, Deem SL, Oppenheimer J, Shapiro B, Wang T, Cherry S, Coyne CB, Handley SA, Landis MJ, Fremont DH, Diamond MS. 2020. An Evolutionary Insertion in the Mxra8 Receptor-Binding Site Confers Resistance to Alphavirus Infection and Pathogenesis. Cell Host Microbe 27:428–440.e9.

181. Diez-Roux G, Banfi S, Sultan M, Geffers L, Anand S, Rozado D, Magen A, Canidio E, Pagani M, Peluso I, Lin-Marq N, Koch M, Bilio M, Cantiello I, Verde R, De Masi C, Bianchi SA, Cicchini J, Perroud E, Mehmeti S, Dagand E, Schrinner S, Nürnberger A, Schmidt K, Metz K, Zwingmann C, Brieske N, Springer C, Hernandez AM, Herzog S, Grabbe F, Sieverding C, Fischer B, Schrader K, Brockmeyer M, Dettmer S, Helbig C, Alunni V, Battaini M-A, Mura C, Henrichsen CN, Garcia-Lopez R, Echevarria D, Puelles E, Garcia-Calero E, Kruse S, Uhr M, Kauck C, Feng G, Milyaev N, Ong CK, Kumar L, Lam M, Semple CA, Gyenesei A, Mundlos S, Radelof U, Lehrach H, Sarmientos P, Reymond A, Davidson DR, Dollé P, Antonarakis SE, Yaspo M-L, Martinez S, Baldock RA, Eichele G, Ballabio A. 2011. A high-resolution anatomical atlas of the transcriptome in the mouse embryo. PLoS Biol 9:e1000582.

182. Ranganathan S, Noyes NC, Migliorini M, Winkles JA, Battey FD, Hyman BT, Smith E, Yepes M, Mikhailenko I, Strickland DK. 2011. LRAD3, a novel low-density lipoprotein receptor family member that modulates amyloid precursor protein trafficking. J Neurosci 31:10836–10846.

183. Prado Acosta M, Geoghegan EM, Lepenies B, Ruzal S, Kielian M, Martinez MG. 2019. Surface (S) Layer Proteins of Lactobacillus acidophilus Block Virus Infection via DC-SIGN Interaction. Front Microbiol 10:810.

184. Froelich S, Tai A, Kennedy K, Zubair A, Wang P. 2011. Pseudotyping lentiviral vectors with aura virus envelope glycoproteins for DC-SIGN-mediated transduction of dendritic cells. Hum Gene Ther 22:1281–1291.

185. Morizono K, Chen ISY. 2014. Role of phosphatidylserine receptors in enveloped virus infection. J Virol 88:4275–4290.

186. Jemielity S, Wang JJ, Chan YK, Ahmed AA, Li W, Monahan S, Bu X, Farzan M, Freeman GJ, Umetsu DT, Dekruyff RH, Choe H. 2013. TIM-family proteins promote infection of multiple enveloped viruses through virion-associated phosphatidylserine. PLoS Pathog 9:e1003232.

187. Wang KS, Kuhn RJ, Strauss EG, Ou S, Strauss JH. 1992. High-affinity laminin receptor is a receptor for Sindbis virus in mammalian cells. J Virol 66:4992–5001.

188. Malygin AA, Bondarenko EI, Ivanisenko VA, Protopopova EV, Karpova GG, Loktev VB. 2009. C-terminal fragment of human laminin-binding protein contains a receptor domain for venezuelan equine encephalitis and tick-borne encephalitis viruses. Biochemistry (Mosc) 74:1328–1336.

189. Kuadkitkan A, Wikan N, Fongsaran C, Smith DR. 2010. Identification and characterization of prohibitin as a receptor protein mediating DENV-2 entry into insect cells. Virology 406:149–161.

190. Kielian M, Chanel-Vos C, Liao M. 2010. Alphavirus Entry and Membrane Fusion. Viruses 2:796–825.

191. Erbacher A, Gieseke F, Handgretinger R, Müller I. 2009. Dendritic cells: functional aspects of glycosylation and lectins. Hum Immunol 70:308–312.

192. Zhou T, Chen Y, Hao L, Zhang Y. 2006. DC-SIGN and immunoregulation. Cell Mol Immunol 3:279–283.

193. Rogers KM, Heise M. 2009. Modulation of cellular tropism and innate antiviral response by viral glycans. J Innate Immun 1:405–412.

194. Long KM, Whitmore AC, Ferris MT, Sempowski GD, McGee C, Trollinger B, Gunn B, Heise MT. 2013. Dendritic cell immunoreceptor regulates Chikungunya virus pathogenesis in mice. J Virol 87:5697–5706.

195. Moller-Tank S, Maury W. 2014. Phosphatidylserine receptors: enhancers of enveloped virus entry and infection. Virology 468–470:565–580.

196. Lemke G. 2019. How macrophages deal with death. Nat Rev Immunol 19:539–549.

197. Nelson J, McFerran NV, Pivato G, Chambers E, Doherty C, Steele D, Timson DJ. 2008. The 67 kDa laminin receptor: structure, function and role in disease. Biosci Rep 28:33–48.

198. Merkwirth C, Langer T. 2009. Prohibitin function within mitochondria: essential roles for cell proliferation and cristae morphogenesis. Biochim Biophys Acta 1793:27–32.

199. Aquino RS, Park PW. 2016. Glycosaminoglycans and infection. Front Biosci (Landmark Ed) 21:1260–1277.

200. Ströh LJ, Stehle T. 2014. Glycan engagement by viruses: receptor switches and specificity. Annu Rev Virol 1:285–306.

201. Raman R, Tharakaraman K, Sasisekharan V, Sasisekharan R. 2016. Glycan-protein interactions in viral pathogenesis. Curr Opin Struct Biol 40:153–162.

202. Thompson AJ, de Vries RP, Paulson JC. 2019. Virus recognition of glycan receptors. Curr Opin Virol 34:117–129.

203. Gardner CL, Choi-Nurvitadhi J, Sun C, Bayer A, Hritz J, Ryman KD, Klimstra WB. 2013. Natural variation in the heparan sulfate binding domain of the eastern equine encephalitis virus E2 glycoprotein alters interactions with cell surfaces and virulence in mice. J Virol 87:8582–8590.

204. Gardner CL, Ebel GD, Ryman KD, Klimstra WB. 2011. Heparan sulfate binding by natural eastern equine encephalitis viruses promotes neurovirulence. Proc Natl Acad Sci USA 108:16026–16031.

205. Byrnes AP, Griffin DE. 1998. Binding of Sindbis virus to cell surface heparan sulfate. J Virol 72:7349–7356.

206. Zhang W, Heil M, Kuhn RJ, Baker TS. 2005. Heparin binding sites on Ross River virus revealed by electron cryo-microscopy. Virology 332:511–518.

207. WuDunn D, Spear PG. 1989. Initial interaction of herpes simplex virus with cells is binding to heparan sulfate. J Virol 63:52–58.

208. Roderiquez G, Oravecz T, Yanagishita M, Bou-Habib DC, Mostowski H, Norcross MA. 1995. Mediation of human immunodeficiency virus type 1 binding by interaction of cell surface heparan sulfate proteoglycans with the V3 region of envelope gp120-gp41. J Virol 69:2233–2239.

209. Watterson D, Kobe B, Young PR. 2012. Residues in domain III of the dengue virus envelope glycoprotein involved in cell-surface glycosaminoglycan binding. J Gen Virol 93:72–82.

210. Dechecchi MC, Tamanini A, Bonizzato A, Cabrini G. 2000. Heparan sulfate glycosaminoglycans are involved in adenovirus type 5 and 2-host cell interactions. Virology 268:382–390.

211. Giroglou T, Florin L, Schäfer F, Streeck RE, Sapp M. 2001. Human papillomavirus infection requires cell surface heparan sulfate. J Virol 75:1565–1570.

212. Hallak LK, Collins PL, Knudson W, Peeples ME. 2000. Iduronic acid-containing glycosaminoglycans on target cells are required for efficient respiratory syncytial virus infection. Virology 271:264–275.

213. Wang E, Brault AC, Powers AM, Kang W, Weaver SC. 2003. Glycosaminoglycan binding properties of natural venezuelan equine encephalitis virus isolates. J Virol 77:1204–1210.

214. Tan CW, Poh CL, Sam I-C, Chan YF. 2013. Enterovirus 71 uses cell surface heparan sulfate glycosaminoglycan as an attachment receptor. J Virol 87:611–620.

215. Bartlett AH, Park PW. 2011. Heparan sulfate proteoglycans in infection, p. 31–62. *In* Pavão, MSG (ed.), Glycans in diseases and therapeutics. Springer Berlin Heidelberg, Berlin, Heidelberg.

216. Chen Y, Götte M, Liu J, Park PW. 2008. Microbial subversion of heparan sulfate proteoglycans. Mol Cells 26:415–426.

217. Klimstra WB, Heidner HW, Johnston RE. 1999. The furin protease cleavage recognition sequence of Sindbis virus PE2 can mediate virion attachment to cell surface heparan sulfate. J Virol 73:6299–6306.

218. Sahoo B, Chowdary TK. 2019. Conformational changes in Chikungunya virus E2 protein upon heparan sulfate receptor binding explain mechanism of E2-E1 dissociation during viral entry. Biosci Rep 39.

219. Ryman KD, Gardner CL, Burke CW, Meier KC, Thompson JM, Klimstra WB. 2007. Heparan sulfate binding can contribute to the neurovirulence of neuroadapted and nonneuroadapted Sindbis viruses. J Virol 81:3563–3573.

220. Bernard KA, Klimstra WB, Johnston RE. 2000. Mutations in the E2 glycoprotein of Venezuelan equine encephalitis virus confer heparan sulfate interaction, low morbidity, and rapid clearance from blood of mice. Virology 276:93–103.

221. Chen C-L, Hasan SS, Klose T, Sun Y, Buda G, Sun C, Klimstra WB, Rossmann MG. 2020. Cryo-EM structure of eastern equine encephalitis virus in complex with heparan sulfate analogues. Proc Natl Acad Sci USA 117:8890–8899.

222. Kesari AS, Sharkey CM, Sanders DA. 2019. Role of heparan sulfate in entry and exit of Ross River virus glycoprotein-pseudotyped retroviral vectors. Virology 529:177–185.

223. Klimstra WB, Ryman KD, Johnston RE. 1998. Adaptation of Sindbis virus to BHK cells selects for use of heparan sulfate as an attachment receptor. J Virol 72:7357–7366.

224. McAllister N, Liu Y, Silva LM, Lentscher AJ, Chai W, Wu N, Raghunathan K, Vang L, Alexander J, Warfield K, Diamond MS, Feizi T, Silva LA, Dermody TS. 2020. Chikungunya virus strains from each genetic clade bind sulfated glycosaminoglycans as attachment factors. J Virol.

225. Smit JM, Waarts B-L, Kimata K, Klimstra WB, Bittman R, Wilschut J. 2002. Adaptation of alphaviruses to heparan sulfate: interaction of Sindbis and Semliki forest viruses with liposomes containing lipid-conjugated heparin. J Virol 76:10128–10137.

226. Ciano KA, Saredy JJ, Bowers DF. 2014. Heparan sulfate proteoglycan: an arbovirus attachment factor integral to mosquito salivary gland ducts. Viruses 6:5182–5197.

227. Gardner CL, Burke CW, Higgs ST, Klimstra WB, Ryman KD. 2012. Interferon-alpha/beta deficiency greatly exacerbates arthritogenic disease in mice infected with wild-type

chikungunya virus but not with the cell culture-adapted live-attenuated 181/25 vaccine candidate. Virology 425:103–112.

228. Ferguson MC, Saul S, Fragkoudis R, Weisheit S, Cox J, Patabendige A, Sherwood K, Watson M, Merits A, Fazakerley JK. 2015. Ability of the Encephalitic Arbovirus Semliki Forest Virus To Cross the Blood-Brain Barrier Is Determined by the Charge of the E2 Glycoprotein. J Virol 89:7536–7549.

229. Bear JS, Byrnes AP, Griffin DE. 2006. Heparin-binding and patterns of virulence for two recombinant strains of Sindbis virus. Virology 347:183–190.

230. Klimstra WB, Ryman KD, Bernard KA, Nguyen KB, Biron CA, Johnston RE. 1999. Infection of neonatal mice with sindbis virus results in a systemic inflammatory response syndrome. J Virol 73:10387–10398.

231. Lindahl U, Couchman J, Kimata K, Esko JD. 2015. Proteoglycans and sulfated glycosaminoglycans, p. . *In* Varki, A, Cummings, RD, Esko, JD, Stanley, P, Hart, GW, Aebi, M, Darvill, AG, Kinoshita, T, Packer, NH, Prestegard, JH, Schnaar, RL, Seeberger, PH (eds.), Essentials of Glycobiology, 3rd ed. Cold Spring Harbor Laboratory Press, Cold Spring Harbor (NY).

232. Dinglasan RR, Alaganan A, Ghosh AK, Saito A, van Kuppevelt TH, Jacobs-Lorena M. 2007. Plasmodium falciparum ookinetes require mosquito midgut chondroitin sulfate proteoglycans for cell invasion. Proc Natl Acad Sci USA 104:15882–15887.

233. Kusche-Gullberg M, Kjellén L. 2003. Sulfotransferases in glycosaminoglycan biosynthesis. Curr Opin Struct Biol 13:605–611.

234. Prydz K. 2015. Determinants of glycosaminoglycan (GAG) structure. Biomolecules 5:2003–2022.

235. Couchman JR, Pataki CA. 2012. An introduction to proteoglycans and their localization. J Histochem Cytochem 60:885–897.

236. Sarrazin S, Lamanna WC, Esko JD. 2011. Heparan sulfate proteoglycans. Cold Spring Harb Perspect Biol 3.

237. Dreyfuss JL, Regatieri CV, Jarrouge TR, Cavalheiro RP, Sampaio LO, Nader HB. 2009. Heparan sulfate proteoglycans: structure, protein interactions and cell signaling. An Acad Bras Cienc 81:409–429.

238. Iozzo RV, Schaefer L. 2015. Proteoglycan form and function: A comprehensive nomenclature of proteoglycans. Matrix Biol 42:11–55.

239. Couchman JR. 2010. Transmembrane signaling proteoglycans. Annu Rev Cell Dev Biol 26:89–114.

240. Esko JD, H. Prestegard J, Linhardt RJ. 2015. Proteins that bind sulfated glycosaminoglycans, p. . *In* Varki, A, Cummings, RD, Esko, JD, Stanley, P, Hart, GW, Aebi, M, Darvill, AG, Kinoshita, T, Packer, NH, Prestegard, JH, Schnaar, RL, Seeberger, PH (eds.), Essentials of Glycobiology, 3rd ed. Cold Spring Harbor Laboratory Press, Cold Spring Harbor (NY).

241. Nizet V, Varki A, Aebi M. 2015. Microbial lectins: hemagglutinins, adhesins, and toxins, p. . *In* Varki, A, Cummings, RD, Esko, JD, Stanley, P, Hart, GW, Aebi, M, Darvill, AG, Kinoshita, T, Packer, NH, Prestegard, JH, Schnaar, RL, Seeberger, PH (eds.), Essentials of Glycobiology, 3rd ed. Cold Spring Harbor Laboratory Press, Cold Spring Harbor (NY).

242. Xu D, Esko JD. 2014. Demystifying heparan sulfate-protein interactions. Annu Rev Biochem 83:129–157.

243. Rabenstein DL. 2002. Heparin and heparan sulfate: structure and function. Nat Prod Rep 19:312–331.

244. Sinnis P, Coppi A, Toida T, Toyoda H, Kinoshita-Toyoda A, Xie J, Kemp MM, Linhardt RJ. 2007. Mosquito heparan sulfate and its potential role in malaria infection and transmission. J Biol Chem 282:25376–25384.

245. Kim SY, Koetzner CA, Payne AF, Nierode GJ, Yu Y, Wang R, Barr E, Dordick JS, Kramer LD, Zhang F, Linhardt RJ. 2019. Glycosaminoglycan Compositional Analysis of Relevant Tissues in Zika Virus Pathogenesis and in Vitro Evaluation of Heparin as an Antiviral against Zika Virus Infection. Biochemistry 58:1155–1166.

246. Kato M, Wang H, Bernfield M, Gallagher JT, Turnbull JE. 1994. Cell surface syndecan-1 on distinct cell types differs in fine structure and ligand binding of its heparan sulfate chains. J Biol Chem 269:18881–18890.

247. Ledin J, Staatz W, Li J-P, Götte M, Selleck S, Kjellén L, Spillmann D. 2004. Heparan sulfate structure in mice with genetically modified heparan sulfate production. J Biol Chem 279:42732–42741.

248. Cadwallader AB, Yost HJ. 2013. The Glycocode: Translating Heparan Sulfate Fine Structure into Developmental Function, p. 3–18. *In* DeSimone, DW, Mecham, RP (eds.), Extracellular matrix in development. Springer Berlin Heidelberg, Berlin, Heidelberg.

249. Mikami T, Kitagawa H. 2017. Sulfated glycosaminoglycans: their distinct roles in stem cell biology. Glycoconj J 34:725–735.

250. Hardingham T, Muir H. 1972. The specific interaction of hyaluronic acid with cartilage proteoglycans. Biochimica et Biophysica Acta (BBA) - General Subjects 279:401–405.

251. Rosenberg LC, Choi HU, Poole AR, Lewandowska K, Culp LA. 1986. Biological roles of dermatan sulphate proteoglycans. Ciba Found Symp 124:47–68.

252. Hascall V, Esko JD. 2015. Hyaluronan, p. . *In* Varki, A, Cummings, RD, Esko, JD, Stanley, P, Hart, GW, Aebi, M, Darvill, AG, Kinoshita, T, Packer, NH, Prestegard, JH, Schnaar, RL, Seeberger, PH (eds.), Essentials of Glycobiology, 3rd ed. Cold Spring Harbor Laboratory Press, Cold Spring Harbor (NY).

253. Szymanski CM, Schnaar RL, Aebi M. 2015. Bacterial and viral infections, p. . *In* Varki, A, Cummings, RD, Esko, JD, Stanley, P, Hart, GW, Aebi, M, Darvill, AG, Kinoshita, T, Packer, NH, Prestegard, JH, Schnaar, RL, Seeberger, PH (eds.), Essentials of Glycobiology, 3rd ed. Cold Spring Harbor Laboratory Press, Cold Spring Harbor (NY).

254. Bumgarner R. 2013. Overview of DNA microarrays: types, applications, and their future. Curr Protoc Mol Biol Chapter 22:Unit 22.1.

255. Sutandy FXR, Qian J, Chen C-S, Zhu H. 2013. Overview of protein microarrays. Curr Protoc Protein Sci Chapter 27:Unit 27.1.

256. Jawhar NMT. 2009. Tissue Microarray: A rapidly evolving diagnostic and research tool. Ann Saudi Med 29:123–127.

257. Ma H, Horiuchi KY. 2006. Chemical microarray: a new tool for drug screening and discovery. Drug Discov Today 11:661–668.

258. Kiessling LL, Cairo CW. 2002. Hitting the sweet spot. Nat Biotechnol 20:234–235.

259. Wang D, Liu S, Trummer BJ, Deng C, Wang A. 2002. Carbohydrate microarrays for the recognition of cross-reactive molecular markers of microbes and host cells. Nat Biotechnol 20:275–281.

260. Houseman BT, Mrksich M. 2002. Carbohydrate arrays for the evaluation of protein binding and enzymatic modification. Chem Biol 9:443–454.

261. Fukui S, Feizi T, Galustian C, Lawson AM, Chai W. 2002. Oligosaccharide microarrays for high-throughput detection and specificity assignments of carbohydrate-protein interactions. Nat Biotechnol 20:1011–1017.

262. Palma AS, Feizi T, Childs RA, Chai W, Liu Y. 2014. The neoglycolipid (NGL)-based oligosaccharide microarray system poised to decipher the meta-glycome. Curr Opin Chem Biol 18:87–94.

263. Liu Y, Childs RA, Palma AS, Campanero-Rhodes MA, Stoll MS, Chai W, Feizi T. 2012. Neoglycolipid-based oligosaccharide microarray system: preparation of NGLs and their noncovalent immobilization on nitrocellulose-coated glass slides for microarray analyses. Methods Mol Biol 808:117–136.

264. Vanlandingham DL, Hong C, Klingler K, Tsetsarkin K, McElroy KL, Powers AM, Lehane MJ, Higgs S. 2005. Differential infectivities of o'nyong-nyong and chikungunya virus isolates in Anopheles gambiae and Aedes aegypti mosquitoes. Am J Trop Med Hyg 72:616–621.

265. Goo L, Dowd KA, Lin T-Y, Mascola JR, Graham BS, Ledgerwood JE, Pierson TC. 2016. A Virus-Like Particle Vaccine Elicits Broad Neutralizing Antibody Responses in Humans to All Chikungunya Virus Genotypes. J Infect Dis 214:1487–1491.

266. Heinze T, Liebert T, Heublein B, Hornig S. 2006. Functional polymers based on dextran, p. 199–291. *In* Klemm, D (ed.), Polysaccharides II. Springer Berlin Heidelberg.

267. Jones JE, Long KM, Whitmore AC, Sanders W, Thurlow LR, Brown JA, Morrison CR, Vincent H, Peck KM, Browning C, Moorman N, Lim JK, Heise MT. 2017. Disruption of the Opal Stop Codon Attenuates Chikungunya Virus-Induced Arthritis and Pathology. MBio 8.

268. Kotecki M, Reddy PS, Cochran BH. 1999. Isolation and characterization of a near-haploid human cell line. Exp Cell Res 252:273–280.

269. Xu Y, Martinez P, Séron K, Luo G, Allain F, Dubuisson J, Belouzard S. 2015. Characterization of hepatitis C virus interaction with heparan sulfate proteoglycans. J Virol 89:3846–3858.

270. Schowalter RM, Pastrana DV, Buck CB. 2011. Glycosaminoglycans and sialylated glycans sequentially facilitate Merkel cell polyomavirus infectious entry. PLoS Pathog 7:e1002161.

271. Hallak LK, Spillmann D, Collins PL, Peeples ME. 2000. Glycosaminoglycan sulfation requirements for respiratory syncytial virus infection. J Virol 74:10508–10513.

272. Kim SY, Zhao J, Liu X, Fraser K, Lin L, Zhang X, Zhang F, Dordick JS, Linhardt RJ. 2017. Interaction of Zika Virus Envelope Protein with Glycosaminoglycans. Biochemistry 56:1151–1162.

273. Lin J-Y, Shih S-R. 2014. Cell and tissue tropism of enterovirus 71 and other enteroviruses infections. J Biomed Sci 21:18.

274. Tseligka ED, Sobo K, Stoppini L, Cagno V, Abdul F, Piuz I, Meylan P, Huang S, Constant S, Tapparel C. 2018. A VP1 mutation acquired during an enterovirus 71 disseminated infection confers heparan sulfate binding ability and modulates ex vivo tropism. PLoS Pathog 14:e1007190.

275. Kamhi E, Joo EJ, Dordick JS, Linhardt RJ. 2013. Glycosaminoglycans in infectious disease. Biol Rev Camb Philos Soc 88:928–943.

276. Gandhi NS, Mancera RL. 2008. The structure of glycosaminoglycans and their interactions with proteins. Chem Biol Drug Des 72:455–482.

277. Stopschinski BE, Holmes BB, Miller GM, Manon VA, Vaquer-Alicea J, Prueitt WL, Hsieh-Wilson LC, Diamond MI. 2018. Specific glycosaminoglycan chain length and sulfation patterns are required for cell uptake of tau versus α-synuclein and β-amyloid aggregates. J Biol Chem 293:10826–10840.

278. Chandra N, Liu Y, Liu J-X, Frängsmyr L, Wu N, Silva LM, Lindström M, Chai W, Pedrosa Domellöf F, Feizi T, Arnberg N. 2019. Sulfated glycosaminoglycans as viral decoy receptors for human adenovirus type 37. Viruses 11.

279. Bugatti A, Paiardi G, Urbinati C, Chiodelli P, Orro A, Uggeri M, Milanesi L, Caruso A, Caccuri F, D'Ursi P, Rusnati M. 2019. Heparin and heparan sulfate proteoglycans promote HIV-1 p17 matrix protein oligomerization: computational, biochemical and biological implications. Sci Rep 9:15768.

280. Chen Y, Maguire T, Hileman RE, Fromm JR, Esko JD, Linhardt RJ, Marks RM. 1997. Dengue virus infectivity depends on envelope protein binding to target cell heparan sulfate. Nat Med 3:866–871.

281. Gama CI, Tully SE, Sotogaku N, Clark PM, Rawat M, Vaidehi N, Goddard WA, Nishi A, Hsieh-Wilson LC. 2006. Sulfation patterns of glycosaminoglycans encode molecular recognition and activity. Nat Chem Biol 2:467–473.

282. Peerboom N, Block S, Altgärde N, Wahlsten O, Möller S, Schnabelrauch M, Trybala E, Bergström T, Bally M. 2017. Binding Kinetics and Lateral Mobility of HSV-1 on End-Grafted Sulfated Glycosaminoglycans. Biophys J 113:1223–1234.

283. Tiwari V, Clement C, Xu D, Valyi-Nagy T, Yue BYJT, Liu J, Shukla D. 2006. Role for 3-O-sulfated heparan sulfate as the receptor for herpes simplex virus type 1 entry into primary human corneal fibroblasts. J Virol 80:8970–8980.

284. Shukla D, Liu J, Blaiklock P, Shworak NW, Bai X, Esko JD, Cohen GH, Eisenberg RJ, Rosenberg RD, Spear PG. 1999. A novel role for 3-O-sulfated heparan sulfate in herpes simplex virus 1 entry. Cell 99:13–22.

285. LyonS M, Deakin J, Gallagher J. 1994. Liver Heparan Sulfate Structure. J Biol Chem 269:11208–1121.

286. de Agostini AI, Watkins SC, Slayter HS, Youssoufian H, Rosenberg RD. 1990. Localization of anticoagulantly active heparan sulfate proteoglycans in vascular endothelium: antithrombin binding on cultured endothelial cells and perfused rat aorta. J Cell Biol 111:1293–1304.

287. Herrero LJ, Foo S-S, Sheng K-C, Chen W, Forwood MR, Bucala R, Mahalingam S. 2015. Pentosan Polysulfate: a Novel Glycosaminoglycan-Like Molecule for Effective Treatment of Alphavirus-Induced Cartilage Destruction and Inflammatory Disease. J Virol 89:8063–8076.

288. Modhiran N, Gandhi NS, Wimmer N, Cheung S, Stacey K, Young PR, Ferro V, Watterson D. 2019. Dual targeting of dengue virus virions and NS1 protein with the heparan sulfate mimic PG545. Antiviral Res 168:121–127.

289. Supramaniam A, Liu X, Ferro V, Herrero LJ. 2018. Prophylactic Antiheparanase Activity by PG545 Is Antiviral In Vitro and Protects against Ross River Virus Disease in Mice. Antimicrob Agents Chemother 62.

290. Supramaniam A, Bielefeldt-Ohmann H, Rudd PA, Webster J, Ferro V, Herrero LJ. 2019. PG545 treatment reduces RRV-induced elevations of AST, ALT with secondary lymphoid organ alterations in C57BL/6 mice. PLoS One 14:e0217998.

291. Rohatgi A, Corbo JC, Monte K, Higgs S, Vanlandingham DL, Kardon G, Lenschow DJ. 2014. Infection of myofibers contributes to increased pathogenicity during infection with an epidemic strain of chikungunya virus. J Virol 88:2414–2425.

292. Heil ML, Albee A, Strauss JH, Kuhn RJ. 2001. An amino acid substitution in the coding region of the E2 glycoprotein adapts Ross River virus to utilize heparan sulfate as an attachment moiety. J Virol 75:6303–6309.

293. Vallet SD, Clerc O, Ricard-Blum S. 2020. Glycosaminoglycan-Protein Interactions: The First Draft of the Glycosaminoglycan Interactome. J Histochem Cytochem 22155420946403.

294. Hileman RE, Fromm JR, Weiler JM, Linhardt RJ. 1998. Glycosaminoglycan-protein interactions: definition of consensus sites in glycosaminoglycan binding proteins. Bioessays 20:156–167.

295. Kreuger J, Matsumoto T, Vanwildemeersch M, Sasaki T, Timpl R, Claesson-Welsh L, Spillmann D, Lindahl U. 2002. Role of heparan sulfate domain organization in endostatin inhibition of endothelial cell function. EMBO J 21:6303–6311.

296. Mulloy B, Forster MJ, Jones C, Davies DB. 1993. N.m.r. and molecular-modelling studies of the solution conformation of heparin. Biochem J 293 (Pt 3):849–858.

297. Faham S, Hileman RE, Fromm JR, Linhardt RJ, Rees DC. 1996. Heparin structure and interactions with basic fibroblast growth factor. Science 271:1116–1120.

298. Cardin AD, Weintraub HJ. 1989. Molecular modeling of protein-glycosaminoglycan interactions. Arterioscler Thromb Vasc Biol 9:21–32.

299. Rudd TR, Preston MD, Yates EA. 2017. The nature of the conserved basic amino acid sequences found among 437 heparin binding proteins determined by network analysis. Mol Biosyst 13:852–865.

300. Sarkar A, Desai UR. 2015. A Simple Method for Discovering Druggable, Specific Glycosaminoglycan-Protein Systems. Elucidation of Key Principles from Heparin/Heparan Sulfate-Binding Proteins. PLoS One 10:e0141127.

301. Mosier PD, Krishnasamy C, Kellogg GE, Desai UR. 2012. On the specificity of heparin/heparan sulfate binding to proteins. Anion-binding sites on antithrombin and thrombin are fundamentally different. PLoS One 7:e48632.

302. Desai UR, Petitou M, Björk I, Olson ST. 1998. Mechanism of heparin activation of antithrombin. Role of individual residues of the pentasaccharide activating sequence in the recognition of native and activated states of antithrombin. J Biol Chem 273:7478–7487.

303. Torrent M, Nogués MV, Andreu D, Boix E. 2012. The "CPC clip motif": a conserved structural signature for heparin-binding proteins. PLoS One 7:e42692.

304. Olson ST, Halvorson HR, Björk I. 1991. Quantitative characterization of the thrombin-heparin interaction. Discrimination between specific and nonspecific binding models. J Biol Chem 266:6342–6352.

305. Richard B, Swanson R, Olson ST. 2009. The signature 3-O-sulfo group of the anticoagulant heparin sequence is critical for heparin binding to antithrombin but is not required for allosteric activation. J Biol Chem 284:27054–27064.

306. Turnbull JE, Fernig DG, Ke Y, Wilkinson MC, Gallagher JT. 1992. Identification of the basic fibroblast growth factor binding sequence in fibroblast heparan sulfate. J Biol Chem 267:10337–10341.

307. Lortat-Jacob H, Turnbull JE, Grimaud JA. 1995. Molecular organization of the interferon gamma-binding domain in heparan sulphate. Biochem J 310 (Pt 2):497–505.

308. Spillmann D, Witt D, Lindahl U. 1998. Defining the interleukin-8-binding domain of heparan sulfate. J Biol Chem 273:15487–15493.

309. Mukhopadhyay S, Zhang W, Gabler S, Chipman PR, Strauss EG, Strauss JH, Baker TS, Kuhn RJ, Rossmann MG. 2006. Mapping the structure and function of the E1 and E2 glycoproteins in alphaviruses. Structure 14:63–73.

310. Asnet Mary J, Paramasivan R, Tyagi BK, Surender M, Shenbagarathai R. 2013. Identification of structural motifs in the E2 glycoprotein of Chikungunya involved in virus-host interaction. J Biomol Struct Dyn 31:1077–1085.

311. Voet D, Voet JG. 2000. Amino Acids, p. 67–81. *In* Voet, D, Voet, JG (eds.), Biochemistry, 4th ed. John Wiley & Sons, Hoboken, NJ.

312. Smith SA, Silva LA, Fox JM, Flyak AI, Kose N, Sapparapu G, Khomandiak S, Ashbrook AW, Kahle KM, Fong RH, Swayne S, Doranz BJ, McGee CE, Heise MT, Pal P, Brien JD, Austin SK, Diamond MS, Dermody TS, Crowe JE. 2015. Isolation and Characterization of Broad and Ultrapotent Human Monoclonal Antibodies with Therapeutic Activity against Chikungunya Virus. Cell Host Microbe 18:86–95.

313. Fox JM, Long F, Edeling MA, Lin H, van Duijl-Richter MKS, Fong RH, Kahle KM, Smit JM, Jin J, Simmons G, Doranz BJ, Crowe JE, Fremont DH, Rossmann MG, Diamond MS. 2015. Broadly neutralizing alphavirus antibodies bind an epitope on E2 and inhibit entry and egress. Cell 163:1095–1107.

314. Bishop JR, Schuksz M, Esko JD. 2007. Heparan sulphate proteoglycans fine-tune mammalian physiology. Nature 446:1030–1037.

315. Bachvarova V, Dierker T, Esko J, Hoffmann D, Kjellen L, Vortkamp A. 2020. Chondrocytes respond to an altered heparan sulfate composition with distinct changes of heparan sulfate structure and increased levels of chondroitin sulfate. Matrix Biol.

316. Silva JC, Carvalho MS, Han X, Xia K, Mikael PE, Cabral JMS, Ferreira FC, Linhardt RJ. 2019. Compositional and structural analysis of glycosaminoglycans in cell-derived extracellular matrices. Glycoconj J 36:141–154.

317. Roberts GC, Zothner C, Remenyi R, Merits A, Stonehouse NJ, Harris M. 2017. Evaluation of a range of mammalian and mosquito cell lines for use in Chikungunya virus research. Sci Rep 7:14641.

318. Pudney M, Varma MGR, Leake CJ. 1979. Establishment of cell lines from larvae of culicine (Aedes species) and anopheline mosquitoes. Tca Manual 5:997–1002.

319. Siu RWC, Fragkoudis R, Simmonds P, Donald CL, Chase-Topping ME, Barry G, Attarzadeh-Yazdi G, Rodriguez-Andres J, Nash AA, Merits A, Fazakerley JK, Kohl A. 2011. Antiviral RNA interference responses induced by Semliki Forest virus infection of mosquito cells: characterization, origin, and frequency-dependent functions of virus-derived small interfering RNAs. J Virol 85:2907–2917.

320. Lan Q, Fallon AM. 1990. Small heat shock proteins distinguish between two mosquito species and confirm identity of their cell lines. Am J Trop Med Hyg 43:669–676.

321. Igarashi A. 1978. Isolation of a Singh's Aedes albopictus cell clone sensitive to Dengue and Chikungunya viruses. J Gen Virol 40:531–544.

322. Mohamed Ali S, Amroun A, de Lamballerie X, Nougairède A. 2018. Evolution of chikungunya virus in mosquito cells. Sci Rep 8:16175.

323. de Witte L, Bobardt M, Chatterji U, Degeest G, David G, Geijtenbeek TBH, Gallay P. 2007. Syndecan-3 is a dendritic cell-specific attachment receptor for HIV-1. Proc Natl Acad Sci USA 104:19464–19469.

324. Kalia M, Chandra V, Rahman SA, Sehgal D, Jameel S. 2009. Heparan sulfate proteoglycans are required for cellular binding of the hepatitis E virus ORF2 capsid protein and for viral infection. J Virol 83:12714–12724.

325. Shi Q, Jiang J, Luo G. 2013. Syndecan-1 serves as the major receptor for attachment of hepatitis C virus to the surfaces of hepatocytes. J Virol 87:6866–6875.

326. Surviladze Z, Sterkand RT, Ozbun MA. 2015. Interaction of human papillomavirus type 16 particles with heparan sulfate and syndecan-1 molecules in the keratinocyte extracellular matrix plays an active role in infection. J Gen Virol 96:2232–2241.

327. Bartlett AH, Park PW. 2010. Proteoglycans in host-pathogen interactions: molecular mechanisms and therapeutic implications. Expert Rev Mol Med 12:e5.

328. Koganti R, Suryawanshi R, Shukla D. 2020. Heparanase, cell signaling, and viral infections. Cell Mol Life Sci.

329. Elfenbein A, Simons M. 2013. Syndecan-4 signaling at a glance. J Cell Sci 126:3799–3804.

330. Christianson HC, Belting M. 2014. Heparan sulfate proteoglycan as a cell-surface endocytosis receptor. Matrix Biol 35:51–55.

331. Lee CHR, Mohamed Hussain K, Chu JJH. 2019. Macropinocytosis dependent entry of Chikungunya virus into human muscle cells. PLoS Negl Trop Dis 13:e0007610.

332. Makkonen K-E, Turkki P, Laakkonen JP, Ylä-Herttuala S, Marjomäki V, Airenne KJ. 2013. 6-o- and N-sulfated syndecan-1 promotes baculovirus binding and entry into Mammalian cells. J Virol 87:11148–11159.

333. Bacsa S, Karasneh G, Dosa S, Liu J, Valyi-Nagy T, Shukla D. 2011. Syndecan-1 and syndecan-2 play key roles in herpes simplex virus type-1 infection. J Gen Virol 92:733–743.

334. Mis EK, Liem KF, Kong Y, Schwartz NB, Domowicz M, Weatherbee SD. 2014. Forward genetics defines Xylt1 as a key, conserved regulator of early chondrocyte maturation and skeletal length. Dev Biol 385:67–82.

335. Mizumoto S, Yamada S, Sugahara K. 2014. Human genetic disorders and knockout mice deficient in glycosaminoglycan. Biomed Res Int 2014:495764.

336. Mizumoto S, Ikegawa S, Sugahara K. 2013. Human genetic disorders caused by mutations in genes encoding biosynthetic enzymes for sulfated glycosaminoglycans. J Biol Chem 288:10953–10961.

337. Condac E, Silasi-Mansat R, Kosanke S, Schoeb T, Towner R, Lupu F, Cummings RD, Hinsdale ME. 2007. Polycystic disease caused by deficiency in xylosyltransferase 2, an initiating enzyme of glycosaminoglycan biosynthesis. Proc Natl Acad Sci USA 104:9416–9421.

338. Götting C, Kuhn J, Zahn R, Brinkmann T, Kleesiek K. 2000. Molecular cloning and expression of human UDP-d-Xylose:proteoglycan core protein beta-d-xylosyltransferase and its first isoform XT-II. J Mol Biol 304:517–528.

339. Pönighaus C, Ambrosius M, Casanova JC, Prante C, Kuhn J, Esko JD, Kleesiek K, Götting C. 2007. Human xylosyltransferase II is involved in the biosynthesis of the uniform tetrasaccharide linkage region in chondroitin sulfate and heparan sulfate proteoglycans. J Biol Chem 282:5201–5206.

340. Lu Q, Shur B. Sperm from b 1,4-galactosyltransferase-null mice are refractory to ZP3-induced acrosome reactions and penetrate the zona pellucida poorly.

341. Izumikawa T, Kanagawa N, Watamoto Y, Okada M, Saeki M, Sakano M, Sugahara K, Sugihara K, Asano M, Kitagawa H. 2010. Impairment of embryonic cell division and glycosaminoglycan biosynthesis in glucuronyltransferase-I-deficient mice. J Biol Chem 285:12190–12196.

342. Izumikawa T, Sato B, Kitagawa H. 2014. Chondroitin sulfate is indispensable for pluripotency and differentiation of mouse embryonic stem cells. Sci Rep 4:3701.

343. Wilson DG, Phamluong K, Lin WY, Barck K, Carano RAD, Diehl L, Peterson AS, Martin F, Solloway MJ. 2012. Chondroitin sulfate synthase 1 (Chsy1) is required for bone development and digit patterning. Dev Biol 363:413–425.

344. Ogawa H, Hatano S, Sugiura N, Nagai N, Sato T, Shimizu K, Kimata K, Narimatsu H, Watanabe H. 2012. Chondroitin sulfate synthase-2 is necessary for chain extension of chondroitin sulfate but not critical for skeletal development. PLoS One 7:e43806.

345. Watanabe Y, Takeuchi K, Higa Onaga S, Sato M, Tsujita M, Abe M, Natsume R, Li M, Furuichi T, Saeki M, Izumikawa T, Hasegawa A, Yokoyama M, Ikegawa S, Sakimura K, Amizuka N, Kitagawa H, Igarashi M. 2010. Chondroitin sulfate N-acetylgalactosaminyltransferase-1 is required for normal cartilage development. Biochem J 432:47–55.

346. Sato T, Kudo T, Ikehara Y, Ogawa H, Hirano T, Kiyohara K, Hagiwara K, Togayachi A, Ema M, Takahashi S, Kimata K, Watanabe H, Narimatsu H. 2011. Chondroitin sulfate N-acetylgalactosaminyltransferase 1 is necessary for normal endochondral ossification and aggrecan metabolism. J Biol Chem 286:5803–5812.

347. Takeuchi K, Yoshioka N, Higa Onaga S, Watanabe Y, Miyata S, Wada Y, Kudo C, Okada M, Ohko K, Oda K, Sato T, Yokoyama M, Matsushita N, Nakamura M, Okano H, Sakimura K, Kawano H, Kitagawa H, Igarashi M. 2013. Chondroitin sulphate N-acetylgalactosaminyl-transferase-1 inhibits recovery from neural injury. Nat Commun 4:2740.

348. Maccarana M, Kalamajski S, Kongsgaard M, Magnusson SP, Oldberg A, Malmström A. 2009. Dermatan sulfate epimerase 1-deficient mice have reduced content and changed distribution of iduronic acids in dermatan sulfate and an altered collagen structure in skin. Mol Cell Biol 29:5517–5528.

349. Bartolini B, Thelin MA, Svensson L, Ghiselli G, van Kuppevelt TH, Malmström A, Maccarana M. 2013. Iduronic acid in chondroitin/dermatan sulfate affects directional migration of aortic smooth muscle cells. PLoS One 8:e66704.

350. Bartolini B, Thelin MA, Rauch U, Feinstein R, Oldberg A, Malmström A, Maccarana M. 2012. Mouse development is not obviously affected by the absence of dermatan sulfate

epimerase 2 in spite of a modified brain dermatan sulfate composition. Glycobiology 22:1007–1016.

351. Lin X, Wei G, Shi Z, Dryer L, Esko JD, Wells DE, Matzuk MM. 2000. Disruption of gastrulation and heparan sulfate biosynthesis in EXT1-deficient mice. Dev Biol 224:299–311.

352. Stickens D, Zak BM, Rougier N, Esko JD, Werb Z. 2005. Mice deficient in Ext2 lack heparan sulfate and develop exostoses. Development 132:5055–5068.

353. Nadanaka S, Kagiyama S, Kitagawa H. 2013. Roles of EXTL2, a member of the EXT family of tumour suppressors, in liver injury and regeneration processes. Biochem J 454:133–145.

354. Nadanaka S, Zhou S, Kagiyama S, Shoji N, Sugahara K, Sugihara K, Asano M, Kitagawa H. 2013. EXTL2, a member of the EXT family of tumor suppressors, controls glycosaminoglycan biosynthesis in a xylose kinase-dependent manner. J Biol Chem 288:9321–9333.

355. Takahashi I, Noguchi N, Nata K, Yamada S, Kaneiwa T, Mizumoto S, Ikeda T, Sugihara K, Asano M, Yoshikawa T, Yamauchi A, Shervani NJ, Uruno A, Kato I, Unno M, Sugahara K, Takasawa S, Okamoto H, Sugawara A. 2009. Important role of heparan sulfate in postnatal islet growth and insulin secretion. Biochem Biophys Res Commun 383:113–118.

356. Stanford KI, Wang L, Castagnola J, Song D, Bishop JR, Brown JR, Lawrence R, Bai X, Habuchi H, Tanaka M, Cardoso WV, Kimata K, Esko JD. 2010. Heparan sulfate 2-O-sulfotransferase is required for triglyceride-rich lipoprotein clearance. J Biol Chem 285:286–294.

357. Axelsson J, Xu D, Kang BN, Nussbacher JK, Handel TM, Ley K, Sriramarao P, Esko JD. 2012. Inactivation of heparan sulfate 2-O-sulfotransferase accentuates neutrophil infiltration during acute inflammation in mice. Blood 120:1742–1751.

358. Merry CL, Bullock SL, Swan DC, Backen AC, Lyon M, Beddington RS, Wilson VA, Gallagher JT. 2001. The molecular phenotype of heparan sulfate in the Hs2st-/- mutant mouse. J Biol Chem 276:35429–35434.

359. HajMohammadi S, Enjyoji K, Princivalle M, Christi P, Lech M, Beeler D, Rayburn H, Schwartz JJ, Barzegar S, de Agostini AI, Post MJ, Rosenberg RD, Shworak NW. 2003. Normal levels of anticoagulant heparan sulfate are not essential for normal hemostasis. J Clin Invest 111:989–999.

360. Habuchi H, Nagai N, Sugaya N, Atsumi F, Stevens RL, Kimata K. 2007. Mice deficient in heparan sulfate 6-O-sulfotransferase-1 exhibit defective heparan sulfate biosynthesis, abnormal placentation, and late embryonic lethality. J Biol Chem 282:15578–15588.

361. Anower-E-Khuda MF, Habuchi H, Nagai N, Habuchi O, Yokochi T, Kimata K. 2013. Heparan sulfate 6-O-sulfotransferase isoform-dependent regulatory effects of heparin on

the activities of various proteases in mast cells and the biosynthesis of 6-O-sulfated heparin. J Biol Chem 288:3705–3717.

362. Soares da Costa D, Reis RL, Pashkuleva I. 2017. Sulfation of glycosaminoglycans and its implications in human health and disorders. Annu Rev Biomed Eng 19:1–26.

363. Rek A, Krenn E, Kungl AJ. 2009. Therapeutically targeting protein-glycan interactions. Br J Pharmacol 157:686–694.

364. Miura Y, Fukuda T, Seto H, Hoshino Y. 2016. Development of glycosaminoglycan mimetics using glycopolymers. Polym J 48:229–237.

365. Muñoz EM, Linhardt RJ. 2004. Heparin-binding domains in vascular biology. Arterioscler Thromb Vasc Biol 24:1549–1557.

366. Herbert JM, Hérault JP, Bernat A, van Amsterdam RG, Lormeau JC, Petitou M, van Boeckel C, Hoffmann P, Meuleman DG. 1998. Biochemical and pharmacological properties of SANORG 34006, a potent and long-acting synthetic pentasaccharide. Blood 91:4197–4205.

367. Choay J, Petitou M, Lormeau JC, Sinaÿ P, Casu B, Gatti G. 1983. Structure-activity relationship in heparin: a synthetic pentasaccharide with high affinity for antithrombin III and eliciting high anti-factor Xa activity. Biochem Biophys Res Commun 116:492–499.

368. Bouvière J, Trignol A, Hoang D-H, Del Carmine P, Goriot M-E, Ben Larbi S, Barritault D, Banzet S, Chazaud B. 2019. Heparan sulfate mimetics accelerate postinjury skeletal muscle regeneration. Tissue Eng Part A 25:1667–1676.

369. Morla S. 2019. Glycosaminoglycans and glycosaminoglycan mimetics in cancer and inflammation. Int J Mol Sci 20.

370. Almer J, Gesslbauer B, Kungl AJ. 2018. Therapeutic strategies to target microbial protein-glycosaminoglycan interactions. Biochem Soc Trans 46:1505–1515.

371. Chandra N, Frängsmyr L, Arnberg N. 2019. Decoy Receptor Interactions as Novel Drug Targets against EKC-Causing Human Adenovirus. Viruses 11.

372. Hidari KIPJ, Abe T, Suzuki T. 2013. Carbohydrate-related inhibitors of dengue virus entry. Viruses 5:605–618.

373. Lee EC, Davis-Poynter N, Nguyen CTH, Peters AA, Monteith GR, Strounina E, Popat A, Ross BP. 2016. GAG mimetic functionalised solid and mesoporous silica nanoparticles as viral entry inhibitors of herpes simplex type 1 and type 2 viruses. Nanoscale 8:16192–16196.

374. Aguilar JS, Rice M, Wagner EK. 1999. The polysulfonated compound suramin blocks adsorption and lateral difusion of herpes simplex virus type-1 in vero cells. Virology 258:141–151.

375. Palma AS, Liu Y, Childs RA, Herbert C, Wang D, Chai W, Feizi T. 2011. The human epithelial carcinoma antigen recognized by monoclonal antibody AE3 is expressed on a sulfoglycolipid in addition to neoplastic mucins. Biochem Biophys Res Commun 408:548–552.

376. Liu Y, McBride R, Stoll M, Palma AS, Silva L, Agravat S, Aoki-Kinoshita KF, Campbell MP, Costello CE, Dell A, Haslam SM, Karlsson NG, Khoo K-H, Kolarich D, Novotny MV, Packer NH, Ranzinger R, Rapp E, Rudd PM, Struwe WB, Tiemeyer M, Wells L, York WS, Zaia J, Kettner C, Paulson JC, Feizi T, Smith DF. 2017. The minimum information required for a glycomics experiment (MIRAGE) project: improving the standards for reporting glycan microarray-based data. Glycobiology 27:280–284.